Assessing and Communicating Climate and Water Ecosystem Services of the City of Ann Arbor Greenbelt Program

by

Jackie Edinger, Jessica Einck, Sebastian Kasparian, and Lavran Pagano

Faculty Advisors: Dr. Sheila Schueller and Shannon Brines

Client Organizations:

1. City of Ann Arbor Greenbelt Advisory Commission and Office of Sustainability and Innovations
2. The Conservation Fund

A project submitted in partial fulfillment of the requirements for the degree of Master of Science at the University of Michigan (School for Environment and Sustainability)

April 2021

Executive Summary

The Open Space and Parkland Preservation Millage was approved by the residents of Ann Arbor in November 2003 as a way to protect productive farmland, prevent the destruction of natural landscapes, and preserve the rural character surrounding Ann Arbor. Commonly known as the Greenbelt Program, the millage provides funds to preserve and protect open space, farmland, natural habitats, and the City's source waters inside and outside the city limits. More than halfway through the 30-year millage in 2021, the Greenbelt Program consists of over 6,200 acres of protected land on more than 70 parcels. While successful, the program lacks adequate ways to report impact and motivate support beyond acres preserved and funds leveraged. Like many organizations working to protect land, they are in need of additional ways to assess and communicate more meaningful measures of conservation value, such as quantifying ecosystem services.

Our goal was to develop a series of dynamic geoprocessing tools to quantify specific ecosystem service value of the Greenbelt's current portfolio of properties and any new properties added in the future. This will allow the City staff and residents of Ann Arbor to have an ongoing understanding of and ability to communicate the value of individual properties and entire land conservation programs. We focused on two categories of ecosystem services: (1) above and belowground carbon storage and (2) water quality.

Aboveground Carbon Storage

We used a combination of field-collected and available remote sensing data to develop a model for measuring the amount of carbon stored in trees within forested areas of the Greenbelt. We acquired LiDAR (light detection and ranging) data of Washtenaw County from 2017 to estimate tree height and volume, and we measured tree species and diameter at three sites located in Washtenaw County to estimate tree biomass using allometric equations from the literature. Using these data sources, we compared the effectiveness of various modeling methods to predict biomass across sites. We found that a Power Law model allowed us to best estimate aboveground carbon storage. We were able to estimate both per-parcel and total aboveground carbon stored in the Ann Arbor Greenbelt, which as of April 2021 totals 32,595,817 kg C, or 119,519 metric tons of CO_2. This is equivalent to the annual CO_2 emissions of 2,716 average Ann Arbor households, 80,682,715 passenger vehicle miles, or 1,348,245 airline miles. This equates to a value of $6,095,473.15 when using the 2021 EPA social cost of carbon value of $51 per metric ton of CO_2.

Belowground Carbon Storage

To estimate the amount of carbon stored in the soil of Greenbelt properties we used available spatial data on soil type together with standards from the literature for calculating carbon stored in the organic matter of soils. We used the National Resources Conservation Service (NRCS) Web Soil Survey to determine which soil types are present in the forested and wetland areas of the Greenbelt District and which characteristics, including horizon depth, bulk density, and organic matter content, are known to be associated with these soil types. Transferring these values into ArcGIS Pro allowed us to provide low, medium, and high estimates of carbon storage for each soil type and develop a model to calculate soil carbon

stored at an individual property level. We found that the estimated carbon contained in the uppermost horizon of forested and wetland soils of the Greenbelt properties as of April 2021 totals 50,005,732 kg C, or 183,356 metric tons of CO_2. This is equivalent to the annual CO_2 emissions of 4,167 average Ann Arbor households, 123,776,564 passenger vehicle miles, or 2,068,363 airline miles. Using the EPA's 2021 social cost of carbon value, we found that the Greenbelt properties have a value of $9,351,156.96. Agricultural soils were not included in estimates given that soil carbon would depend highly on specific cultivation practices, which are neither constant nor easy to assess.

Water Quality

To evaluate how land protection under the Greenbelt program contributes to water ecosystem services, we compared tools that assess the impact of land conversion on water quality. Based on this review we recommended amendments to existing tools that would improve their applicability to the Greenbelt Program and accessibility for other land conservancies in Southeast Michigan. Specifically, we provided an updated web-based version of the EPA Region 5 Conservation Easement Load Reduction Worksheet and identified the Michigan State University Institute of Water Research's Great Lakes Watershed Management System (GLWMS) as the optimal tool for future water quality analyses within Washtenaw County. We recommend further collaboration with the Institute of Water Research to expand the spatial scope of its tool to include the Huron River Watershed.

Future Projects and Recommendations

While we achieved our project goals of providing tools that can allow the Greenbelt Program to assess certain ecosystem services, the accuracy and broader applicability of our assessment methods can be improved with future work. Aboveground carbon storage evaluations could incorporate more diverse field data, including both coniferous and deciduous trees across the county, to allow our approach to be applied on a broader variety of forest types. As tree heights change over time, the model we developed may also need to be updated with current LiDAR and field data. To expand the soil carbon storage model to include agricultural soils, it would be necessary to know what agricultural practices are being used and the differential impacts of these practices on soil carbon storage. Other potential projects can consider drone-based biomass estimation, community engagement, and interactive maps of public lands to educate Ann Arbor residents on the value of ecosystem services. Assessing ecosystem services in feasible and meaningful ways as we did in this project has broad application to global land conservation efforts and should continue to be tailored for specific ecosystems.

Acknowledgements

We would like to express our sincere gratitude to our faculty advisors, Dr. Sheila Schueller and Shannon Brines, for helping to develop this project, review drafts of this report, and provide moral support throughout the duration of this project. Without their expert guidance this project would not have been possible.

We would like to acknowledge and thank our client representative Remy Long, Manager of the City of Ann Arbor Greenbelt Program. We also want to thank Dr. Missy Stults and Thea Yagerlener at the City of Ann Arbor Office of Sustainability and Innovations for their support of this project, as well as Scott Harrod, GIS Coordinator for the City of Ann Arbor. This project was completed using funds provided by the City of Ann Arbor's Office of Sustainability and Innovations.

We would like to thank Jason Tallant at the University of Michigan Biological Station for his guidance with developing a method for assessing aboveground carbon storage through LiDAR data. Our fieldwork design and methods for measuring carbon storage were inspired by the 2020 SEAS Properties Master's Project team, including Maxwell DeYoung, Zimeng Ding, Zhengyu Li, Lara O'Brien, Peter Siciliano, and Cyrus Van Haitsma. This work would not be possible without the assistance of Manish Verma at Consulting for Statistics, Computing and Analytics Research, and Bennet Fauber and Shelly Johnson at the University of Michigan Information and Technology Services, Advanced Research Computing group. We would also like to thank Jeremiah Asher at the Institute of Water Research for his assistance with the Great Lakes Watershed Management System tool, as well as Kevin Harnish and Colin Carroll at The Conservation Fund, and Tristan Goulden and Courtney Meier at the National Ecological Observatory Network (NEON).

We also extend our appreciation to several SEAS faculty members who informally advised us on this project including: Dr. Kathleen Bergen, Dr. Jennifer Blesh, Dr. Silvia Cordero-Sancho, Dr. Stella Cousins, Dr. Drew Gronewold, Dr. Brendan O'Neill, Dr. Catherine Riseng, Dr. Paul Seelbach, Dr. Derek Van Berkel, and Dr. Don Zak.

We would like to acknowledge the members of the Huron River Watershed Council, Sleeping Bear Dunes, and SEAS Bees Master's Project teams for their moral support throughout the 16 months completing this project. We would also like to thank our Graduate Student Instructors, Emily Blackmer and Calli VanderWilde for their feedback in developing this report.

Finally, but certainly not least, we would like to acknowledge and thank our families and friends for their love and support over the past two years.

This research was done using resources provided by the Open Science Grid (Pordes, et al., 2007; Sfiligoi et al., 2009), which is supported by the National Science Foundation award #2030508. This work used resources provided by the OSiRIS Project, which is supported by the National Science Foundation under Grant Number 1541335.

Table of Contents

Chapter 1:

Ecosystem Services and the Greenbelt Program

Introduction to the Problem

Ecosystem services are defined as the collection of biological processes required to sustain human life and provide a good quality of living (Cardinale et al., 2019). These services are grouped into four categories: (1) Provisioning: products obtained from ecosystems, such as food, water, and raw materials; (2) Regulating: benefits from the regulation of ecosystem processes, such as air and water purification, climate regulation, and erosion control; (3) Supporting: ecological processes that control the functioning of ecosystems, including biomass production, decomposition, and nutrient cycling; and (4) Cultural: nonmaterial benefits obtained from ecosystems, including recreation, ecotourism, health, and well-being (Leeans & De Groot, 2003).

Regulating and supporting services are both ecological processes that may go unnoticed, but are critical for human life on earth. Carbon regulating services are often the most frequently studied regulating ecosystem service studied at present, due to carbon's connection with climate change mitigation. Water-related services have also received increased attention, as water is vital to life on Earth and its value is easily appreciated by humans (Karabulut et al., 2016). For example, water ecosystem services could consist of water purification and water supply provided to agriculture (Brander et al., 2006).

Ecosystem services can be *quantified* with an ecological production function, and this can then be translated to some form of human *value*, which include monetary value or human well-being (Summers et al., 2012). For example, carbon storage can be measured directly as gigatons of carbon stored per hectare. This carbon amount can also be quantified in terms of how much carbon dioxide is prevented from entering the atmosphere. These avoided emissions can be assigned a monetary value where carbon-valuation mechanisms exist, such as emissions trading schemes, carbon taxes, and voluntary markets (Hungate et al., 2017). For example, Costanza et al. (1997) estimated the value of the world's ecosystem services to be in the range of US $16-54 trillion per year, with an average of US $33 trillion.

There have been significant advances in the development of the ecosystem service concept, but quantifying and valuing ecosystem services in ways that are useful for communication and decision-making remains challenging, especially at a local scale and in data-scarce regions (Pandeya et al., 2016). Great interest currently exists for developing ecosystem models that allow the user to forecast how ecosystem services may change under alternative land use and climate futures (Feng et al., 2011). Geoprocessing models such as ARIES, InVEST, and Marxan have aimed to quantify ecosystem services in a way that acknowledges complexity and its consequences, while making sure that models are sufficiently simple to remain tractable and scalable to varying levels of detail and data availability (Villa et al., 2014).

Despite increased research and interest in development of tools to actually measure ecosystem services, they can be difficult for practitioners to apply in land use planning. In part this is simply because the literature outlining methodologies is often not accessible to practitioners (Knight et al., 2008). Even if that information is accessible, most assessments require significant field data collection time, for which organizations may have limited capacity. For example, carbon storage and sequestration are of particular interest to decision makers, because of their direct impact on climate regulation. However, carbon stocks in forest soils and forest floors are highly variable annually, seasonally and spatially, because they depend on physical conditions and tree species. For example, Schulp et al. (2008) found that in the Netherlands, forest floor carbon stocks ranged from 11.1 Mg C ha^{-1} for beech trees to 29.6 Mg C ha^{-1} for larch trees.

The need for more accessible and feasible ecosystem service assessments is critical to the future of land protection efforts. Uncoordinated development around urban areas is associated with the loss and fragmentation of rural open space, wildlife habitat, and wetlands, and the consequential decline in biodiversity. If protected from development, land has the potential to provide numerous ecosystem services, such as water purification, climate change mitigation, food production, and opportunities for recreational and aesthetic enjoyment. However, organizations that are working to protect land often lack the capacity to communicate the incremental and overall meaningful value of that land to potential supporters and decision-makers. They require feasible ecosystem service assessment methods.

Client & Site Background

The Greenbelt Program is an example of the City of Ann Arbor's efforts to protect land. They, like other organizations, require ecosystem service assessment methods that would assist in project selection and in reporting within the Greenbelt Program, as well as progress reporting of the City's sustainability efforts. Due to the fact that Washtenaw County has lost 223,785 acres of farmland since 1935, conservation easements of remaining land are necessary to maintain vital ecosystem services. Concurrently, in the state of Michigan, the equivalent of 2 acres of farmland have been lost every hour since 2007, which is the equivalent of 2 farms each day (The Conservation Fund, 2019).

The creation of the City of Ann Arbor Greenbelt Program was predicated on the passage of the Open Space and Parkland Preservation Millage. The millage started in 2003 when 67% of Ann Arbor voters approved a 30-year, 0.5 million tax levy, which funds new parkland acquisitions within the City limits and the purchase of development rights outside the City but within the Greenbelt District. The purpose of this initiative is to provide funds to preserve and protect open space, farmland, natural habitats, and the city's source waters inside and outside the City limits. A breakdown of the millage revenue is shown in Figure 1.1 below.

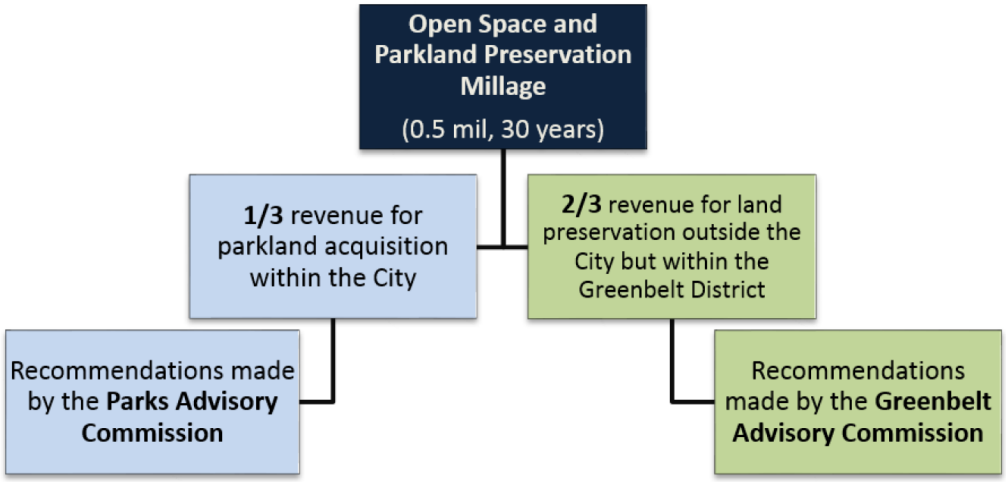

Figure 1.1. Open Space and Parkland Preservation Millage revenue, from 2019 Strategic Plan (The Conservation Fund, 2019)

Chapter 42 of the City Code of Ann Arbor outlines the use of the millage funds. It also establishes the Greenbelt Advisory Commission (GAC). GAC is appointed by the City Council of Ann Arbor and is composed of nine members: one City Council representative, one farmer, one developer, two environmentalists, one biologist, and three community members. GAC reviews applications for the purchase of Greenbelt District properties, advises City Council on monitoring and enforcement of development rights and conservation easements acquired by the Greenbelt District, and prepares an annual budget for land rights acquisition, preservation, and management (Open Space and Parkland Preservation Ordinance, 2004).

Land preservation for the Greenbelt program occurs in two primary forms:

1. **Fee Simple Ownership**, where an entity such as the City or County owns land outright, usually for the purpose of public recreation
2. **Purchase of Development Rights**, where an entity secures a voluntary and perpetual contract with a private landowner to restrict the current and future potential for development, providing public benefits without requiring public ownership

Purchasing development rights helps keep land in private ownership and also ensures that the land is preserved in perpetuity. This is a cost effective approach for the City to achieve land preservation at a fraction of the market cost. For a property to be accepted into the Greenbelt, it typically takes about 18-36 months for the process to be completed after the property owner first submits their application to the Greenbelt Program. During that time, the application is evaluated, matching funds are secured, and the project is reviewed and approved by GAC and the Ann Arbor City Council (City of Ann Arbor, 2021a).

The City of Ann Arbor employs an external consultant to manage all acquisitions and administration of the Open Space and Parkland Preservation Program. The current external consultant retained by the City is The Conservation Fund, a national non-profit organization that protects land and water resources through land acquisition, sustainable community and

economic development, and leadership training. The Conservation Fund is responsible for overseeing the logistics of each land or easement acquisition, from reviewing applications and securing funds for the purchases to navigating the review process using advice and oversight provided by the City.

To assess each prospective acquisition, GAC uses scoring criteria as a way to review and identify high-quality parcels that should be prioritized for protection. The scoring criteria assesses the characteristics and context of the land, as well as potential acquisition considerations. Typically, aerial imagery and GIS are used to conduct these assessments. After an application report is prepared, the prospective project is presented to GAC, and GAC then chooses whether or not to proceed by authorizing an appraisal of the property. If approved, an appraisal is commissioned. If both the applicant and GAC agree that the valuation is an accurate reflection of the Fair Market Value, the project proceeds. Next, project partners and matching funds are sought for each acquisition. These partners often include Washtenaw County, townships within the Greenbelt District, local nonprofit land conservancies, and federal agencies. After the project package is prepared, it is presented to GAC for review. If GAC approves of the project's structure and partnerships, a final recommendation is made to City Council for approving the acquisition. A final resolution to approve the acquisition is then presented to City Council for their consideration.

Once approved, the necessary due diligence is completed and, in accordance with the City's Conservation Easement Deed, each Greenbelt property is placed under several restrictions, encumbering the property's development rights (City of Ann Arbor, 2021a). For instance, the conservation easement may include some or all of the following provisions (Open Space and Parkland Preservation Ordinance, 2004), among many others:

- The property will be subject to a Conservation Plan which is approved by the Natural Resources Conservation Service (NRCS), to promote the long term viability of the land to meet the conservation easement and Conservation Plan purposes.
- No more than 2% of the protected property may be improved or altered with impervious surfaces that limit rainfall infiltration, excluding NRCS-approved conservation practices.
- Oil, gas, or mineral exploration and extraction are prohibited.
- Timber harvest must follow specific rules that include if the protected property contains 40 contiguous acres of forest or 20 percent of the protected property is forestland, then forest management and timber harvesting must be performed in accordance with a written forest management plan. The goals of commercial timber harvest must also include the preservation of scenic characteristics and assure sustainable forest productivity.

Generally these provisions ensure that the conservation value of the property - its wetlands, forests, agricultural soil, etc. - will remain protected from development or over-exploitation in perpetuity.

Excluding the city, the Ann Arbor Greenbelt District encompasses approximately 87,500 acres, 25,000 of which are currently in active agricultural production (The Conservation Fund, 2019). Now in its 18th year (over halfway through the 30-year millage), the Greenbelt Program has protected over 6,200 acres of open space surrounding the city and has leveraged over $24M in Greenbelt funds by securing matching grants, landowner donations, and contributions from other locally funded programs totalling over $29M. As of April 2021, there are 70 parcels

ranging from 7 to 286 acres in size. The properties protected by the Greenbelt Program collectively account for 3,737 acres of active farmland and 2,817 acres of natural areas, including forests, prairies, and wetlands. A map of the Ann Arbor Greenbelt District boundary is shown below in Figure 1.2.

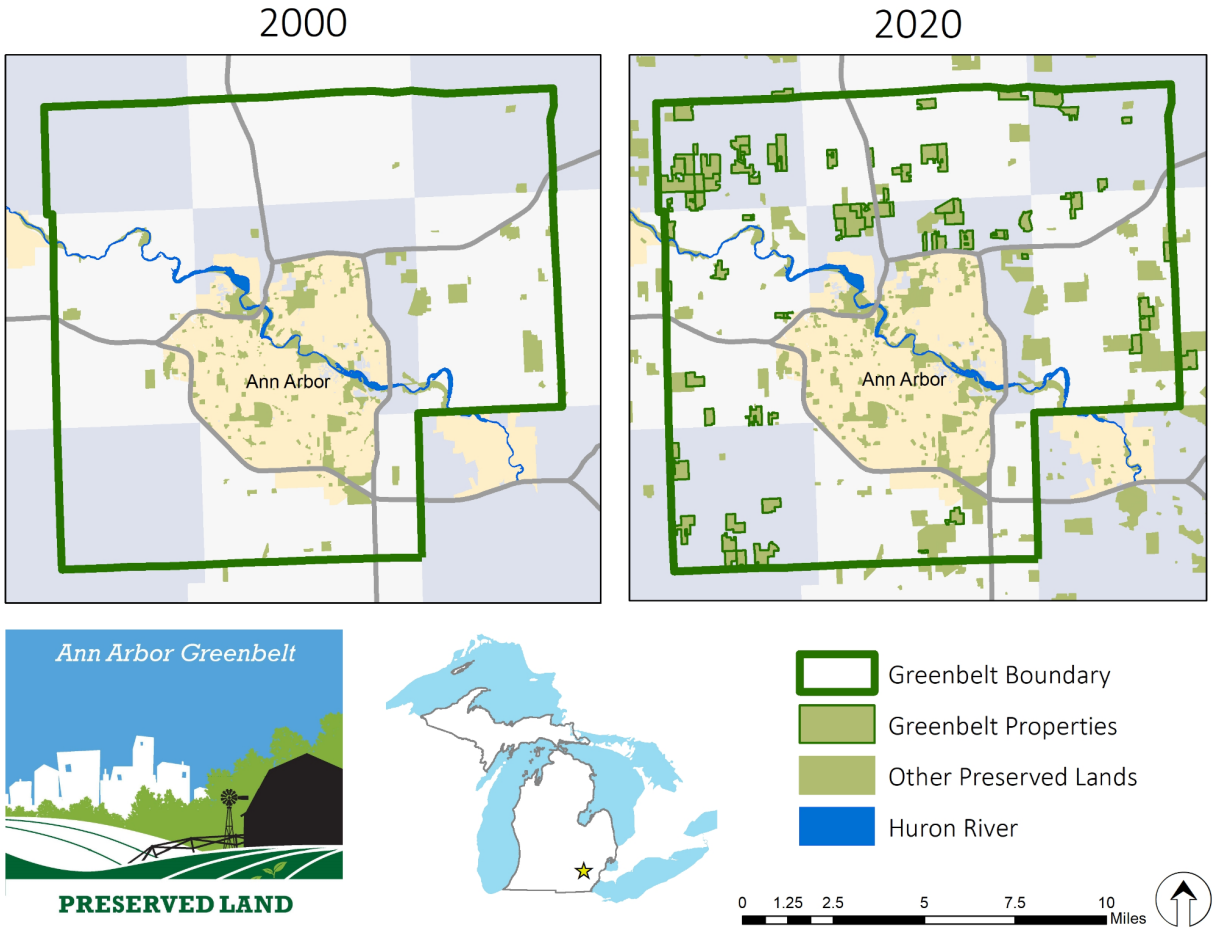

Figure 1.2. Map of Ann Arbor Greenbelt District (City of Ann Arbor, 2021b)

A variety of aquatic and terrestrial ecosystems, and therefore ecosystem services, are protected by the Greenbelt Program. The Greenbelt Program has protected over 28 miles of river, stream and water frontage, and 60% of these waterways are within the Huron River Watershed, contributing to the filtration and protection of the City's drinking water (The Conservation Fund, 2019). Wetlands protected by the Greenbelt provide flood protection, pollution control, and essential breeding and feeding grounds for many species of fish and wildlife (Federal Geographic Data Committee, 2013). Forested areas that can store carbon in trees within the Greenbelt District include species such as white oak (*Quercus alba*), northern red oak (*Quercus rubra*), sugar maple (*Acer saccharum*), and American basswood (*Tilia americana*). Forest vegetation can also be dominated by invasive shrubs such as common buckthorn (*Rhamnus cathartica*), autumn-olive (*Elaeagnus umbellata*), and Oriental bittersweet (*Celastrus orbiculatus*) (Barnes & Wagner, 2004). As a temperate system, the area experiences

high seasonality in temperature and precipitation. A summary of total acreage of various land cover types is shown in Table 1.1.

Table 1.1. Summary of Land Cover Types within Greenbelt District. Soils refer to prime, local importance, and prime if drained only soils. Total acreage is from May 2020. These numbers were provided by the City of Ann Arbor.

Land Cover Type	**Acres within Greenbelt District**	**Acres within Greenbelt Properties**	**% of Total Area of Greenbelt Properties**
Woodland	33,524	1,341	5.0%
Wetlands	24,611	1,476	6.6%
Soils	96,985	5,575	6.9%
Agriculture	24,469	3,737	15.3%
Total	**105,675**	**5,923**	

Project Goals

While the Greenbelt Program has been successful at preserving land with conservation easements, it currently faces two major limitations:

1) A lack of capacity to *report* success in terms beyond acres and money leveraged to values that are important to a larger audience of decision-makers and funders, including being able to communicate contributions to carbon neutrality and watershed protection initiatives in the area, and
2) Inadequate information to make parcel-level *decisions* based on actual information about key criteria deemed in a recent strategic review as especially important goals of the program: climate mitigation and water quality protection.

The goal of this project is to provide the City of Ann Arbor Greenbelt Program with the ability to assess and report on the ecosystem services of individual parcels and over the total acreage already protected, as well as each new or potential parcel acquisition, especially in terms of 1) climate regulation services through carbon storage, and 2) water quality. This information will be used to assist in reviewing potential parcel acquisitions and in reporting and leveraging support for the Greenbelt program.

Project Significance

With this project, the Greenbelt Program Manager will be able to communicate to various entities, including landowners in the Greenbelt area, Ann Arbor City Council, and Ann Arbor residents, the return on investment provided by continued land purchases for protection.

Additionally, because the Greenbelt Program is funded by the 30-year millage, our project will help provide Ann Arbor residents with adequate information to consider renewal of the millage in 2034.

Between 2004 and 2018, all applications for private land to be added as Greenbelt properties were approved by the Ann Arbor City Council. However, in 2019, Council concerns with a particular Greenbelt acquisition brought to light a critical lack of understanding of the conservation values of each potential Greenbelt acquisition. Communicating this value requires having compelling data to share. The Greenbelt Program Manager aims to build understanding among residents and City Council of the value and benefits of the existing portfolio of Greenbelt acquisitions, and offer them more crucial information regarding each future project so they can make informed decisions and utilize the voter's tax dollars efficiently and effectively. Additionally, Ann Arbor residents have expressed interest in carbon storage and water quality. Water quality is an integral part of the Greenbelt mission, and carbon is a common subject in public commentary and connects with the City's carbon neutrality goals.

City Council has already placed an emphasis on the Greenbelt Program to leverage the City's funds to the best of its ability. The processing tool we create provides City staff with data to inform the City Council about a parcel's ecosystem services so that they can weigh these benefits with the acquisition costs.

Broader Theory and Practice

As discussed above, the need for more accessible and feasible ecosystem service assessments is critical to the future of land protection efforts. Beyond the Ann Arbor Greenbelt, our project deliverables can be adapted to serve as an invaluable resource for regional land trusts to improve the way they assess and report the value of land protection. Similar greenbelts, greenways, or other land use planning efforts to curb suburban sprawl or maintain natural areas close to cities have been implemented throughout the world with varying degrees of support and success. According to the 2015 National Land Trust Census Report, 56 million acres were conserved by state, local and national land trusts by the end of 2015 (Land Trust Alliance, 2015).

Approach & Chapter Overview

We developed ecosystem service assessment methods specific to above- and below-ground carbon and the impact of land conversion on water quality by using a variety of available data sources and tools to generate new models. To measure carbon storage with minimal field work, we developed separate geoprocessing tools for the aboveground (trees and shrubs) and belowground (soil) components to estimate the carbon storage of Greenbelt properties remotely. In Chapter 2, we lay out our method to measure aboveground carbon storage using a combination of field data and LiDAR remote sensing data. We test the statistical significance of various modeling techniques to determine which model best predicts biomass, and calculate aboveground carbon of Greenbelt properties using this model. In Chapter 3, we use existing research and data on soil properties and land use/land cover to estimate carbon storage in soils of forested and wetland segments of Greenbelt properties. For both above and belowground carbon we demonstrate how to convert the amount of carbon stored into more

easily understood values, such as average household annual emissions, airline mile, and passenger vehicle mile equivalents. Finally, in Chapter 4, we consider which aspects of water quality can be quantified and recommend amendments to currently-used tools and the adoption of outside tools for future analysis. Our key research questions are summarized in Figure 1.3. Together, these approaches provide the Greenbelt Program with a way to continue to assess specific ecosystem services without further field data collection while also providing a landmark example of how ecosystem service assessment can be made feasible. Ultimately, this project meets the Greenbelt Program's need to report the value of land protection beyond acreage.

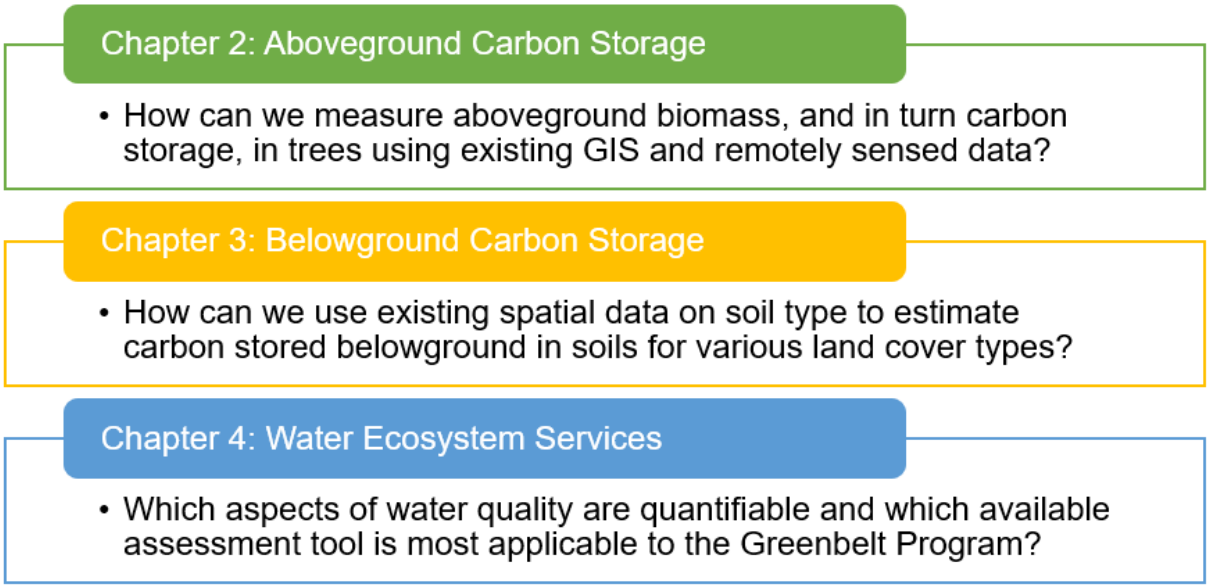

Figure 1.3. Chapter Overview and Key Research Questions

Literature Cited

Barnes, B. V. (2004). *Michigan trees, revised and updated: a guide to the trees of the Great Lakes region*. University of Michigan Press.

Brander, L. M., Florax, R. J., & Vermaat, J. E. (2006). The empirics of wetland valuation: a comprehensive summary and a meta-analysis of the literature. *Environmental and Resource Economics, 33*(2), 223-250. https://doi.org/10.1007/s10640-005-3104-4

Cardinale, B., Prinack, R., & Murdoch, J. (2019). Biodiversity and Ecosystem Services. In *Conservation Biology*, Sinauer Associates.

City of Ann Arbor (2021). *Application Process*. https://www.a2gov.org/greenbelt/Pages/ApplicationProcess.aspx

City of Ann Arbor. (2021). *Greenbelt*. https://www.a2gov.org/greenbelt/Pages/greenbelthome.aspx

Costanza, R., d'Arge, R., De Groot, R., Farber, S., Grasso, M., Hannon, B., ... & Van Den Belt, M. (1997). The value of the world's ecosystem services and natural capital. *Nature, 387*(6630), 253-260.

Federal Geographic Data Committee. (2013). Classification of wetlands and deepwater habitats of the United States. FGDC-STD-004-2013. Second Edition. Wetlands Subcommittee, Federal Geographic Data Committee and U.S. Fish and Wildlife Service, Washington, DC.

Feng, M., Liu, S., Euliss Jr, N. H., Young, C., & Mushet, D. M. (2011). Prototyping an online wetland ecosystem services model using open model sharing standards. *Environmental Modelling & Software, 26*(4), 458-468. https://doi.org/10.1016/j.envsoft.2010.10.008

Hungate, B. A., Barbier, E. B., Ando, A. W., Marks, S. P., Reich, P. B., Van Gestel, N., ... & Cardinale, B. J. (2017). The economic value of grassland species for carbon storage. *Science Advances, 3*(4), e1601880.

Karabulut, A., Egoh, B. N., Lanzanova, D., Grizzetti, B., Bidoglio, G., Pagliero, L., ... & Mubareka, S. (2016). Mapping water provisioning services to support the ecosystem–water–food–energy nexus in the Danube river basin. *Ecosystem Services, 17*, 278-292.

Knight, A. T., Cowling, R. M., Rouget, M., Balmford, A., Lombard, A. T., & Campbell, B. M. (2008). Knowing but not doing: selecting priority conservation areas and the research–implementation gap. *Conservation Biology, 22*(3), 610-617. https://doi.org/10.1111/j.1523-1739.2008.00914.x

Land Trust Alliance. (2015). 2015 National Land Trust Census Report [PDF file]. http://s3.amazonaws.com/landtrustalliance.org/2015NationalLandTrustCensusReport.pdf

Leemans, R., & De Groot, R. S. (2003). Millennium Ecosystem Assessment: Ecosystems and human well-being: a framework for assessment.

Open Space and Parkland Preservation Ordinance, 42 § 3 (2004).

Pandeya, B., Buytaert, W., Zulkafli, Z., Karpouzoglou, T., Mao, F., & Hannah, D. M. (2016). A comparative analysis of ecosystem services valuation approaches for application at the local scale and in data scarce regions. *Ecosystem Services, 22*, 250-259. https://doi.org/10.1016/j.ecoser.2016.10.015

Schulp, C. J., Nabuurs, G. J., Verburg, P. H., & de Waal, R. W. (2008). Effect of tree species on carbon stocks in forest floor and mineral soil and implications for soil carbon inventories. *Forest Ecology and Management, 256*(3), 482-490. https://doi.org/10.1016/j.foreco.2008.05.007

Summers, J. K., Smith, L. M., Case, J. L., & Linthurst, R. A. (2012). A review of the elements of human well-being with an emphasis on the contribution of ecosystem services. *Ambio, 41*(4), 327-340. https://doi.org/10.1007/s13280-012-0256-7

The Conservation Fund. (2019). City of Ann Arbor Greenbelt Program: Strategic Plan. Revised 2019. [PDF file]. Retrieved from https://www.a2gov.org/greenbelt/Pages/greenbelthome.aspx

Villa, F., Bagstad, K. J., Voigt, B., Johnson, G. W., Portela, R., Honzák, M., & Batker, D. (2014). A methodology for adaptable and robust ecosystem services assessment. *PloS One, 9*(3), e91001. https://doi.org/10.1371/journal.pone.0091001

Chapter 2:

Aboveground Carbon Storage: Alternative Methods for Measuring Biomass in Practice

Relevant Appendices
Appendix A: Maps of Field Sample Plot Locations
Appendix B: Field Data
Appendix C: Summary of Aboveground Carbon Storage by Property

Introduction

Well informed and sustainable land use planning and prioritization require knowledge of ecosystem services and how they are affected by different land use decisions. The need for more accessible and feasible ecosystem service assessments is critical to the future of land protection efforts, especially when conservation funds are limited. Capacity-limited organizations, including non-profits, city governments, and even private landowners, lack the resources to accurately assess carbon storage and other ecosystem service metrics necessary for financing conservation efforts.

Here, we use the City of Ann Arbor Greenbelt Program as a case study to develop a model for estimating aboveground carbon storage with minimal fieldwork. The Greenbelt Program was developed in 2003 to preserve and protect open space, farmland, and natural habitats. The Greenbelt District contains 33,524 acres of forested land, and over 1,000 acres of this have been protected with conservation easements. As the Greenbelt Program continues to expand, there is a growing desire to improve the City's ability to assess and communicate the value of the Greenbelt Program. Quantifying the carbon stored via conservation easements would allow the City of Ann Arbor Greenbelt Program to meet their goals laid out in the City's A2Zero Carbon Neutrality Plan, which aims to divert 2.1 million metric tons of CO_2 equivalent annually (A2Zero, 2020).

The purpose of this chapter is to determine the best model for predicting aboveground biomass and, in turn, carbon storage using a limited amount of field data together with existing remote sensing data. In this study, we compare four modeling techniques - Ordinary Least Squares (OLS) Regression, Power Law, Random Forest (RF), and Support Vector Regression (SVR) - for estimating biomass at the plot level. We assess each of these models' statistical significance to determine which model type is best suited for estimating biomass and which set of predictor variables is best for predicting biomass at three study sites. Finally, we use the best model to estimate the total amount of biomass for all Greenbelt properties and thus the carbon stored. Figure 2.1 provides an overview of the process we used to build a model that would allow for this large-scale aboveground carbon estimation using minimal field data combined with LiDAR data.

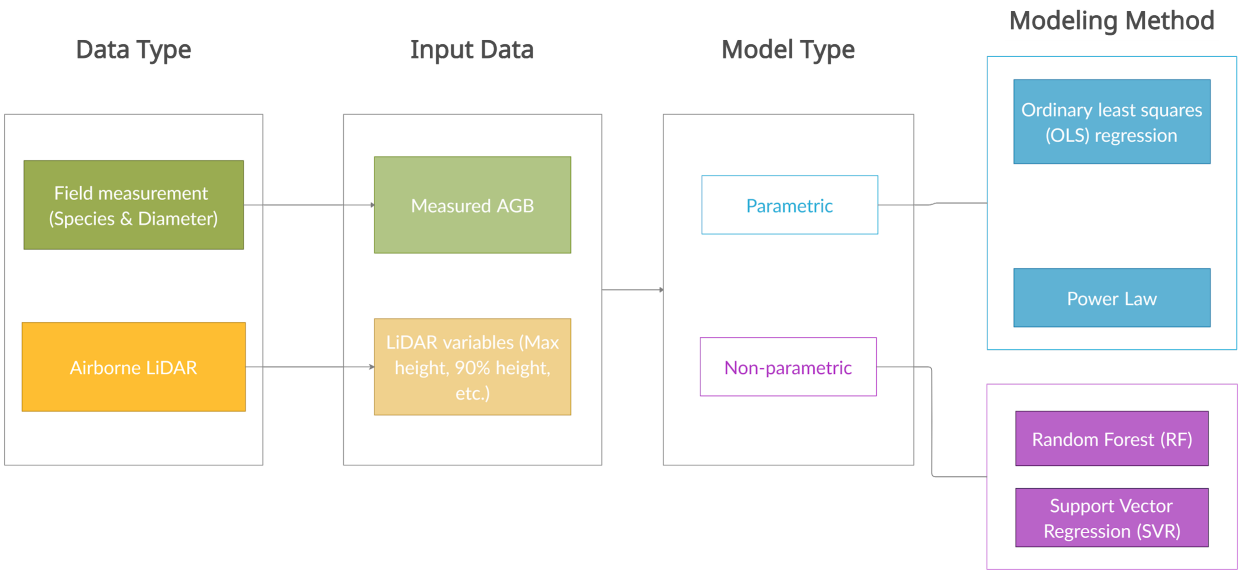

Figure 2.1. Process of using a combination of field and LiDAR data to inform a model to estimate above ground carbon on a large scale. AGB = Aboveground biomass.

I. Traditional Methods of Measuring Aboveground Carbon Storage

Aboveground carbon storage can be calculated from field-based measures of biomass. The aboveground biomass of a tree is defined as the weight of the portion of the tree found above the ground surface when oven-dried (Jenkins et al., 2003). It is also equal to the amount of tree volume multiplied by wood density specific to the tree species type (Ali et al., 2015). Plot-level biomass measures are usually expressed on a per-unit-area basis, such as kg/m^2, and calculated as the sum of biomass values for individual trees in a plot (Jenkins et al., 2003). It is widely assumed that the carbon content of a tree is 50% of its biomass. Once the biomass is known, carbon content can easily be calculated by multiplying by a factor of 0.5 (Fang et al., 2001).

Biomass can be measured by taking measurements of individual tree diameters in the field and applying allometric regression equations based on tree species. “Allometric” refers to size-correlated variations in organic form and metabolism (Niklas, 1994). There is an allometric relationship between plant dimensions, such as diameter and height, and biomass for groups of similar species (Jenkins et al., 2003), thus making it possible to estimate the biomass of a tree given its species and diameter. Historically, allometric equations were site-specific and inconsistent, making them unsuitable for large-scale forest carbon estimation. Jenkins et al. (2003) reviewed existing diameter-based allometric equations and developed a new series of equations that could be applied across regional boundaries. They developed ten sets of parameters and equations for estimating total aboveground biomass of hardwood and softwood species in the United States, of which at least four can be found across the Greenbelt.

Although field-based estimates of biomass using allometric equations have a long history in forestry operations worldwide (Goetz et al., 2009), measuring tree species and diameter on

the ground is time-consuming and labor-intensive. Estimating biomass over large areas requires a dense network of inventory plots, which is infeasible in many regions due to high costs and required labor (Fassnacht et al., 2014). For this reason, there is growing interest in estimating forest biomass using novel remote sensing approaches.

II. Remote Sensing Approaches to Measuring Biomass

Although aboveground biomass is traditionally estimated based on measurements collected on the ground, more recent studies have incorporated remotely sensed data into biomass estimations. Advantages of using remotely sensed data as opposed to data collected on the ground include the ability to measure all areas within the forest of interest, the speed of collecting and processing data, and the ability to collect data in areas that are difficult to access on the ground (Bortolot & Wynne, 2005).

Remote sensing methods vary by platform type (airborne or spaceborne) and sensor type (optical, radar, and LiDAR) (Zolkos et al., 2013). Remote sensors generally fit into two categories, passive and active, which have both been used in biomass estimation. Passive optical sensors measure the reflected or emitted electromagnetic radiation from the Sun. Alternatively, active sensors detect reflected responses from artificially generated energy sources, such as photons in LiDAR (light detection and ranging) and microwave energy in radar (radio detection and ranging) (Shugart et al., 2010).

Passive remote sensors are helpful in the acquisition of imagery at high spatial and temporal resolution, but only active remote sensors can provide three-dimensional data that is necessary for estimating biomass. Landsat Thematic Mapper (TM) is one type of passive remote sensing data type that can provide reasonable estimations of secondary forest biomass, but it results in large uncertainty for mature forests with high biomass density (Lu et al., 2012). The reflectance of forested land cover mostly originates from reflections of sunlight in the topmost part of the canopy (Fassnacht et al., 2014). In dense forest canopies, spectral signatures become insensitive due to the complexity of stand structure. Lu et al. (2012) found that biomass density of greater than 150 T/ha, such as that found in the Brazilian Amazon, could not be accurately predicted by optical/passive remote sensing alone. In other words, passive sensors cannot provide information about the vertical structure of a forest because only the upper canopy is represented. Because active sensors penetrate into vegetation canopies, they are more sensitive to forest structure than passive sensors (Koch, 2010). Since vertical structure relates to tree heights, and height directly relates to biomass and therefore carbon stored, remote sensing that captures structure information can provide a better assessment of carbon storage.

III. Use of LiDAR Data to Measure Biomass

Zolkos et al. (2013) found that LiDAR-based models are significantly better at predicting biomass than models that use passive optical metrics alone. One of the earliest attempts at using LiDAR to predict forest stand structure was completed by Maclean and Krabill (1986). They were able to explain 92% of the variation in timber volume using LiDAR data in addition to tree species composition for a pine forest in the southeastern United States (Lefsky et al.,

2005). In a LiDAR system, a short pulse of laser light is emitted from an aircraft. When the laser pulse reaches the forest canopy, a portion of the pulse is reflected back to the aircraft. The remaining energy proceeds through the canopy and is reflected off the forest floor. The time interval between the initial return from the tree canopy and the secondary return from the forest floor can be converted to a height measurement using the speed of light (Maclean & Krabill, 1986). It is important to note that no sensor can directly measure biomass (Fassnacht et al., 2014). Moreover, no single sensor, regardless of whether it is passive or active, can be expected to provide consistently infallible estimates of biomass (Goetz et al., 2009). Recent research has aimed to extract descriptive variables from LiDAR and apply machine learning approaches to estimate biomass (García-Gutiérrez et al., 2015). LiDAR-derived height percentiles have been shown to be effective at estimating biomass, however, for the majority of studies commonalities between reported predictor variables are rare, suggesting that predictor variables are likely to be study- and site-specific (Lim & Treitz, 2004).

Overview of Model Types

Methods to predict biomass from LiDAR data have evolved rapidly due to improvements in LiDAR technology and the development of statistical models that use automated tree crown delineation and machine learning (Koch, 2010; Gleason & Im, 2012; Fassnacht et al., 2014). Regression approaches for forest attribute estimations using LiDAR data can generally be divided into two groups: parametric and non-parametric. Linear regression models are parametric approaches that define linear relationships between forest variables such as tree height and volume (Shataee, 2013). Though linear regressions are by far the most common prediction method (Fassnacht et al., 2014), they often do not have the ability to characterize forest complexity at fine spatial scales or in mixed forest types (Shataee, 2013). Non-parametric machine learning techniques include decision tree algorithms such as Random Forest (RF) and statistical learning theory-based algorithms, such as Support Vector Regression (SVR). Each parametric and non-parametric approach has advantages and disadvantages and model effectiveness can vary by site and spatial scale. Here we first review these approaches and then test their effectiveness specifically using the field and LiDAR data we acquired to be able to estimate carbon on Greenbelt properties.

1. Ordinary Least Squares (OLS) Regression

Ordinary Least Squares (OLS) Regression has been widely used for LiDAR biomass estimation due to its simplicity (García-Gutiérrez et al., 2015). Linear models have several disadvantages, however. They are less flexible than non-parametric models, are affected by multicollinearity, are less versatile in identifying complex nonlinear relationships, and struggle to deal with high data dimensionality (Almeida et al., 2019). In addition, OLS cannot produce robust predictions if the assumptions of linearity, independence, homoscedasticity, and normality are not met (Osborne & Waters, 2002).

Despite the limitations of linear regression models, several studies have found success in estimating carbon storage using this method. For instance, Means et al. (1999) used a linear regression model that explained 96% of the variation in aboveground biomass from mean

canopy height derived from LiDAR returns in coniferous forests in the Pacific Northwest. Popescu (2007) developed a model for loblolly pine stands in the southeastern United States that explained 88% of the variation in biomass calculated with LiDAR-estimated diameter at breast height (DBH). Almeida et al. (2019) compared different linear models for estimating biomass in the Brazilian Amazon and found that a linear model with regularization (a way of shrinking the coefficients of redundant predictor variables) could solve the issue of multicollinearity.

There are a myriad of different variations of linear models that have been used to estimate above-ground biomass. Salas et al. (2010) compared the effectiveness of ordinary least squares (OLS), generalized least squares (GLS) with a non-null correlation structure, linear mixed-effects (LME), and geographically weighted regression (GWR). They found that root mean square prediction errors with LME were the lowest, followed by GWR, then by OLS and GLS. The advantages of mixed-effects models are their flexibility in modeling when modeling covariates are grouped by one or more classification factors. Pinheiro and Bates (2006) discuss their advantages and applications in great detail. However, mixed-effects models are not applicable at the plot level as there are no well-defined groups within which the random effects structure can vary (Gleason & Im, 2012).

A common problem with linear models is that the relationship between predicted and measured biomass differs strongly between sites (Foody et al., 2003). Furthermore, linear regression rarely fully captures the complex relationships between forest variables (Chen & Hay, 2011). Linear models are also less flexible than nonparametric techniques because they demand large sample sizes and are affected by multicollinearity (Li et al., 2014). Nonparametric machine learning techniques, such as Support Vector Regression (SVR), Random Forest (RF), and Cubist, are more versatile than linear regression models in identifying complex nonlinear relationships (Almeida et al., 2019).

2. *Power Law (PL)*

Power Law, or log linear, models in the form of $y = ax^b$ are one of the most common patterns in biology (Xiao et al., 2011). Because in situ field biomass estimations through allometric models are based on a Power Law relationship between tree diameter and biomass, it should be expected that tree diameter and biomass are nonlinearly related to tree height (Lu et al., 2016). While Power Law models have been found to successfully predict biomass in predominantly coniferous Scandinavian forests (Næsset, 1997; Næsset et al., 2011), they have been shown to produce inaccurate biomass estimations in the United States and Canada. For example, Nelson et al. (2017) found that, compared to existing national forest inventory plots, linear models overestimated in situ biomass by 7.5%, whereas a Power model overestimated ground results by 261%.

Power Law models however have shown to be more effective than simple ordinary least squares regression models, in some cases yielding R^2 values between 0.76 and 0.89 compared to OLS R^2 values ranging from 0.03 to 0.28 (Næsset et al., 2011). Other studies have also explained the majority of the variance between LiDAR-derived covariates and predicted biomass with Power Law models with R^2 values equal to 0.63 (Ws et al., 2017) and 0.64 (Vaglio Laurin et al., 2014).

3. *Random Forest (RF)*

Random Forest (RF) is a non-parametric modeling approach that is relatively robust to outliers and noise (Breiman, 2001). RF models randomly and iteratively sample the data to generate a large group of classification and regression trees (Hudak et al., 2008). A *random forest* is made up of *decision trees*, which perform the task of aggregation or regression by recursively asking true or false questions that split the data into subgroups. Instead of building only one decision tree for prediction, the idea behind RF is to combine many trees into a robust ensemble, or "forest" (Kern et al., 2019). To make a prediction, each decision tree "votes" by making its own prediction and the average over all trees becomes the output of the RF. The prediction of many models is more likely to be correct than the prediction of any single model. Because decision trees "disagree" on what the predictions are, the forest is shielded from the errors of individual trees. An example of what decision trees look like is shown below in Figure 2.2.

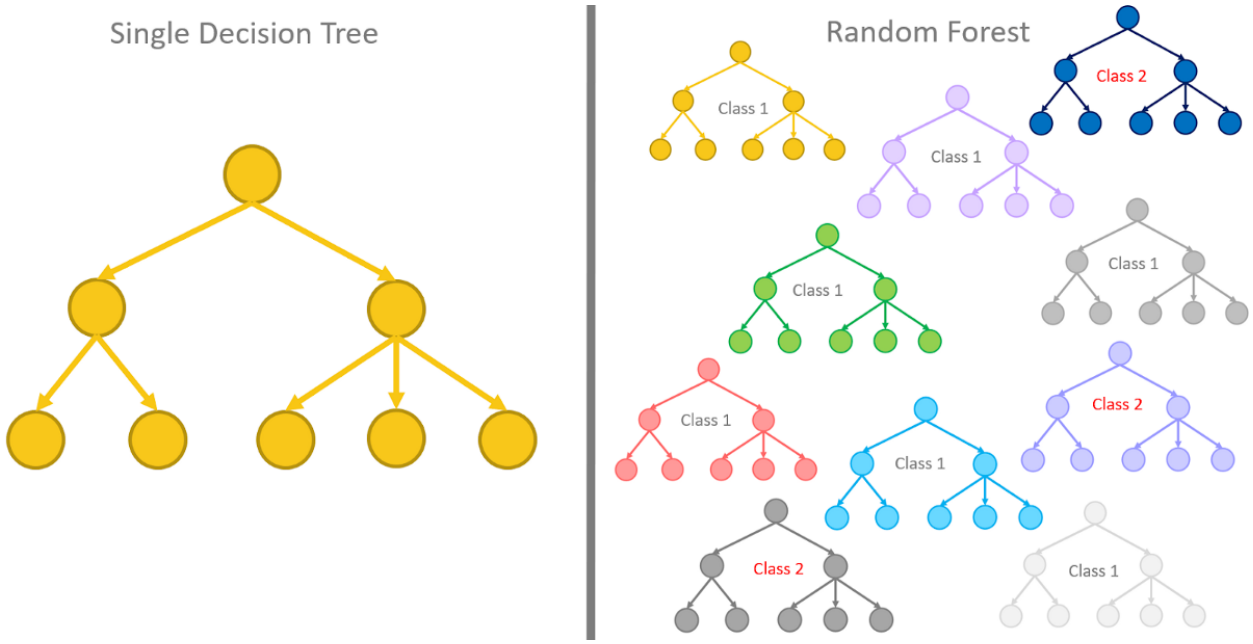

Figure 2.2. Decision Trees in a Random Forest algorithm. Sourced from Silipo (2019).

RF models have been shown to reduce bias and overfitting. Random forests do not overfit as more trees are added, because the average will always converge according to the mathematical law of large numbers (Breiman, 2001). Different LiDAR metrics can be objectively selected for predicting the response variables, helping to prevent arbitrary decisions in which predictor variables to use. Hudak et al. (2012) ran a Model Improvement Ratio (MIR) function to objectively choose the most important LiDAR metrics. Their function selected from 62 LiDAR metrics including mean height, maximum height, various percentiles of height, intensity, and slope, excluding highly correlated predictor variables (Pearson's $r > 0.9$). This model was used to observe changes in biomass due to forest growth over a six-year period.

Many studies have found RF models to be the best at capturing non-linear relationships between remote sensing data and biomass density. Powell et al. (2010) found RF to be the most accurate model for predicting biomass change using Landsat data at locations in Arizona and Minnesota, in comparison to other non-parametric model types. Avitabile et al. (2012) compared a RF model with a single regression tree model and a multilinear regression model for a low-biomass density forest in Uganda and found that the variance explained by RF was 14-17% higher than that explained by a single tree model. Mascaro et al. (2014) tested the effect of incorporating spatial context into a RF model for a heterogeneous region of Northern Peru. The RF model with spatial context explained 59% of LiDAR-based carbon estimates, compared to 37% for a traditional stratified sampling and upscaling (non-machine learning) model and 43% for a RF model without spatial context.

RF has both advantages and disadvantages over other models. RF has also been shown to produce more stable predictions than the other model types (Gleason & Im, 2012). However, at small sample sizes, RF explains a smaller proportion of the variation at both plot and individual tree levels than other model types, including SVR, linear regression, and Cubist. Additionally, RF models are known to increase spatial autocorrelation among the model residuals and, in some cases, actually overfit to spatial data, even though they are theoretically less prone to overfitting (Mascaro et al., 2014).

4. Support Vector Regression (SVR)

Support vector machines (SVM) are not as well-known as other classifiers in the remote sensing community, but are becoming more popular due to their ability to match or even exceed the performance of more established methods (Mountrakis et al., 2011). Support vector regression (SVR) is a regression technique that uses a SVM algorithm. This method solves binary classification problems by transforming a nonlinear regression problem into a linear one by using kernel functions that map the original input space into a new, multidimensional feature space (Chen & Hay, 2011). SVR assumes that each set of input parameters (canopy volume, maximum height, crown geometric volume, etc.) will have a unique relation to its response variable (biomass). The groupings and relations of these predictors to one another is sufficient to identify rules for predicting biomass (Gleason & Im, 2012).

A SVR algorithm aims to find a *hyperplane* that separates the data into a discrete number of classes. *Support vector* refers to the points that lie on the margin, which are used to define the hyperplane. The optimal hyperplane will have a decision boundary that minimizes misclassifications (Mountrakis et al., 2011). To achieve this, the algorithm finds the maximum margin separating the hyperplane while correctly classifying as any training points as possible (Awad & Khanna, 2015). Each response variable is plotted in a multidimensional feature space with axes that represent each input variable, as shown in Figure 2.3. As a supervised learning technique, SVR iteratively assigns hyperplanes in the data and adjusts them to minimize errors (Gleason & Im, 2012).

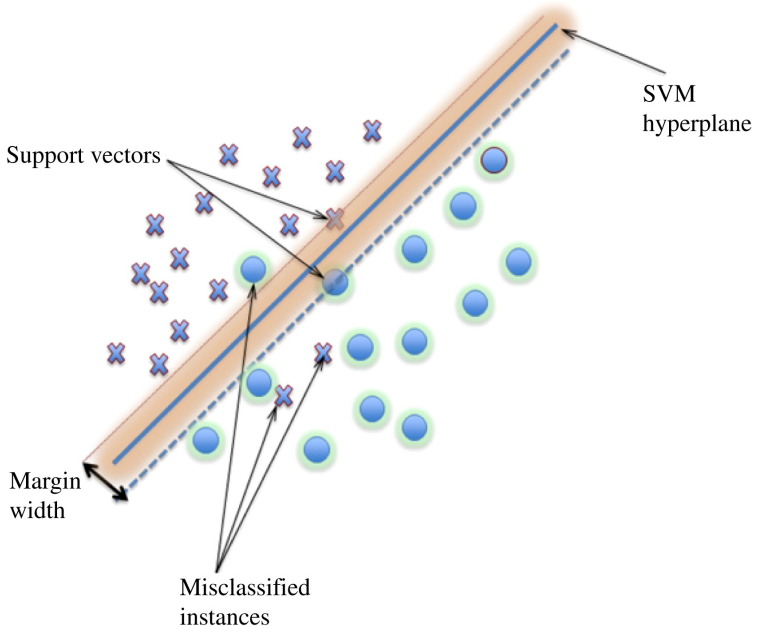

Figure 2.3. Linear support vector machine example. Sourced from Mountrakis et al. (2011)

SVR is among the most common machine learning regression techniques recently published in the literature (García-Gutiérrez et al., 2015). Chen and Hay (2011) used SVR to estimate canopy height, aboveground biomass, and volume from LiDAR data and multispectral QuickBird imagery for a predominantly coniferous forest in British Columbia, Canada. The use of SVR dramatically improved height estimation performance for both coniferous and deciduous trees in comparison to multilinear regression. They found a strong relationship between predicted and field-estimated canopy height, and were able to explain 81% of the variation. Gleason and Im (2012) also found that SVR explained the largest fraction of the variation when estimating biomass at the plot level, when compared to linear mixed-effects (LME) regression, RF, and Cubist.

A major advantage of SVR is its ability to generalize well, even with limited training samples (Mountrakis et al., 2011). Despite having only 18 plots available for plot level estimation, Gleason and Im (2012) produced a SVR model with an R^2 value of 0.93, in comparison to their RF model with an R^2 value of 0.22. They also compared RF and SVR at the individual tree level and found better results with a SVR model. An underlying principle of SVR is structural risk minimization, in which the algorithm minimizes classification error on unseen data without making prior assumptions on the data's probability distribution (Mountrakis et al., 2011). Li et al. (2014) and García-Gutiérrez et al. (2015) also found that SVMs statistically outperformed all other models they tested.

A potential disadvantage of SVR is that it can lead to less stable predictions of biomass than RF. Both RF and SVR models contain some degree of randomness, resulting in a different biomass model each time they are applied to the same data. Gleason and Im (2012) found the standard deviation of root mean square errors (RMSEs) were smaller for RF (up to 16.64 kg) than for SVR (up to 109 kg). Out of the 17 models tested by García-Gutiérrez et al. (2015), SVR had the highest maximum RMSE (91.224%) and the highest mean RMSE (91.981%).

Methods

We compared the ability of the four modeling techniques reviewed above to estimate biomass at the plot level using limited field data together with existing remote sensing data.

I. Study sites

Three sites in Washtenaw County, Michigan, were selected for field data collection: Scio Woods Preserve, Brauer Preserve, and Creekshead Preserve. Scio Woods Preserve is a 91-acre property owned and operated by the Washtenaw County Parks and Recreation Commission and was purchased with financial support from the Greenbelt Program in 2008. It contains oak-hickory forest in areas with drier soils and beech-sugar maple forest in areas with wetter soils. Brauer Preserve is an 85-acre property operated by Washtenaw County. Upland forest types include dry-mesic and dry Southern forest and wetland types include Southern swamp, marsh, and open water. Creekshead Nature Preserve is a 27-acre property located 12 miles north of Ann Arbor, owned and managed by Legacy Land Conservancy, a nonprofit land conservation organization in Southern Michigan. Creekshead Preserve consists of mature beech-maple-basswood forest. A summary of the three sampling locations can be found below in Table 2.1.

Table 2.1. Summary of sample plots

	Scio Woods Preserve	**Brauer Preserve**	**Creekshead Preserve**
Location	42.2559°N, 83.8081°W	42.2374°N, 83.8964°W	42.3816°N, 83.6072°W
Number of plots	33	24	12
Number of trees measured	138	77	66
Mean DBH (cm)	26.4	33.3	25.7
Std dev DBH (cm)	13.8	19.1	14.4
*Basal area (m^2/ha)	29.07	36.93	37.38
Mean plot biomass (kg)	2524.39	3565.98	2846.70
Std dev plot biomass (kg)	1736.07	3206.99	1705.95
Species	Sugar maple, American basswood, white oak, pignut hickory, hop-hornbeam, bitternut hickory, black cherry, shagbark hickory, American beech, black walnut, tuliptree, Northern red oak, Eastern cottonwood, white willow, Ailanthus	Silver maple, red maple, American elm, black cherry, black oak, bur oak, sugar maple, Northern red oak, bigtooth aspen, black walnut, American ash	Sugar maple, American basswood, American beech, bur oak, red maple, Northern red oak, bitternut hickory, black maple, silver maple

* Basal area was calculated including the three plots at Scio Woods and three plots at Brauer which had no trees greater than 10cm DBH, resulting in lower values of basal area than if these plots were removed

II. Field Data Collection

A total of 69 field plots of 10 m x 10 m were established at the three sites (33 at Scio, 24 at Brauer, and 12 at Creekshead) between September and November 2020. For each site, random plot locations were generated and then superimposed on leaf-on NearMap imagery. Plot locations were randomly placed using the Create Random Points tool in ArcGIS Pro. Maps of the field sites were exported as PDFs and uploaded to the Avenza Maps app and used along with a handheld compass and Trimble R1 unit to navigate to plot locations in the field. Each random point was marked as the southwest corner of the plot, and the square plot extended 10 meters True North and 10 meters East. These maps can be found in Appendix A.

Data collected included tree species, tree stem diameter at breast height (DBH) measured at 4.5 feet above the ground, and relative crown position (understory vs. overstory). Standard DBH measuring protocols were followed according to standards described by West (2015). Over the 69 plots, measurements of a total of 281 live trees with a minimum DBH of 10 c.m. from 23 species (Table 2.2). Three out of 33 plots at Scio Woods and three out of 24 plots at Brauer Preserve contained no live trees greater than 10 c.m. in DBH and were excluded from biomass calculations due to concerns that plots containing 0 kg of tree biomass would lead to arbitrary underestimates of biomass. An additional plot located in Scio Woods was also thrown out due to questionable GPS accuracy. Field-collected tree data are listed in Appendix B.

Table 2.2. Tree species of field plots

Scientific Name	Common Name	*Species Group	**Tree Count by Site	Total Tree Count
Acer nigrum	Black maple	MO	0, 0, 1	1
Acer rubrum	Red maple	MB	0, 12, 7	19
Acer saccharinum	Silver maple	MB	0, 36, 1	37
Acer saccharum	Sugar maple	MO	63, 2, 20	85
Ailanthus altissima	Ailanthus	MH	1, 0, 0	1
Carya cordiformis	Bitternut hickory	MO	5, 0, 2	7
Carya glabra	Pignut hickory	MO	7, 0, 0	7
Carya ovata	Shagbark hickory	MO	4, 0, 0	4
Fagus grandifolia	American beech	MO	3, 0, 10	13
Fraxinus americana	White ash	MH	0, 1, 0	1
Juglans nigra	Black walnut	MH	3, 1, 0	4
Liriodendron tulipifera	Tuliptree	MH	3, 0, 0	3
Ostrya virginiana	Hop-hornbeam	MH	7, 0, 0	7
Populus deltoides	Eastern cottonwood	AA	2, 0, 0	2
Populus grandidentata	Bigtooth aspen	AA	0, 1, 0	1
Prunus serotina	Black cherry	MH	5, 6, 0	11
Quercus alba	White oak	MO	14, 0, 0	14
Quercus macrocarpa	Bur oak	MO	0, 2, 7	9
Quercus rubra	Northern red oak	MO	3, 1, 4	8
Quercus velutina	Black oak	MO	0, 4, 0	4
Salix alba	White willow	AA	2, 0, 0	2
Tilia americana	American basswood	MH	16, 0, 14	30
Ulmus americana	American elm	MH	0, 11, 0	11

*Species groups include aspen/cottonwood/willow (AA), soft maple/birch (MB), mixed hardwood (MH), and hard maple/oak/hickory/beech (MO) (Jenkins et al., 2003)

**Tree count in order of Scio Woods Preserve, Brauer Preserve, Creekshead Preserve

The aboveground biomass of individual trees based on species group and DBH was estimated using the following equation (Jenkins et al., 2003):

$$biomass = Exp(\beta_0 + \beta_1 \ln DBH)$$

where

biomass = total aboveground biomass (kg) for trees 10 c.m. DBH and larger
DBH = diameter at breast height (c.m.)
Exp = exponential function
ln = natural log base “e” (2.718282)

The β coefficients from the above equation are found in Table 2.3.

Table 2.3. Parameters for biomass equations

Species Group	β_0 Parameter	β_1 Parameter
Aspen/alder/cottonwood/willow (AA)	-2.2094	2.3867
Soft maple/birch (MB)	-1.9123	2.3651
Mixed hardwood (MH)	-2.4800	2.4835
Hard maple/oak/hickory/beach (MO)	-2.0127	2.4342

Species groups and parameters found in Jenkins et al. (2003)

III. LiDAR Data Acquisition

LiDAR data was acquired from the University of Michigan Biological Station which was acquired from the Southeast Michigan Council of Governments (SEMCOG) flight of Washtenaw County in 2017. Each LAS tile used covers an area measuring 2,500 feet by 2,500 feet and contains the point clouds for each laser pulse that is returned to the LiDAR sensor. The density of LiDAR returns varies depending on forest density. For example, an area that is mostly cropland and forest has 2,220,767 total LiDAR returns per tile and a point density of 3.82 points/m^2. Meanwhile, an area of the same size at Stinchfield Woods, which is more densely forested, has a total of 5,016,515 LiDAR returns and a point density of 8.64 points/m^2.

IV. Canopy Height Model Creation

Canopy height models were created in R version 4.0.3. LiDAR returns were processed into canopy height models with the lidR package using the pit-free canopy height algorithm proposed by Khosravipour et al. (2014). Inverse distance weighting was used to normalize all canopy height models and a Gaussian filter was applied to remove spurious points, using a moving window with a radius of 2 feet. All resulting canopy height models had a spatial resolution of 0.25 feet (0.075 meters) and all subsequent analysis was conducted in the Michigan State Plane projected coordinate system.

V. Model and Predictor Variable Selection

Choosing appropriate predictor variables from LiDAR-derived forest measurements that are correlated with aboveground forest biomass is necessary to create a parsimonious model for biomass estimation (Gleason & Im, 2012). In this study, several LiDAR-derived predictor variables were explored that were assumed to be correlated with biomass. Predictor variables were obtained from Gleason and Im and expanded upon, resulting in a list of predictor variables that included the maximum and minimum pixel height values within each plot, as well as the LiDAR-derived height percentiles (10th, 20th, 30th, 40th, 50th, 60th, 70th, 80th, and 90th) for each plot.

We considered four models including Ordinary Least Squares Regression (OLS), Power Law (PL), Random Forest (RF), and Support Vector Regression (SVR). For the parametric models, the optimal model was chosen by which combination of predictor variables yielded the model with the lowest Akaike information criterion (AIC) value. For the PL model, only height percentiles above the 40th percentile were considered to avoid log transforming height percentiles that were equal to zero. Because AIC values are not applicable for non-parametric machine learning models, predictor variables for RF and SVR were selected using a RF classifier which has been found in other studies to provide valuable insight regarding the discriminative ability of individual predictor variables (Archer & Kimes, 2008). Ranked predictor variable importance were, in descending order, Maximum Height, Minimum Height, 90th percentile, 10th percentile, 20th percentile, 50th percentile, 30th percentile, 80th percentile, 40th percentile, 60th percentile, and lastly the 70th percentile. Predictor variables were then added in order of ranked importance to the model until the addition of additional predictor variables resulted in a model with poorer model performance (lower cross validated R^2 and Root Mean Squared Error (RMSE)). All resulting predictor variables are shown in Table 2.4.

To measure the accuracy of each model type, a 10-fold cross-validation scheme was used due to the limited available training data. R^2 values and RMSE were calculated for each model type along with the standard error for each model metric. Adjusted R^2 and p-values were also calculated on the entire dataset for each model.

Table 2.4. Displays the predictor variables used in each of the four models. “Maximum Height” refers to the maximum height pixel value of a given plot. “Minimum Height” refers to the minimum height pixel value of a given plot. “Height xth” refers to the xth height percentile for a given plot. For example, “Height 30th” is the 30th height percentile of the pixel distribution of a given plot.

Model Type	Predictor Variables Used	AIC
Ordinary Least Squares (OLS) Regression	Maximum Height, Height 80th, Height 60th, Height 40th, Height 30th	1114.438
Power Law (PL)	Maximum Height, Height 80th, Height 60th, Height 50th	163.4564
Random Forest (RF)	Maximum Height, Height 90th, Height 20th, Height 10th, Minimum Height	NA
Support Vector Regression (SVR)	Maximum Height, Height 10th, Minimum Height	NA

The R code for extracting LiDAR predictor variables and comparing model types can be found at this link: https://github.com/UMGreenbelt/Greenbelt21

VI. Estimating Carbon Storage on Greenbelt Properties

To estimate the biomass of individual properties, a PL model was used to predict the biomass of a given property by creating a biomass raster with a 10-meter by 10-meter pixel size (the same size as our sampled plots). To develop a biomass raster for the entire Greenbelt District, multiple computing machines were necessary. We used Open Storage Research Infrastructure (OSiRIS) to process large amounts of LiDAR data in the form of LAS files. First, we copied LiDAR files covering the entirety of the Greenbelt District over to OSiRIS. Next, we set up jobs to run on the Open Science Grid (OSG). Each tile was analyzed using R version 4.0.4 and the lidR package in R, with one tile per job. Then, each output file was copied back from OSiRIS. Output TIF images were then mosaiced into a single raster in ArcGIS Pro. Any cells of the mosaiced raster that fell outside of a manually digitized forest land cover feature class provided by the City of Ann Arbor were set to equal zero in order to prevent buildings from erroneously contributing to the final biomass calculations. The total biomass of a single property was considered to be the summation of all pixel values that fell within or intersected the digitized property boundary. This was calculated by using the Zonal Statistics as Table tool in ArcGIS Pro. The total carbon storage of a given property was then assumed to be 50% of the total biomass at that property. All biomass estimations for Greenbelt properties can be found in Appendix C.

Results & Discussion

Ordinary Least Squares (OLS) Regression

Of the various model types used in this study, OLS explained the least amount of variation within the dataset and within cross-validated testing datasets, as shown in Table 2.5. Given the clustered nature of the training data, it is expected that OLS would explain a small fraction of the variation as with limited data the assumptions of linear regression, such as independence of observations, are difficult to meet. These results are consistent with several studies such as Baccini et al. (2008) who found that RF explained 11% more of the variation in the data set than OLS. However, many studies have used OLS models to effectively predict biomass (Means et al., 1999; Popescu, 2007; Almeida et al., 2019), and given the simplicity of OLS, it is an attractive option for practitioners to consider. However, in order for OLS to be effective, it is necessary to have independence among observations to produce accurate predictions of biomass, which may be difficult to achieve with clustered field data.

Power Law (PL)

The PL model proved to arguably be the most appropriate model for estimating biomass from the LiDAR-derived predictor variables. It had by far the highest adjusted R^2 and cross-validated R^2 values. The PL model outperformed OLS in almost every metric, proving to

be consistent with the findings of Næsset et al. (2011). However, though the PL model had the highest RMSE of all models, all of the models had relatively the same RMSE and the PL model had the second smallest RMSE standard error between folds. This is an interesting result because studies such as Næsset et al. (2011) created effective PL models in coniferous forests whereas our study took place in primarily deciduous forests. Future research should explore the overall effectiveness of PL models on biomass estimation in forests with varying heterogeneity. Overall, the PL model is a relatively simple model and a very useful tool for practitioners to consider when estimating biomass in similar conditions.

Random Forest (RF)

RF was arguably the second most appropriate model for estimating biomass of the models tested. The RF model was likely affected by the relatively small sample size, and with larger sample size, it could potentially be more suitable than the PL model because even with limited data the RF model yielded the second-lowest RMSE. Our results are consistent with the findings of Gleason and Im (2012) who yielded a slightly lower R^2 of 0.22, though their sample size was even smaller (n=18). Practitioners interested in using RF or other machine learning models would require access to large datasets in order to expect accurate results. While designed to prevent overfitting, as noted by Mascaro et al. (2014), RF models can increase spatial autocorrelation among the model residuals and overfit spatial data. Given our small sample size, this is likely a large contributing factor to the performance of the model.

Support Vector Regression (SVR)

SVR performed similarly to RF, which was surprising given SVR's ability to generalize well with limited training samples (Mountrakis et al., 2011). SVR was arguably the least stable of all model types explored, as it had the highest standard error between folds. SVR is an important model to consider given its success at predicting biomass in other studies such as García-Gutiérrez et al. (2015). Given the results of our study, however, RF is a comparable and arguably better machine learning algorithm to estimate biomass with limited training data in densely forested conditions in Southeast Michigan. It is also important to consider the steep learning curve and the necessity to parameterize the model properly. This alone may make SVR a less appealing choice compared to RF or PL models for practitioners to estimate biomass.

Table 2.5. Displays the Adjusted R^2 values, p-values, 10-fold cross-validated R^2 values (CV R^2), 10-fold cross-validated RMSE (CV RMSE kg of biomass), and the standard error for all cross-validated model metrics for each model type.

Model Metric	Ordinary Least Squares (OLS) Regression	Power Law (PL)	Random Forest (RF)	Support Vector Regression (SVR)
Adj. R^2	0.21	0.43	NA	NA
p-value	0.00	0.00	NA	NA
CV RMSE kg of biomass	2060.99	2452.93	2074.94	2101.89
CV R^2	0.27	0.37	0.28	0.28
CV RMSE Standard Error	50.07	56.33	58.60	61.73
CV R^2 Standard Error	0.02	0.02	0.02	0.02

Conclusion

Overall Model Effectiveness Comparison

As shown in Table 2.5, overall a moderate to low amount of variation was explained from the LiDAR-derived predictor variables and the plot-level forest inventory data that were collected. This is perhaps due to several factors, including but not limited to the fact that three years had passed between the LiDAR flight and when the training data were collected and the limited diversity of the forested properties sampled. Future studies should seek to obtain the most recent and robust airborne LiDAR and field data that was collected at approximately the same time period. Unfortunately, that might not be practical for small land conservancies and poorly funded government agencies. Therefore, these results are within the range of estimation accuracy one should expect if a similar study design is conducted on dense deciduous forests with limited training data in Southeast Michigan. Given these conditions, however, a major conclusion that can be drawn is that the Power Law model arguably proved to be the most appropriate for explaining the relationship between tree height and biomass. All model types produced similar RMSE values and fairly stable predictions of biomass, only varying a few kilograms of biomass between folds. Furthermore, given that the R^2 values standard error between folds varied on average only around 0.02, this suggests that any of the models explored would be able to consistently explain relatively the same amount of variation when presented with plots with similar forest composition to the training data. Overall, our study demonstrates that LiDAR biomass estimation models are worth further exploration to estimate

carbon storage even with suboptimal access to robust LiDAR and field data collection capabilities by practitioners.

Future Recommendations

Our study demonstrates the relative effectiveness of LiDAR biomass estimation in Southeast Michigan and serves as a template for future studies in the region. However, there are several attributes of our experimental design that can be improved upon. First, we only sampled forests that were predominantly composed of maples, oaks, and other hardwoods clustered in three locations. The separation in time from when the LiDAR flight was conducted to when the training data was collected will likely affect the accuracy of our analysis as well. Therefore, it is recommended that future studies collect a more diverse set of training data from various forest types and spatial locations in the area of interest.

Our approach produces estimates that are not as exact as direct field measures and could still be improved upon with additional sampling data to train the model. However, our feasible approach does at the very least provide a reasonable estimate of overall aboveground carbon that can be used for communication purposes of overall carbon storage. We would caution against using this approach being used for the carbon market or for fine scale comparison of properties with very similar values, but as data availability and methods evolve, perhaps that would be feasible in the future.

Literature Cited

A2Zero. (2020). Ann Arbor's Living Carbon Neutrality Plan [PDF file]. https://www.a2gov.org/departments/sustainability/Documents/A2Zero%20Climate%20Action%20Plan%20_3.0.pdf

Ali, I., Greifeneder, F., Stamenkovic, J., Neumann, M., & Notarnicola, C. (2015). Review of machine learning approaches for biomass and soil moisture retrievals from remote sensing data. *Remote Sensing, 7*(12), 16398-16421.

Almeida, C. T. de, Galvão, L. S., Aragão, L. E. de O. C. e, Ometto, J. P. H. B., Jacon, A. D., Pereira, F. R. de S., Sato, L. Y., Lopes, A. P., Graça, P. M. L. de A., Silva, C. V. de J., Ferreira-Ferreira, J., & Longo, M. (2019). Combining LiDAR and hyperspectral data for aboveground biomass modeling in the Brazilian Amazon using different regression algorithms. *Remote Sensing of Environment, 232*, 111323. https://doi.org/10.1016/j.rse.2019.111323

Archer, K. J., & Kimes, R. V. (2008). Empirical characterization of random forest variable importance measures. *Computational statistics & data analysis*, *52*(4), 2249-2260.

Avitabile, V., Baccini, A., Friedl, M. A., & Schmullius, C. (2012). Capabilities and limitations of Landsat and land cover data for aboveground woody biomass estimation of Uganda. *Remote Sensing of Environment, 117*, 366-380. https://doi.org/10.1016/j.rse.2011.10.012

Awad, M., & Khanna, R. (2015). *Support Vector Regression*. In M. Awad & R. Khanna (Eds.), Efficient Learning Machines: Theories, Concepts, and Applications for Engineers and System Designers. Apress. https://doi.org/10.1007/978-1-4302-5990-9_4

Baccini, A., Laporte, N., Goetz, S. J., Sun, M., & Dong, H. (2008). A first map of tropical Africa's above-ground biomass derived from satellite imagery. *Environmental Research Letters, 3*(4), 045011. https://doi.org/10.1088/1748-9326/3/4/045011

Bortolot, Z. J., and Wynne, R. H. (2005). Estimating Forest Biomass Using Small Footprint LiDAR Data: An Individual Tree-Based Approach That Incorporates Training Data. *ISPRS Journal of Photogrammetry and Remote Sensing 59*(6), 342-60. https://doi.org/10.1016/j.isprsjprs.2005.07.001

Breiman, L. (2001). Random Forests. *Machine Learning 45*(1), 5-32. https://doi.org/10.1023/A:1010933404324

Chen, G., & Hay, G. J. (2011). A support vector regression approach to estimate forest biophysical parameters at the object level using airborne lidar transects and quick bird data. *Photogrammetric Engineering and Remote Sensing, 77*(7), 733-741. https://doi.org/10.14358/PERS.77.7.733

Fang, J., Chen, A., Peng, C., Zhao, S., & Ci, L. (2001). Changes in Forest Biomass Carbon Storage in China Between 1949 and 1998. *Science, 292*(5525), 2320-2322. https://doi.org/10.1126/science.1058629

Fassnacht, F. E., Hartig, F., Latifi, H., Berger, C., Hernández, J., Corvalán, P., & Koch, B. (2014). Importance of sample size, data type and prediction method for remote sensing-based

estimations of aboveground forest biomass. *Remote Sensing of Environment, 154*, 102-114. https://doi.org/10.1016/j.rse.2014.07.028

Foody, G. M., D. S. Boyd, & M. E. J. Cutler. (2003). Predictive Relations of Tropical Forest Biomass from Landsat TM Data and Their Transferability between Regions. *Remote Sensing of Environment 85*(4), 463-74. https://doi.org/10.1016/S0034-4257(03)00039-7

García-Gutiérrez, J., Martínez-Álvarez, F., Troncoso, A., & Riquelme, J. C. (2015). A comparison of machine learning regression techniques for LiDAR-derived estimation of forest variables. *Neurocomputing, 167*, 24-31. https://doi.org/10.1016/j.neucom.2014.09.091

Gleason, C. J., & Im, J. (2012). Forest biomass estimation from airborne LiDAR data using machine learning approaches. *Remote Sensing of Environment, 125*, 80-91. https://doi.org/10.1016/j.rse.2012.07.006

Goetz, S. J., Baccini, A., Laporte, N. T., Johns, T., Walker, W., Kellndorfer, J., Houghton, R. A., & Sun, M. (2009). Mapping and monitoring carbon stocks with satellite observations: A comparison of methods. *Carbon Balance and Management, 4*(1). https://doi.org/10.1186/1750-0680-4-2

Hudak, A. T., Crookston, N. L., Evans, J. S, Hall, D. E., & Falkowski, M. J. (2008). Nearest Neighbor Imputation of Species-Level, Plot-Scale Forest Structure Attributes from LiDAR Data. *Remote Sensing of Environment 112*(5), 2232-45. https://doi.org/10.1016/j.rse.2007.10.009

Hudak, A. T., Strand, E. K., Vierling, L. A., Byrne, J. C., Eitel, J. U. H., Martinuzzi, S., & Falkowski, M. J. (2012). Quantifying aboveground forest carbon pools and fluxes from repeat LiDAR surveys. *Remote Sensing of Environment, 123*, 25-40. https://doi.org/10.1016/j.rse.2012.02.023

Jenkins, J. C., Chojnacky, D. C., Heath, L. S., & Birdsey, R. A. (2003). National Scale Biomass Estimators for United States Tree Species. *Forest Science, 49*, 12-35.

Kern, C., Klausch, T., & Kreuter, F. (2019). Tree-Based Machine Learning Methods for Survey Research. *Survey Research Methods 13*(1), 73-93.

Khosravipour, A., Skidmore, A. K., Isenburg, M., Wang, T., & Hussin, Y. A. (2014). Generating pit-free canopy height models from airborne lidar. *Photogrammetric Engineering & Remote Sensing*, *80*(9), 863-872.

Koch, B. (2010). Status and future of laser scanning, synthetic aperture radar and hyperspectral remote sensing data for forest biomass assessment. *ISPRS Journal of Photogrammetry and Remote Sensing, 65*(6), 581-590. https://doi.org/10.1016/j.isprsjprs.2010.09.001

Lefsky, M. A., Hudak, A. T., Cohen, W. B., & Acker, S. A. (2005). Geographic variability in lidar predictions of forest stand structure in the Pacific Northwest. *Remote Sensing of Environment, 95*(4), 532-548. https://doi.org/10.1016/j.rse.2005.01.010

Li, M., Im, J., Quackenbush, L. J., & Liu, T. (2014). Forest Biomass and Carbon Stock Quantification Using Airborne LiDAR Data: A Case Study Over Huntington Wildlife

Forest in the Adirondack Park. *IEEE Journal of Selected Topics in Applied Earth Observations and Remote Sensing 7*(7), 3143-56. https://doi.org/10.1109/JSTARS.2014.2304642

Lim, K. S., & Treitz, P. M. (2004). Estimation of above ground forest biomass from airborne discrete return laser scanner data using canopy-based quantile estimators. *Scandinavian Journal of Forest Research, 19*(6), 558-570.

Lu, D., Chen, Q., Wang, G., Liu, L., Li, G., & Moran, E. (2016). A survey of remote sensing-based aboveground biomass estimation methods in forest ecosystems. *International Journal of Digital Earth, 9*(1), 63-105. https://doi.org/10.1080/17538947.2014.990526

Lu, D., Chen, Q., Wang, G., Moran, E., Batistella, M., Zhang, M., Vaglio Laurin, G., & Saah, D. (2012). Aboveground Forest Biomass Estimation with Landsat and LiDAR Data and Uncertainty Analysis of the Estimates. *International Journal of Forestry Research, 2012*, 1-16. https://doi.org/10.1155/2012/436537

Maclean, G. A., & Krabill, W. B. (1986). Gross-Merchantable Timber Volume Estimation Using an Airborne Lidar System. *Canadian Journal of Remote Sensing, 12*(1), 7-18. https://doi.org/10.1080/07038992.1986.10855092

Mascaro, J., Asner, G. P., Knapp, D. E., Kennedy-Bowdoin, T., Martin, R. E., Anderson, C., Higgins, M., & Chadwick, K. D. (2014). A Tale of Two "Forests": Random Forest Machine Learning Aids Tropical Forest Carbon Mapping. *PloS One, 9*(1), e85993. https://doi.org/10.1371/journal.pone.0085993

Means, J. E., Acker, S.A., Harding, D. J., Blair, J. B., Lefsky, M. A., Cohen, W. B., Harmon, M. E., & McKee, W. A. (2009). Use of Large-Footprint Scanning Airborne Lidar To Estimate Forest Stand Characteristics in the Western Cascades of Oregon. *Remote Sensing of Environment, 67*(3), 298-308. https://doi.org/10.1016/S0034-4257(98)00091-1

Mountrakis, G., Im, J., & Ogole, C. (2011). Support vector machines in remote sensing: A review. *ISPRS Journal of Photogrammetry and Remote Sensing, 66*(3), 247-259. https://doi.org/10.1016/j.isprsjprs.2010.11.001

Naesset, E. (1997). Estimating timber volume of forest stands using airborne laser scanner data. *Remote Sensing of Environment*, *61*(2), 246-253. https://doi.org/10.1016/S0034-4257(97)00041-2

Næsset, E., Gobakken, T., Solberg, S., Gregoire, T. G., Nelson, R., Ståhl, G., & Weydahl, D. (2011). Model-assisted regional forest biomass estimation using LiDAR and InSAR as auxiliary data: A case study from a boreal forest area. *Remote Sensing of Environment, 115*(12), 3599-3614. https://doi.org/10.1016/j.rse.2011.08.021

Nelson, R., Margolis, H., Montesano, P., Sun, G., Cook, B., Corp, L., Andersen, H.-E., deJong, B., Pellat, F. P., Fickel, T., Kauffman, J., & Prisley, S. (2017). Lidar-based estimates of aboveground biomass in the continental US and Mexico using ground, airborne, and satellite observations. *Remote Sensing of Environment, 188*, 127-140. https://doi.org/10.1016/j.rse.2016.10.038

Niklas, K. J. (1994). *Plant Allometry: The Scaling of Form and Process*. University of Chicago Press.

Osborne, J., & Waters, E. (2002). Four Assumptions of Multiple Regression That Researchers Should Always Test. *Practical Assessment, Research, and Evaluation, 8*(1). https://doi.org/10.7275/r222-hv23

OSiRIS: a distributed Ceph deployment using software defined networking for multi-institutional research, DOI https://doi.org/10.1088/1742-6596/898/6/062045

OSiRIS: A Distributed Storage and Networking Project Update, DOI https://doi.org/10.1051/epjconf/202024504012

Pinheiro, J., & Bates, D. (2006). *Mixed-effects models in S and S-PLUS*. Springer Science & Business Media.

Popescu, S. C. (2007). Estimating Biomass of Individual Pine Trees Using Airborne Lidar. *Biomass and Bioenergy, 31*(9), 646-55. https://doi.org/10.1016/j.biombioe.2007.06.022

Pordes, R. et al. (2007). "The Open Science Grid", J. Phys. Conf. Ser. 78, 012057.doi:10.1088/1742-6596/78/1/012057.

Powell, S. L., Cohen, W. B., Healey, S. P., Kennedy, R. E., Moisen, G. G., Pierce, K. B., & Ohmann, J. L. (2010). Quantification of live aboveground forest biomass dynamics with Landsat time-series and field inventory data: A comparison of empirical modeling approaches. *Remote Sensing of Environment, 114*(5), 1053-1068. https://doi.org/10.1016/j.rse.2009.12.018

Salas, C., Ene, L., Gregoire, T. G., Næsset, E., & Gobakken, T. (2010). Modelling tree diameter from airborne laser scanning derived variables: A comparison of spatial statistical models. *Remote Sensing of Environment, 114*(6), 1277-1285. https://doi.org/10.1016/j.rse.2010.01.020

Sfiligoi, I., Bradley, D. C., Holzman, B., Mhashilkar, P., Padhi, S., & Wurthwein, F. (2009, March). The pilot way to grid resources using glideinWMS, In *2009 WRI World congress on computer science and information engineering* (Vol. 2, pp. 428-432). IEEE. doi:10.1109/CSIE.2009.950

Shataee, S. (2013). Forest attributes estimation using aerial laser scanner and TM data. *Forest Systems, 22*(3), 484-496.

Shugart, H. H., Saatchi, S., & Hall, F. G. Importance of Structure and Its Measurement in Quantifying Function of Forest Ecosystems. *Journal of Geophysical Research: Biogeosciences, 115*, (G2). https://doi.org/10.1029/2009JG000993

Silipo, R. (2019, October 1). *From a Single Decision Tree to a Random Forest*. Towards Data Science. https://towardsdatascience.com/from-a-single-decision-tree-to-a-random-forest-b9523be65147

Vaglio Laurin, G., Chen, Q., Lindsell, J. A., Coomes, D. A., Frate, F. D., Guerriero, L., Pirotti, F., & Valentini, R. (2014). Above ground biomass estimation in an African tropical forest with lidar and hyperspectral data. *ISPRS Journal of Photogrammetry and Remote Sensing, 89*, 49-58. https://doi.org/10.1016/j.isprsjprs.2014.01.001

West, P. W. (2015). *Tree and forest measurement*. Springer.

Ws, W.-M.-J., Ih, W., Ca, S., H, O., & At, H. (2017). Modelling individual tree aboveground biomass using discrete return LiDAR in lowland dipterocarp forest of Malaysia. *Journal of Tropical Forest Science, 29*(4), 465-484. https://doi.org/10.26525/jtfs2017.29.4.465484

Xiao, X., White, E. P., Hooten, M. B., & Durham, S. L. (2011). On the use of log‐transformation vs. nonlinear regression for analyzing biological power laws. *Ecology, 92*(10), 1887-1894. https://doi.org/10.1890/11-0538.1

Zolkos, S. G., S. J. Goetz, & R. Dubayah. (2013). A Meta-Analysis of Terrestrial Aboveground Biomass Estimation Using Lidar Remote Sensing. *Remote Sensing of Environment, 128*, 289-98. https://doi.org/10.1016/j.rse.2012.10.017

Chapter 3:

Belowground Carbon Storage: Measuring Organic Carbon Content in Soils

Relevant Appendices
Appendix D: Map of Soil Types Found in the Greenbelt District
Appendix E: Summary of Aboveground Carbon Storage by Property

Introduction

Terrestrial ecosystems consist of two distinct compartments: aboveground and belowground (Kardol & Wardle, 2010), and the ecosystem service value of carbon storage is relevant to both. The Ann Arbor Greenbelt Program, which protects open space, farmland, and natural habitats, can benefit from measures of carbon storage that communicate its value to carbon neutrality and climate mitigation efforts. In Chapter 2, we looked at the amount of carbon stored in part of the aboveground compartment (i.e. trees and shrubs). As shown in Figure 3.1, approximately 40% of carbon stored in a Great Lakes forest is contained in aboveground tree trunks and branches. In this chapter, we address the carbon in the belowground component. Specifically, we focus on carbon in soil organic matter. Other aspects of belowground carbon, such as tree roots, are not considered here because they are not as easily quantifiable. It is also not possible to measure tree roots using remote sensing and they are not included in publicly available GIS datasets. Our estimates of aboveground and belowground soil carbon storage together make up 85% of total carbon storage in a forested ecosystem.

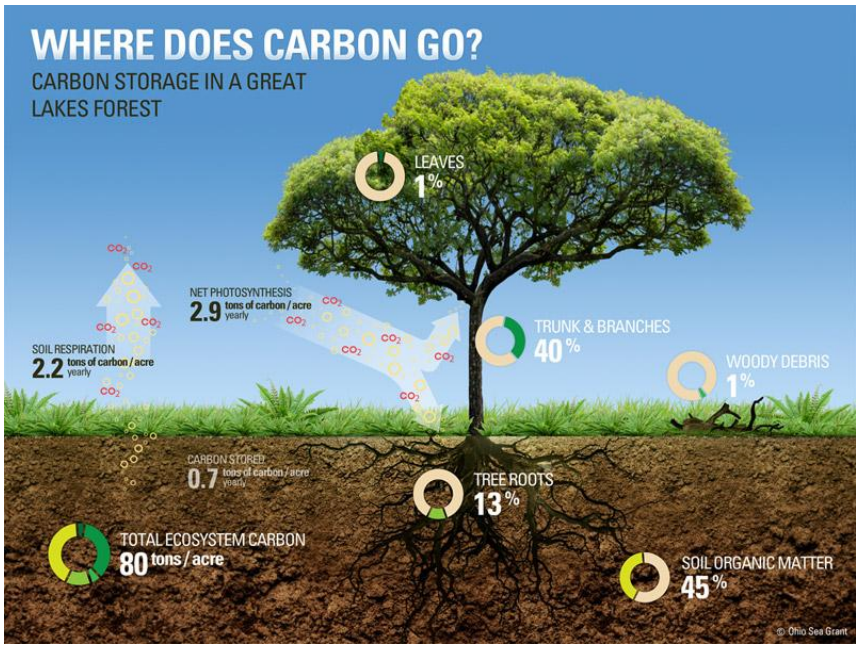

Figure 3.1. Carbon Storage Distribution Aboveground and Belowground in a typical Great Lakes forest. Sourced from Dierkes (2011).

In this chapter, we produce a method and calculate estimates of soil carbon for Greenbelt properties by first reviewing what is known about the importance of measuring soil carbon storage, the amount of soil carbon in different land cover types (forest, wetland, and agricultural), and appropriate methods for estimating soil carbon. Our guiding research questions are summarized in Box 3.1:

Box 3.1. Research questions to understand belowground carbon storage in the Ann Arbor Greenbelt

I. **Importance of Carbon in Soils:** What is soil organic carbon and why measure it?
II. **Carbon in Forest and Wetland Soils:** How much carbon is contained in relatively undisturbed land cover types?
III. **Carbon in Agricultural Soils:** What impact does agriculture have on soil carbon?
IV. **Soil Carbon Estimation:** What existing methods can be used to estimate soil carbon?

I. Importance of Carbon Storage in Soils

A significant proportion of the world's carbon is stored in soils. The amount of carbon stored in soils is nearly three times that in aboveground biomass and double that in the atmosphere (Schlesinger, 1986; Eswaran et al., 1993). Soil organic carbon (SOC) represents the amount of carbon found in soil organic matter (Figure 3.1), and is usually expressed in kilograms or kilograms per unit area. Soil organic matter consists of litter and decomposing organic matter on the soil surface and decomposing leaves and other plant material in the soil horizons (Schlesinger, 1986). SOC is estimated to be 47% of the mass of soil organic matter (Don Zak, pers. comm., 18 June 2020), though some researchers have shown it is closer to 58% (Burt, 2014), the rest being inorganic material.

Attempts to estimate global and regional soil carbon reveal how significant the quantity of carbon stored in the soil is. Lal (2007) estimated that 1550 petagrams (Pg) of carbon (C) is stored as SOC in soils worldwide. A more recent estimate is 1460.5 Pg C, representing the median of SOC estimates from 27 different studies (Scharlemann et al., 2014). These estimates only include carbon in the top 1 meter of soil. Global SOC storage in the top 3 meters is estimated at 2344 Pg C, which is over 50% more than the amount contained in the top 1 m (Jobbágy & Jackson, 2000). However, it is important to note that methods to measure soil carbon vary by region and there is no consensus on the amount of carbon stored in terrestrial ecosystems (Scharlemann et al., 2014). In the United States, the estimated total SOC storage is 73 Pg C, according to a study by the U.S. Geological Survey. Of this, 25 Pg C are contained in forest and woodland soils (Sundquist et al., 2009).

Though land use change can have substantial impacts on SOC (Scharlemann et al., 2014), there is still a significant amount of carbon stored in urban areas and urban soil. Churkina et al. (2010) estimated that in the year 2000, 18 Pg of carbon was stored in human settlements of the contiguous United States. This is 10% of the U.S. total land carbon storage, and the majority of that 18 Pg (64%) was in the soil.

Clearly carbon stored in soils is a significant portion of total carbon storage across different regions and habitat types, so current estimates of soil carbon are necessary to serve as a baseline for assessing potential future carbon storage gains or losses (Sundquist et al., 2009). Not only is estimating soil carbon important for climate regulation, but soil carbon management can also have effects on other ecosystem services. Soils with higher carbon content have increased water and nutrient storage and greater resistance to erosion (Scharlemann et al., 2014). Although these other ecosystem services of soil carbon can be difficult to quantify, they support the Greenbelt's mission to protect natural areas and water quality.

II. Carbon in Forest and Wetland Soils

The Ann Arbor Greenbelt contains a variety of land cover types, including 1,341 acres of woodlands and 1,476 acres of wetlands. Soil carbon content varies by land cover type, with the highest density of soil organic carbon occurring in forest land cover types, followed by grassland, shrubs, and desert (Wang et al., 2010). Bae and Ryu (2015) estimated SOC stocks up to a depth of 1 m in an urban park in South Korea and found a tenfold difference in SOC stocks across different land cover types, with the highest stocks of SOC occurring in wetlands (~14 kg/m^2) followed by forest, lawn, and bare soils. To accurately assess soil carbon on Greenbelt properties, it is thus essential to understand the nature of soil carbon in forest and wetland land use types specifically.

While forest management has a significant effect on aboveground carbon storage (in the form of tree biomass), it has surprisingly little effect on belowground soil carbon storage. Johnson (1992) examined existing literature on soil carbon change with forest harvesting and found no general trend toward lower soil carbon. More recently, Powers et al. (2011) found that different harvesting treatments, such as individual tree selection and shelterwood treatments, resulted in no significant differences in understory carbon, forest floor carbon, or mineral soil carbon pools. On the other hand, clearing the land for agriculture results in up to 50% loss in soil carbon in most cases (Johnson, 1992). The fact that soil carbon storage does not vary by forest management type is significant for the Greenbelt and other conservation easement programs because soil carbon estimates will be more stable regardless of how forested land is managed. A huge amount of carbon will remain stored in forest soils simply by preventing that land from being developed.

Wetlands contain a disproportionate amount of total soil carbon in comparison to other land cover types. Wetlands occupy 5-8% of the world's land surface (Mitsch et al., 2009) but contain 20-30% of global soil carbon (Nahlik & Fennessy, 2016). A study conducted in a British moorland, a type of wetland in England, found that the soil contained at least 200 times more carbon than the aboveground vegetation (Garnett et al., 2001). The Greenbelt District, or the potential area of the land protection program, contains 24,611 acres of wetlands, making up nearly 25% of the total acreage. Though only 1,476 acres of wetlands were protected by the Greenbelt as of April 2021, the high potential for belowground carbon storage of wetlands indicates the importance of prioritizing wetlands in the Greenbelt Program for their climate mitigation service value.

III. Carbon in Agricultural Soils

The conversion of land to agriculture is generally found to have negative effects on soil carbon storage. Changes in land uses, including agriculture, deforestation, and grazing increase the net transfer of carbon from terrestrial ecosystems to the atmosphere (Davidson & Ackerman, 1993). Many studies have estimated the amount of carbon lost as a result of cultivation. According to a review by Guo and Gifford (2002), converting forest land to cropland decreased soil carbon by an average of 42%. In some cases, 25-50% of SOC in the top 1 meter has been lost as a result of converting native vegetation to cropland (Scharlemann et al., 2014). This depletion occurs over a period of 20 to 50 years in temperate climates (Lal, 2007). Furthermore, the rate of soil carbon loss is highest in the first two or three years following cultivation (Davidson & Ackerman, 1993).

Agriculture decreases SOC for a myriad of reasons. It can cause increases in soil temperature, aeration, and moisture, leading to an increase in decomposition and a decrease in the annual production of plant residues. As a result, there is a decline in the amount of organic matter in the soil surface layers (Schlesinger, 1986). In addition, agriculture decreases the amount of biomass returned to the soil, alters the carbon to nitrogen ratio, and increases soil erosion (Lal, 2005). Though the effects of different agricultural practices, such as no-till farming, on SOC have been a subject of debate in recent years (VandenBygaart, 2016), scientists have concluded that most conventional agricultural practices have a net negative effect on soil carbon (Scharlemann et al., 2014). This is especially true of annually tilled crops, which, at least currently, make up the majority of acres in farmland in the Greenbelt area.

On the other hand, there are certain agricultural practices that are more definitively known to increase soil carbon, including the addition of biochar and compost. Biochar is a carbon-rich product created by pyrolyzing biomass in an environment with little or no oxygen (Sánchez-Reinoso et al., 2020). Once biomass has been burned and turned into biochar it can be mixed into agricultural soils. When mixed, the long residence time and stability of the carbon in biochar from the pyrolysis process helps to increase the amount of carbon that can be stored in agricultural soils (Jha et al., 2010). Lehmann et al. (2006) estimated that by the year 2100, it could be possible to globally store 9.5 billion metric tons of carbon per year in soil with the application of biochar. Similarly, composting incorporates microbial and biochemical processes to create a more controlled and quicker substitute to the decomposition that occurs naturally in soil (Mekki et al., 2019). The effects of compost addition to soil depend on the climate, soil type, and farming practices used at a location, as well as the characteristics of the organic material itself, but adding compost has generally been found to increase soil organic matter across ecosystem types (Canali et al., 2004; Jaiarree et al., 2014; Mekki et al.; 2019).

While assessing carbon in the agricultural soils of the Greenbelt Program is a promising future direction, we chose to limit our evaluation of carbon in soils to only forested and wetland land areas within the Greenbelt properties. The Greenbelt Program by design is aimed at conservation in perpetuity and not in influencing practices, beyond easement restrictions, on that land. Carbon in agricultural soils will vary depending on cultivation, tilling, and composting practices, and can be more labile than carbon in the soil of protected forest or wetland systems. Thus, in assessing soil carbon for Greenbelt properties we exclude agricultural soils and focus instead on assessing carbon in the soil of forests and wetlands.

IV. Soil Carbon Estimation

Estimates of soil carbon storage are calculated based on numerous features of the soil. The most important of these are bulk density, horizon thickness, and carbon concentration (Kimble et al., 2000). Box 3.2 below defines key physical properties of soils.

Box 3.2. Key terms for physical soil properties

- **Horizon depth** - the upper and lower boundaries of each soil layer
- **Bulk density** - the weight of soil (ovendry) per unit volume
- **Organic matter** - the plant and animal residue in the soil at various stages of decomposition, from which carbon concentration can be derived

Source: USDA Natural Resources Conservation Service (Soil Survey Staff)

SOC estimates also depend on other features such as profile characteristics (the layers of soil), position on the landscape, characteristics of the terrain, temperature, and rainfall (Lal, 2007). Concentrations of organic carbon are highest in the uppermost horizons, or layers, because plant residues are located at the surface of the soil. Soil carbon also varies with management (as discussed above), moisture content, and other properties (Kimble et al., 2000), all of which vary too much to be a part of feasible soil carbon estimation for the Greenbelt program.

Unlike some of the less tractable soil features, *soil type* is an easily assessed and stable feature of soil that can be used to identify key variables needed for soil carbon estimation. The Greenbelt District is known to contain over 80 different soil types, which can be categorized into three main types by particle size (Box 3.3). See Appendix D for a map of Greenbelt soil types. Each soil type is associated with a different known bulk density and organic concentration that varies by soil horizon. Thus, having soil type information also provides information on the other key variables needed to estimate soil carbon.

Box 3.3. Definitions of Soil Types

- **Sand** - consists of soil particles that are 0.05 to 2 millimeters in diameter
- **Silt** - consists of mineral soil particles that are 0.002 to 0.05 millimeter in diameter
- **Clay** - consists of mineral soil particles that are less than 0.002 millimeter in diameter

Source: USDA Natural Resources Conservation Service (Soil Science Division Staff)

Given the valuable information soil type provides for carbon estimation, we determined it was the most feasible and accurate way to approach soil carbon estimation of the Greenbelt properties using already available site-specific soil type data. Measuring bulk density and organic matter content in the field is a labor and time-intensive process, so using soil type as a proxy for these features enabled us to get a rough estimate of soil organic carbon across the Greenbelt district without the need to do field work.

Methods

In order to calculate soil carbon for Ann Arbor Greenbelt properties, as well as create a tool to continue assessment of future properties, we used publicly available spatial data from the National Cooperative Soil Survey, which is operated by the USDA Natural Resources Conservation Service (NRCS). The NRCS Web Soil Survey provides access to soil maps and data for more than 95% of the nation's counties (Soil Survey Staff). The Soil Survey Geographic Database (SSURGO) includes, for each soil horizon, measures of horizon depth, bulk density, and organic matter. From these data, we calculated the mass of organic carbon per unit surface area for the top soil horizon.

We filtered GIS data from the NRCS Web Soil Survey to access soil properties specific to the Greenbelt. First, we used the Area of Interest (AOI) tab to input shapefiles for the Greenbelt (Figure 3.2). Because the total area of the Greenbelt District boundary shapefile (105,675 acres, including the City of Ann Arbor), exceeds the AOI limit of 100,000 acres, the shapefile was split in ArcGIS Pro into a North and South section.

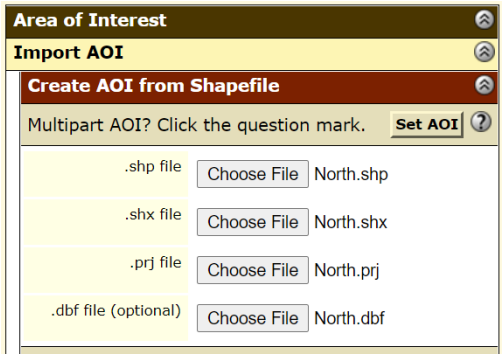

Figure 3.2. Step 1: Define Area of Interest (AOI) for North section of Greenbelt.

Next, we generated a Soil Report for Soil Physical Properties for both the North and South sections (Figure 3.3).

Report — Physical Soil Properties

Three values are provided to identify the expected Low (L), Representative Value (R), and High (H).

Washtenaw County, Michigan

Map symbol and soil name	Depth	Sand	Silt	Clay	Moist bulk density	Saturated hydraulic conductivity	Available water capacity	Linear extensibility	Organic matter	Erosion factors			Wind erodibility group	Wind erodibility index
										Kw	Kf	T		
	In	*Pct*	*Pct*	*Pct*	*g/cc*	*micro m/sec*	*In/In*	*Pct*	*Pct*					
Ad—Adrian muck														
Adrian	0-26	-10-	-50-	-40-	0.30-0.43-0.55	1.40-21.70-42.00	0.35-0.40-0.45	—	75.0-82.5-90.0			1	2	134
	26-60	-92-	- 2-	2-6-10	1.40-1.58-1.75	42.00-92.00-141.00	0.03-0.06-0.08	0.0- 1.5- 2.9	0.0-0.3- 0.5	.02	.02			

Figure 3.3. Step 2: Generate Soil Report for Physical Soil Properties. Here one soil type, Ad-Adrian muck, is shown.

The soil reports were downloaded and values for physical soil properties were entered into an Excel spreadsheet set up to calculate soil carbon estimates (Figure 3.4). The NRCS Web Soil Survey provides low, medium, and high values for bulk density and organic matter content, as shown above in Figure 3.3. We calculated low, medium, and high estimates of soil carbon using a combination of low-low, medium-medium, and high-high moist bulk density and organic matter values.

	A	B	C	D	E	F	G	H	I	J	K	L	M
1	Soil Code	Soil Name	Horizon depth (in)	Horizon depth (cm)	low-bulk density (g/cm3)	med-bulk density (g/cm3)	high-bulk density (g/cm3)	low-OC (%)	med-OC (%)	high-OC (%)	low-Carbon (kg/m^2)	med-Carbon (kg/m^2)	high-Carbon (kg/m^2)
2	Ad	Adrian muck	26	66.04	0.3	0.43	0.55	75	82.5	90	69.8373	110.1101	153.6421
3	BbA	Blount loam	9	22.86	1.3	1.45	1.6	2	2.5	3	2.793492	3.894773	5.157216
4	BnB	Boyer loamy sand	9	22.86	1.45	1.55	1.65	1	1.8	2.5	1.557909	2.997632	4.431983
5	Br	Brookston loam	11	27.94	1.35	1.43	1.5	3	4	5	5.318379	7.51139	9.84885
6	Cc	Cohoctah fine sandy loam	10	25.4	1.2	1.35	1.5	3	9	15	4.29768	14.50467	26.8605
7	CoB	Conover loam	11	27.94	1.4	1.48	1.55	2	2.5	3	3.676904	4.858766	6.106287
8	CpA	Conover-Brookston loams	11	27.94	1.4	1.48	1.55	2	2.5	3	3.676904	4.858766	6.106287
9	Ed	Edwards muck	32	81.28	0.3	0.43	0.55	75	82.5	90	85.9536	135.5202	189.0979
10	FoA	Fox sandy loam	9	22.86	1.3	1.45	1.6	1	2	3	1.396746	3.115818	5.157216

Figure 3.4. Partial list of soils found in Greenbelt District with values taken from Web Soil Survey report.

Soil carbon storage was calculated using the following formula:

$$Carbon\ storage\left(\frac{kg}{m^2}\right) =$$

$$Horizon\ depth\ (cm)\ \times\ Bulk\ Density\ (\frac{g\ soil}{cm^3})\ \times\ Organic\ Matter\ Concentration\ (\%)\ \times\ 0.47\ (\%\ Carbon)$$

The formula above was given to us by Dr. Don Zak, a soil scientist and SEAS faculty member. The values for organic matter content were converted to soil organic carbon by multiplying by 0.47 because 47% is an accepted and conservative estimate of the amount of carbon contained in organic matter (Don Zak, pers. comm., 18 June 2020) This formula was entered into columns K, L, and M (Figure 3.4) to calculate low, medium, and high carbon estimates. Centimeters were converted into meters and grams into kilograms to produce estimates of carbon in kilograms per square meter.

As an example, the low, medium, and high carbon storage values for Blount loam (row 3) were calculated as follows. For low carbon storage, the horizon depth value from column D in Figure 3.4, the low-bulk density value from column E, and the low-OC value from column H were substituted into the equation above. When these values were plugged in, the equation became, 22.86 (cm) x 1.3 (g/cm^3) x 0.02 x 0.47 (% C) = 2.793492 kg/m^2 (in column K in Figure 3.4). The medium carbon storage calculation was done using horizon depth from column D, med-bulk density from column F, and med-OC from column I in Figure 3.4 above. The calculations were done in the same manner as for the low carbon storage value and the output can be seen in column L of Figure 3.4. Finally, horizon depth, high-bulk density and high-OC from columns D, G, and J, respectively, were input into the equation above to determine the high value of carbon storage. The output was recorded in column M.

To assess carbon specifically for forest and wetland land cover types, we used a 30-m spatial resolution National Land Cover Database (NLCD) from 2016 to determine land-use and land-cover in the Greenbelt District. As shown in Figure 3.5, this layer was clipped to the extent of Washtenaw County (as some properties are located just outside the district boundary) and converted from raster to vector format without simplified polygons. Forest and wetland cover types were selected and joined with the CitySoils layer containing soil types of the county. Irrelevant fields were deleted and the Soil Carbon csv (a simplified version of Figure 3.4 with unnecessary fields removed) was joined to the forest and wetland soils layer. The output is stored as a shapefile, labeled as “soil_carbon” at the bottom of Figure 3.5. This shapefile contains soil carbon amount per unit area (kg/m^2).

Figure 3.5. Soil Model 1 (static)
Required input data: NLCD land cover types (nlcd_mi_utm16), aerial image of Washtenaw county (2015_Washtenaw.sid), City Soils data obtained from the City of Ann Arbor (CitySoils), Soil Carbon spreadsheet converted into a CSV (Soil Carbon.csv).

The output of Model 1 was used as input to Model 2 (Figure 3.6) to calculate soil carbon storage for a single Greenbelt Property. Model 1 is a one-time process; assuming land cover types do not change, this model does not need to be run as additional properties are added to the Greenbelt.

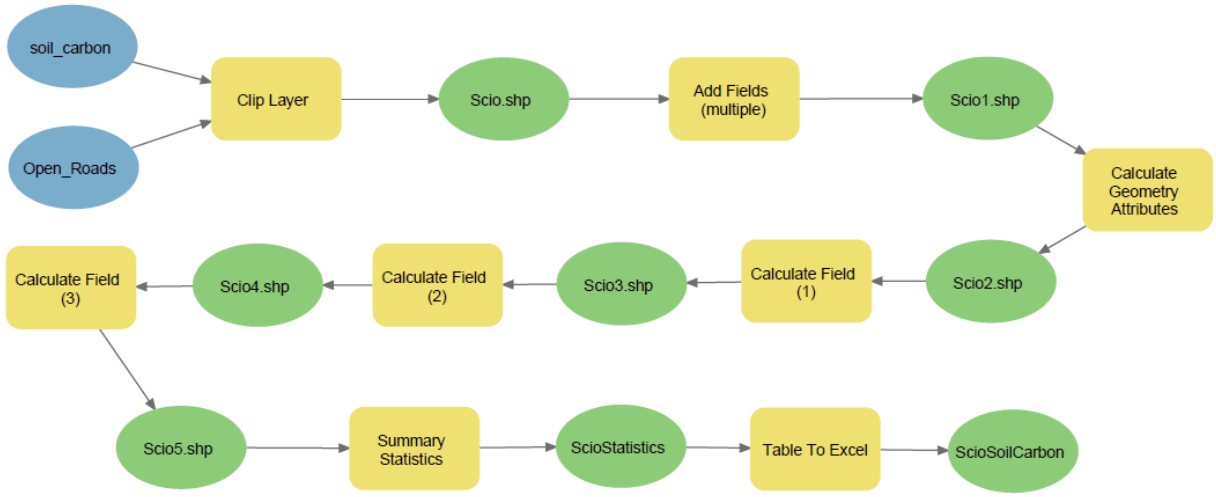

Figure 3.6. Soil Model 2 (dynamic)
Required input data: soil_carbon (output of Model 1) and a shapefile of a single Greenbelt property

Model 2 uses Open_Roads (otherwise known as Scio Woods) as a sample property. The model clips soil_carbon to the property boundary, calculates area in square meters, and calculates total soil carbon storage in kilograms, separated by cover type (forest or wetland) at that property. The result is exported as an Excel spreadsheet containing low, medium, and high carbon storage estimates. Model 2 was exported as a Python file and modified to run a list of all existing Greenbelt properties as of April 2021. This code can be found as "SoilModelTutorial.py" at the following link: https://github.com/UMGreenbelt/Greenbelt21.

Storing carbon in aboveground biomass or as soil organic matter keeps it out of the atmosphere as carbon dioxide, which is a global externality associated with a plethora of economic and social costs (Cai & Lontzek, 2019). In order to connect carbon storage on Greenbelt properties to dollar values, we applied the pricing model used by the EPA where values represent the total long-term damage derived from emitting one ton of carbon as well as the value of the avoided damages due to emission reductions (U.S. EPA, 2016). The EPA model estimates the social cost of emitting one metric ton of carbon at $51 (Interagency Working Group on Social Cost of Greenhouse Gases, 2021), which is currently the official baseline for the EPA and the City of Ann Arbor.

Results

Table 3.1 shows the carbon stored in forested and wetland soils at three sample Greenbelt properties and the total stored in all properties currently protected in the Greenbelt. Forest soils make up 20.6% of the Greenbelt district and wetland soils make up 8.7%. Carbon

stored in forest and wetland soils in various Greenbelt properties, based on NRCS Web Soil Survey results for medium bulk density and organic content. The complete list of properties can be found in Appendix E.

Table 3.1. Soil Carbon Storage in three sample Greenbelt Properties and across all Greenbelt properties (as of April 2021)

	Forest Soil Carbon (kg)	**Wetland Soil Carbon (kg)**	**Total Soil Carbon (kg)**
Sample properties			
Whitney	2,510,091	5,988,566	8,498,657
Botero	262,790	4,212,790	4,475,580
Scio Woods	1,641,390	94,994	1,736,384
Total Greenbelt Properties	23,605,839	26,399,893	50,005,732

To convert mass of carbon stored in kilograms to other metrics that communicate their value, we used a variety of available sources and conversion standards. Table 3.2 shows the social cost and carbon emission equivalents for selected Greenbelt properties as well as for all current Greenbelt properties. The social cost of carbon represents the societal costs, in terms of the long-term damage done to both the environment and human health, that are associated with the emission of one extra ton of CO_2 (U.S. EPA, 2016). Social cost and passenger vehicle mile emission estimates came from the EPA's Greenhouse Gases Equivalencies Calculator, airline mile emission estimates were sourced from BlueSkyModel, and yearly average household emission data was gathered using the CoolClimate Household Calculator (U.S. EPA, 2021; BlueSkyModel; CoolClimate Network).

Table 3.2. Social Cost and Carbon Emission Equivalents

	Social Cost ($)	**Passenger Vehicle Miles Equivalent (mi)**	**Airline Miles Equivalent (mi)**	**Avg. Annual Ann Arbor Household Emission Equivalent (# of households)**
Sample properties				
Whitney	$1,589,263.37	21,036,280	351,526	708
Botero	$836,941.06	11,078,168	185,121	373
Scio Woods	$324,706.75	4,297,980	71,821	145
Total Greenbelt Properties	$9,351,156.96	123,776,564	2,068,363	4,167

A different valuation model from Hungate et al. (2017) estimates the social cost of carbon at $42 to $400 per metric ton of C, with a median value of $137. The estimates from this model are lower than those calculated using the EPA social cost of carbon because the units of this model are metric tons of C while the units for the EPA model are metric tons of CO_2. Using the median value from the Hungate et al. (2017) model, we calculated the social cost of the soil carbon for the three sample properties from Table 3.2. We found that Whitney had a value of $1,164,316.05, Botero had a value of $613,154.46, and Scio Woods had a value of $237,884.60. In total, using this model, we calculated the social cost of belowground soil carbon storage for all Greenbelt properties to be $6,850,785.33.

Discussion

Major Findings

Overall, we have demonstrated that it is feasible to calculate soil carbon storage using a combination of existing GIS data, the NRCS Web Soil Survey, and formulas to calculate total soil carbon for different land cover types. To our knowledge this is the first use of this practical method to assess soil carbon using only available spatial data on soil type and known conversion, without the need for any field data collection. Unlike our assessment of aboveground carbon storage, no field work was necessary to achieve these results. Using the estimates for soil carbon storage at the individual property and Greenbelt-wide levels derived from this method we converted the values into common equivalents, such as average annual Ann Arbor household emissions and passenger vehicle and airline miles. These equivalents allow the value of soil carbon storage to be communicated in a manner beyond kilograms of carbon so the impact of the Greenbelt Program can more easily be understood.

Limitations and Caveats

We believe our estimates of soil carbon are conservative. First, we conservatively calculated soil carbon as 47% of organic matter, but other literature indicates that soil carbon may constitute 58% of organic matter (Burt, 2014). Using a higher percentage of carbon would have increased the carbon estimates for the Greenbelt. In addition, we used the NRCS Web Soil Survey results for medium estimates of bulk density and organic content as opposed to the high estimates. Furthermore, we only calculated soil carbon in the top horizon of soil. Soil carbon exists at other depths of the soil, but in decreasing amounts (Wang et al., 2010). Lastly, we only calculated soil carbon in forested and wetland parts of the Greenbelt, even though agricultural land currently makes up about one quarter of the land cover in the Greenbelt District (not including the City of Ann Arbor). This exclusion of agricultural land makes sense, however, given the likely low carbon storage value of most annual crop fields and the complexities of applying a model based on soil type to agricultural land with variable practices. Future adaptations of the model are presented in the subsequent section.

The dollar values we have calculated and presented above for the social cost of soil carbon represent the value of having the soil protected and kept in place. They are different from the dollar values we calculated in Chapter 2 because the value of soil carbon does not

come from its salable value like aboveground biomass from trees. Instead, the value of soil carbon is derived from it remaining in place and being protected from disturbance in perpetuity.

Uses and Future Applications of Soil Carbon Model

Our soil carbon model is intended to be used for future Greenbelt property acquisitions. The output of Model 1 can be used repeatedly as input to Model 2 for each individual property to calculate forest and wetland soil carbon. That said, if there is a change in land cover type, Model 1 would need to be updated with a more recent NLCD layer. For example, if land that is currently forested is converted to farmland before being added to the Greenbelt, the existing model would erroneously calculate forest soil carbon storage for that land under the 2016 NLCD cover type.

The model is not designed to be used for farmland of any kind, but could be adapted for certain situations. If in the future there is interest in applying the model to agricultural land, Model 1 would need to be modified to select agriculture in addition to forest and wetland land cover types. Roughly 50% of the carbon reported by the model based on soil type can be considered intact, as the rest was depleted due to cultivation (Scharlemann et al., 2014). We caution against using the model for this purpose because our methodology for estimating soil carbon in forests and wetlands is heavily grounded in primary literature, and loosely adapting it for agricultural soils would simply add uncertainty and detract from its overall robustness.

It is possible to increase both the soil organic content and soil quality of agricultural soils. Aticho (2013) recommend that stakeholders focus on management activities that improve SOC and bulk density to increase carbon storage capacity of the soil. As discussed above, biochar and compost amendments can increase soil carbon storage. Increasing soil carbon has implications not only for climate mitigation goals but also, in some cases, for increasing crop yields. The Greenbelt Program, or similar initiatives, could consider incentivizing certain farming practices to increase the amount of carbon stored in agricultural soils as a way to further increase the ecosystem service value of land protected from development.

Literature Cited

Bae, J., & Ryu, Y. Land use and land cover changes explain spatial and temporal variations of the soil organic carbon stocks in a constructed urban park." *Landscape and Urban Planning, 136*, 57-67. https://doi.org/10.1016/j.landurbplan.2014.11.015

BlueSkyModel. https://blueskymodel.org

Burt, R. (Ed.). (2014). Kellogg soil survey laboratory methods manual. United States Department of Agriculture, Natural Resources Conservation Service, National Soil Survey Center, Kellogg Soil Survey Laboratory.

Cai, Y., & Lontzek, T. S. (2019). The social cost of carbon with economic and climate risks. *Journal of Political Economy, 127*(6), 2684-2734.

Canali, S., Trinchera, A., Intrigliolo, F., Pompili, L., Nisini, L., Mocali, S., & Torrisi, B. (2004). Effect of long term addition of composts and poultry manure on soil quality of citrus orchards in Southern Italy. *Biology and Fertility of Soils, 40*(3), 206-210. https://doi.org/10.1007/s00374-004-0759-x

Churkina, G., Brown, D. G., & Keoleian, G. (2010). Carbon stored in human settlements: the conterminous United States. *Global Change Biology, 16*(1), 135-43. https://doi.org/10.1111/j.1365-2486.2009.02002.x

CoolClimate Network. *Household calculator*. https://coolclimate.org/calculator

Davidson, E. A., & Ackerman, I. L. Changes in soil carbon inventories following cultivation of previously untilled soils. *Biogeochemistry, 20*(3), 161-93. https://doi.org/10.1007/BF00000786

Dierkes, C. (2011, June 2). Accounting for Carbon in Great Lakes Forests [PDF file]. http://changingclimate.osu.edu/assets/pubs/articles/accounting-for-carbon.pdf

Eswaran, H., Berg, E., & Reich, P. Organic Carbon in Soils of the World. *Soil Science Society of America Journal, 57*(1), 192-94. https://doi.org/10.2136/sssaj1993.03615995005700010034x

Garnett, M. H., Ineson, P., Stevenson, A. C., & Howard, D. C. (2001). Terrestrial organic carbon storage in a British moorland. *Global Change Biology, 7*(4), 375-388. https://doi.org/10.1046/j.1365-2486.2001.00382.x

Guo, L. B., & Gifford, R. M. (2002). Soil carbon stocks and land use change: a meta analysis. *Global Change Biology, 8*(4), 345-360. https://doi.org/10.1046/j.1354-1013.2002.00486.x

Hungate, B. A., Barbier, E. B., Ando, A. W., Marks, S. P., Reich, P. B., Van Gestel, N., ... & Cardinale, B. J. (2017). The economic value of grassland species for carbon storage. *Science Advances, 3*(4), e1601880.

Interagency Working Group on Social Cost of Greenhouse Gases, United States Government. (2021, February). Technical Support Document: Social Cost of Carbon, Methane, and Nitrous Oxide Interim Estimates under Executive Order 13990 [PDF file].

https://www.whitehouse.gov/wp-content/uploads/2021/02/TechnicalSupportDocument_SocialCostofCarbonMethaneNitrousOxide.pdf

Jaiarree, S., Chidthaisong, A., Tangtham, N., Polprasert, C., Sarobol, E., & Tyler, S. C. (2014). Carbon budget and sequestration potential in a sandy soil treated with compost. *Land Degradation & Development, 25*(2), 120-129. https://doi.org/10.1002/ldr.1152

Jha, P., Biswas, A. K., Lakaria, B. L., & Rao, A. S. (2010). Biochar in agriculture - prospects and related implications. *Current Science, 99*(9), 1218-25.

Jobbágy, E. G., & Jackson, R. B. (2000). The Vertical Distribution of Soil Organic Carbon and Its Relation to Climate and Vegetation. *Ecological Applications, 10*(2), 423-36. https://doi.org/10.1890/1051-0761(2000)010[0423:TVDOSO]2.0.CO;2

Johnson, D. W. (1992). Effects of forest management on soil carbon storage. In *Natural Sinks of CO2* (pp. 83-120). Springer, Dordrecht. https://doi.org/10.1007/978-94-011-2793-6_6

Kardol, P., & Wardle, D. A. (2010). How understanding aboveground-belowground linkages can assist restoration ecology. *Trends in Ecology & Evolution, 25*(11), 670-79. https://doi.org/10.1016/j.tree.2010.09.001

Kimble, J. M., Follett, R. F., & Stewart, B. A. (Eds.). (2000). *Assessment methods for soil carbon*. CRC press.

Lal, R. (2007). Carbon Management in Agricultural Soils. *Mitigation and Adaptation Strategies for Global Change* 12(2), 303-22. https://doi.org/10.1007/s11027-006-9036-7

Lal, R. (2005). Forest soils and carbon sequestration. *Forest Ecology and Management, 220*(1), 242-258. https://doi.org/10.1016/j.foreco.2005.08.015

Lehmann, J., Gaunt, J., & Rondon, M. (2006). Bio-char Sequestration in Terrestrial Ecosystems - a review. *Mitigation and Adaptation Strategies for Global Change*, *11*(2), 403-427. https://doi.org/10.1007/s11027-005-9006-5

Mekki, A., Aloui, F., & Sayadi, S. (2019). Influence of biowaste compost amendment on soil organic carbon storage under arid climate. *Journal of the Air & Waste Management Association, 69*(7), 867-877. https://doi.org/10.1080/10962247.2017.1374311

Mitsch, W. J., Gosselink, J. G., Zhang, L., & Anderson, C. J. (2009). *Wetland ecosystems*. John Wiley & Sons.

Nahlik, A. M., & Fennessy, M. S. Carbon storage in US wetlands. *Nature Communications, 7*(1), 13835. https://doi.org/10.1038/ncomms13835

Powers, M., Kolka, R., Palik, B., McDonald, R., & Jurgensen, M. Long-term management impacts on carbon storage in Lake States forests. *Forest Ecology and Management, 262*(3), 424-31. https://doi.org/10.1016/j.foreco.2011.04.008

Sánchez-Reinoso, A. D., Ávila-Pedraza, E. A., & Restrepo, H. Use of Biochar in agriculture. *Acta Biológica Colombiana, 25*(2), 327-38. https://doi.org/10.15446/abc.v25n2.79466

Scharlemann, J. P. W., Tanner, E. V. J., Hiederer, R., & Kapos, V. Global soil carbon: understanding and managing the largest terrestrial carbon pool. *Carbon Management, 5*(1), 81-91. https://doi.org/10.4155/cmt.13.77

Schlesinger, W. H. (1986). Changes in soil carbon storage and associated properties with disturbance and recovery. In *The changing carbon cycle* (pp. 194-220). Springer, New York, NY. https://doi.org/10.1007/978-1-4757-1915-4_11

Soil Science Division Staff. Ch. 3. Examination and Description of Soil Profiles. U.S. Department of Agriculture, Natural Resources Conservation Service. Available online at https://www.nrcs.usda.gov/wps/portal/nrcs/detail/soils/ref/?cid=nrcs142p2_054253. Accessed January 12, 2021.

Soil Survey Staff, Natural Resources Conservation Service, United States Department of Agriculture. Web Soil Survey. Available online at https://websoilsurvey.nrcs.usda.gov/. Accessed January 16, 2021.

Sundquist, E. T., Ackerman, K. V., Bliss, N. B., Kellndorfer, J. M., Reeves, M. C., & Rollins, M. G. (2009). Rapid assessment of US forest and soil organic carbon storage and forest biomass carbon sequestration capacity. *US Geological Survey Open-File Report, 1283*, 15.

United States Environmental Protection Agency (U.S. EPA). (2016, December). *Social Cost of Carbon* [PDF file]. https://www.epa.gov/sites/production/files/2016-12/documents/social_cost_of_carbon_fact_sheet.pdf

United States Environmental Protection Agency (U.S. EPA). (2021, March 11). *Greenhouse Gases Equivalencies Calculator - Calculations and References*. https://www.epa.gov/energy/greenhouse-gases-equivalencies-calculator-calculations-and-references

VandenBygaart, A. J. (2016). The myth that no-till can mitigate global climate change. *Agriculture, Ecosystems & Environment, 216*, 98–99. https://doi.org/10.1016/j.agee.2015.09.013

Wang, Y., Li, Y., Ye, X., Chu, Y., & Wang, W. (2010). Profile storage of organic/inorganic carbon in soil: From forest to desert. *Science of The Total Environment, 408*(8), 1925-31. https://doi.org/10.1016/j.scitotenv.2010.01.015

Chapter 4:

Water Ecosystem Services

Relevant Appendices
Appendix F: Soil & Water Assessment Tool (SWAT) Input Files

Introduction

Water ecosystem services are ecological processes and outcomes linked directly or indirectly to the hydrological cycle. These services provide us tangible benefits such as water purification, water retention, and climate regulation (Grizzetti et al., 2016). Whereas Chapters 2 and 3 focused on carbon storage as it relates to climate ecosystem services, this chapter serves as a review of the potential impacts of land conversion on water ecosystem services and existing approaches used to measure them. In particular, this chapter will focus on nutrient and heavy metal loading as proxies for water quality, due to their influence on both ecosystem and human health. Our primary research questions are summarized in Box 4.1:

Box 4.1. Key research questions to understand water ecosystem services in the Ann Arbor Greenbelt

I. **Background:** What are the key factors or variables to consider when assessing water-related ecosystem services?
II. **Existing Approaches:** What tools/approaches exist for quantifying water ecosystem services?
III. **Recommendations:** How can the City of Ann Arbor assess water ecosystem services in the Greenbelt district while ensuring broader access to such data?

I. Background

Water ecosystem services are important to measure because they are integral to human life and environmental health, and are also impacted by a vast array of stressors imposed by humans. Streams, lakes, surface water, and groundwater together make up the hydrology of a given landscape. This hydrology affects all types of ecosystem services in different and related ways, including provisioning (clean drinking water), regulating (climate regulation and water purification), supporting (hydrological cycling), and cultural (recreation and aesthetic) services (Leemans & De Groot, 2003). Ensuring the security of these ecosystem services relies on our ability to recognize both the natural resources and associated landscapes that provide us with these benefits and the stressors that threaten them (see Figure 4.1). Water supply and quality are especially impacted by stressors such as groundwater abstractions, point and nonpoint source pollution, and groundwater salinization, just to name a few (Grizzetti et al., 2016).

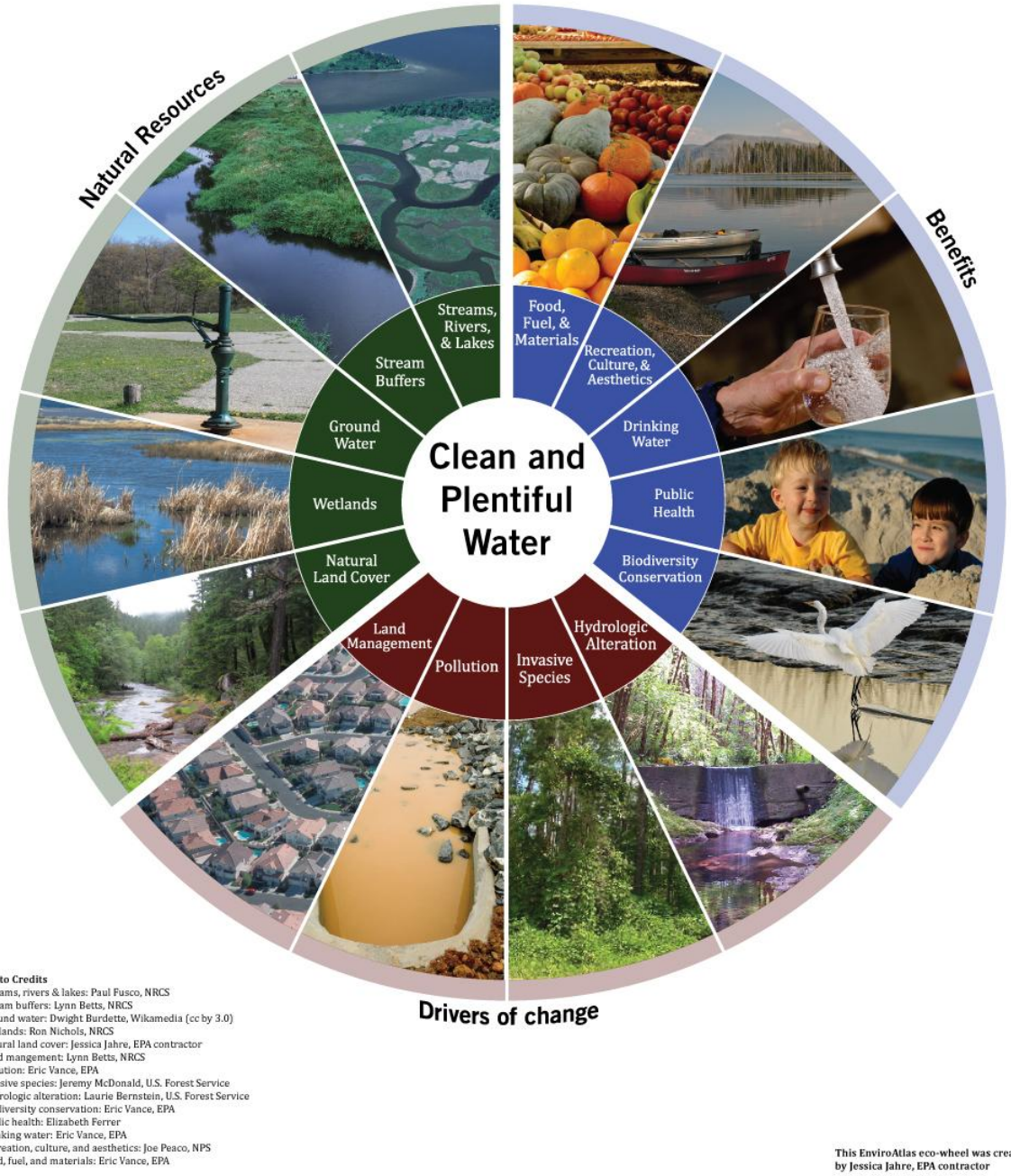

Figure 4.1. The graphic above depicts the relationship between natural resources, water quality benefits, and the drivers of change that threaten them. Sourced from the EPA EnviroAtlas (Jahre, 2020).

Land conservation efforts, such as the Ann Arbor Greenbelt Program, can be an essential tool to protect water ecosystem services from the stressors known to impact water supply and quality. As outlined in the 2019 Greenbelt Strategic Plan, the program's vision for the future highlights the need for conserving parcels that protect Ann Arbor's water resources and support pollution breakdown and absorption (The Conservation Fund, 2019). To assess the progress of the Greenbelt program toward this goal, the impact of different land use on water supply and quality can be quantified on a parcel-by-parcel basis. We focus in particular on

assessing the value of protected land for water *quality*, because nonpoint source pollution is highly quantifiable and can be modeled to estimate both the impacts of development and the value of conservation easements in preventing it. It is especially important for the Greenbelt Program to assess the impact of protected land on water quality because the Greenbelt District overlaps with the Huron River watershed, a key source of City of Ann Arbor drinking water and a favorite recreational area.

Nonpoint source pollution is defined as pollution that comes from many diffuse sources, generally resulting from land runoff, precipitation, atmospheric deposition, drainage, seepage or hydrologic modification. Nonpoint source pollutants include substances such as oil, toxic chemicals, fertilizers, sediments, bacteria, and nutrients such as nitrogen and phosphorus (United States EPA, 2020). Models are useful for understanding water quality and corresponding pollutants because they allow for accurate forecasting and simulation, while simultaneously avoiding the time and labor costs involved in gathering field measurements. In tools designed to assess water quality, nonpoint source pollution is typically modeled as nutrient or heavy metal loading. Nutrient or heavy metal loads represent the rate at which these substances enter the environment from nonpoint sources, and estimated reductions in these loads are often used to justify activities such as environmental stewardship and land conservation. Nutrient and heavy metal loading are important to measure because they can have harmful effects on both environmental and human health. Aquatic ecosystems experiencing heavy nonpoint source pollution may undergo eutrophication, where the influx of excess organic matter and nutrients can result in toxic algal blooms, accelerated succession, and other ecological harms (Khan & Ansari, 2005). Similarly, the introduction of heavy metals into the environment can result in human exposure through biomagnification, where toxicants concentrate along the food chain, or the consumption of contaminated water (Singare et al., 2011).

II. Existing Approaches

The purpose of this section is to compare current approaches used to estimate water quality parameters and how they vary with land cover and land use changes. More specifically, we focused on tools that were capable of modeling nonpoint source pollution through nutrient and heavy metal loading with minimal input data required, noting the additional capabilities of each. The EPA Region 5 Model, Great Lakes Watershed Management System, and Soil & Water Assessment Tool were chosen for evaluation due to their relevance, accessibility, and current use in land conservation efforts.

A. EPA Region 5 Model

The Environmental Protection Agency's Region 5 division is one of ten federal regions created to facilitate easier operations with state and local governments, and represents six states: Illinois, Indiana, Michigan, Minnesota, Ohio, and Wisconsin (Williams, 1993). The EPA Region 5 Model is an Excel workbook that uses data from this geographical region to estimate nutrient and sediment load reductions based on varying land cover and land management practices. The model contains seven distinct worksheets, with focuses ranging from Gully

Stabilization to Urban Runoff. The most relevant of these worksheets to the Greenbelt Program is the Conservation Easement Load Reduction Worksheet, because it allows the user to quantify the water quality benefits of placing conservation easements on land parcels. More specifically, based on data from the Illinois EPA, the Conservation Easement Load Reduction Worksheet allows users to calculate changes in nutrient and heavy metal loading based on the following formula:

$$Load\ Reduction\ =\ (Unit\ Load\ of\ Proposed\ Use \times Area)\ -\ (Unit\ Load\ with\ Easement \times Area)$$

The Region 5 Model requires only two primary inputs to complete a calculation, namely the area of the land parcel in acres (stipulating whether it is sewered or unsewered) and the most probable developed use of the easement area. For the latter input, the user can select Commercial, Industrial, Institutional, Transportation, Multi-Family, Residential, or Agriculture. The nutrient and heavy metal loading calculations are based on a table embedded in the worksheet that contains the average pollutant load by land use type in pounds per acre per year, based on an inventory conducted by the Northeast Illinois Planning Commission in 1993 that was subsequently adopted by the Illinois EPA. In addition to the aforementioned types of developed land use, this table contains average pollutant load data for Open Space and Vacant land use types. In its standard form, the worksheet uses the input data to produce a "Load Reduction with Easement" estimate using the difference between the proposed land use and Open Space loading values, where Open Space refers to undeveloped natural areas.

For the purposes of the Greenbelt Program, The Conservation Fund produced an edited version of this worksheet in 2020 that automatically calculates the proposed difference in loading values for agricultural easements when compared to other developed land uses. The output of the tool shows the predicted change in load values for the following water quality parameters: Biochemical Oxygen Demand (BOD), Chemical Oxygen Demand (COD), Total Suspended Solids (TSS), Total Dissolved Solids (TDS), Total Nitrogen (TN), Total Kjeldahl Nitrogen (TKN), Dissolved Phosphorus (DP), Total Phosphorus (TP), Lead, Copper, Zinc, and Cadmium. Table 4.1 provides an example of this output for a sample area, the entirety of which resides in the River Raisin watershed.

While the EPA Region 5 Model provides its users with a simple method of inputting basic data in order to obtain water pollution estimates, it is entirely based on loading averages that are neither tailored to the study sites in question nor recent literature. The simplicity of the tool hinders the user from accounting for a plethora of variables that could influence nutrient and heavy metal loading, such as soil type, elevation, proximity to waterways, and location within the watershed. Additionally, the Illinois EPA data embedded in the tool has not been updated since 1993, despite the fact that the tool was most recently updated in 2010.

Table 4.1. EPA Region 5 Model output for a sample area (102 acres) in the River Raisin watershed, with most probable developed land use set to 'Residential.' Average pollutant load data sourced from Illinois EPA, representing unit area pollutant load estimates for Lake County, Illinois Lake Michigan Watersheds (August 1993).

Substance	Residential Loading (lbs/yr.)	Agricultural Loading (lbs/yr.)	Load Reduction with Agricultural Easement (lbs/yr.)
Biochemical Oxygen Demand (BOD)	1,122	306	816
Chemical Oxygen Demand (COD)	7,242	2,856	4,386
Total Suspended Solids (TSS)	15,708	15,606	102
Total Dissolved Solids (TDS)	22,236	9,098.4	13,137.6
Total Nitrogen (TN)	316.2	244.8	71.4
Total Kjeldahl Nitrogen (TKN)	163	92.62	70.38
Dissolved Phosphorus (DP)	13.26	8.16	5.1
Total Phosphorus (TP)	40.8	18.36	22.44
Lead	11.93	0.2	11.73
Copper	2.45	0.45	2
Zinc	45.9	7.04	38.86
Cadmium	0.1	0.02	0.08

B. Great Lakes Watershed Management System

The Great Lakes Watershed Management System (GLWMS) is an online tool developed by the Institute of Water Research at Michigan State University. Free to use, it allows users to track and predict a variety of water quality metrics at both coarse and fine scales. These metrics can be aggregated into customized reports and saved as individual projects for future reference. There are five primary modules for assessment in GLWMS: Water Erosion, Groundwater Recharge, Nutrient Loading, Nutrient Loading (enhanced), and Wind Erosion. Using these modules, the tool can be used to estimate the impacts of land-use changes and land management practices for any given area on the virtual map interface. This area can be defined by the user by manually drawing a polygon or by uploading a shapefile, provided it lies within the boundaries of the watersheds available in the tool.

Where the EPA Region 5 tool struggles to combine multiple data sources into one analysis, the GLWMS thrives. All modules can be run simultaneously over an area of interest,

and the parameters of each module can be adjusted to account for different landscape features or management practices. Furthermore, nutrient loading is broken down into two separate modules, standard and enhanced. The standard module uses the Long-Term Hydrological Impact Analysis (L-THIA) framework developed by Purdue University, which estimates changes in recharge, runoff, and nonpoint source pollution using historical land use, soil, and climate data. The enhanced module uses a web-based version of the Spreadsheet Tool for Estimating Pollutant Load (STEPL) framework developed by the EPA, which estimates changes in nonpoint source pollution using soil, wastewater, climate, land use, nutrient concentration, and other data. While both have similar functionality, the L-THIA model focuses more on historical climate data while STEPL focuses more on land management practices (Nejadhashemi et al., 2011). Table 4.2 provides an example of the output of the enhanced Nutrient Loading module for the same sample area in Table 4.1.

Powerful and simple to use, the GLWMS is an ideally designed tool for assessing water ecosystem services on a parcel-by-parcel basis. Its applicability in practice is, however, limited by the number of watersheds included in the interface. Only land parcels within the River Raisin, Shiawassee, and a handful of other watersheds in the Upper Midwest can be modeled, while parcels outside of these boundaries cannot, because the tool does not contain the necessary data for these geographical areas. Currently, the GLWMS does not contain modeling capabilities for the Huron River Watershed, within which a vast majority of Greenbelt properties reside. Moreover, the GLWMS only estimates two pollutants in the STEPL Nutrient Loading module (nitrogen and phosphorus) and four pollutants in the L-THIA Nutrient Loading module (phosphorus, copper, lead, and zinc), whereas the EPA Region 5 model estimates twelve (see Table 4.3 for model comparisons).

Table 4.2. Great Lakes Watershed Management System (GLWMS) enhanced Nutrient Loading module output for the sample area, with proposed land use change set to low density residential. Pollutant load data calculated using the EPA Spreadsheet Tool for Estimating Pollutant Load (STEPL) framework.

Substance	Current Annual Loading (lbs/yr.)	Change in Annual Loading (lbs/yr.)
Phosphorus	399.98	-187.27
Nitrogen	1504.83	-1078.35

C. Soil & Water Assessment Tool

The Soil & Water Assessment Tool (SWAT) is a GIS tool developed by the USDA Agricultural Research Service (ARS). The SWAT model simulates the quality and quantity of surface and ground water at the small watershed to river basin scale using primarily local climate, land cover, and land management information. It is used to predict the environmental impact of land use, land management practices, and climate change on outputs such as sediment yield, nutrient loading, crop yield, surface runoff, stream flow, groundwater flow, and water yield.

SWAT can be used to quantify water ecosystem services that are also related to climate mitigation. For example, Gathenya et al. (2011) applied SWAT to water conservation to simulate

hydrological processes and crop growth based on daily temperature, water availability, and other variables in Tibet. Immerzeel et al. (2008) used SWAT to consider how different climate change scenarios would affect streamflow and sediment yield. Determining the effects of rainfall, temperature, and infiltration capacity of land surface could serve as justification for modifying hydrology or adapting to climate change.

SWAT can run as a GIS extension tool on either ArcGIS or QGIS, but a potential downside to SWAT is the vast number of inputs required to run the tool. The first step in setting up a watershed simulation is to partition the watershed into subunits. Subbasins are the first level of subdivision in a watershed and are spatially related to one another, so outflow from one subbasin enters the adjacent one. This step requires information such as subbasins, channel segments, impoundments, and point sources. After subbasins are delineated, many individual files are required as inputs, including precipitation, temperature, solar radiation, wind speed, relative humidity, weather forecast, land cover, water use, and fertilizer. A full list of all the required and optional input files can be found in Appendix F.

In comparison to the EPA Region 5 Model and GLWMS, SWAT is a much more computationally intensive tool that requires substantial input, which is why it is typically only used by experienced hydrologists (Muleta & Nicklow, 2005). Unlike the other two models, we were unable to produce any results for the Greenbelt using SWAT due to lack of access to detailed input data pertaining to climate, sediment, pesticide use, bacteria, channel and impoundment processes, and land management practices. SWAT does go beyond the other models in terms of assessing not just quality, but also water quantity measures (e.g. stream and groundwater flow), but if the desired focus is water quality (nonpoint source pollution) and soil erosion, the other models are capable of calculating these outputs with greater ease (see Table 4.3).

Table 4.3. Comparison of three tools commonly used to assess land use impact on water ecosystem services: EPA Region 5 Model, Great Lakes Watershed Management System, and Soil & Water Assessment Tool. Data sourced from Illinois EPA, Michigan State University, USDA, and Bukhari et al. (2015).

	EPA Region 5 Model	**Great Lakes Watershed Management System**	**Soil & Water Assessment Tool**
Inputs	Acreage, proposed land use change	Acreage (via shapefile or drawn polygon), proposed land use change, land management practices	Watershed dimensions, climate, hydrologic cycle, sediment, nutrients, pesticides, bacteria, water quality, plants, channel and impoundment processes, land management practices
Outputs	Nutrient and heavy metal loads	Nutrient and heavy metal loads (L-THIA, STEPL), groundwater recharge, water erosion, wind erosion	Nutrient and heavy metal loads, sediment yield, crop yield, surface runoff, stream flow, groundwater flow, water yield
Format	Excel spreadsheet	Website	ArcGIS and QGIS extension
Accessibility	Free download from EPA website	Web tool with free user account activation	Free download but requires GIS software
Ease of Use	Simple spreadsheet interface, minimal data inputs	Simple web interface, several modules and data inputs	Complex GIS interface, difficult to calibrate, many detailed data inputs

III. Recommendations

Based on the information provided in this chapter, we have two primary recommendations for the Greenbelt program to improve and expand its analysis of water ecosystem services:

1. Provide a more accessible web-based version of the EPA Region 5 Model Conservation Easement worksheet; and
2. Work with the Institute of Water Research at Michigan State University to update the Great Lakes Management System to include other watersheds (namely the Huron River watershed) within the Greenbelt District.

To facilitate our first recommendation, we have reformatted the EPA Region 5 Conservation Load Reduction Calculator into a web page and shared it with the City. In addition to internal use, this file will ideally be hosted by the City and become available to all conservation practitioners looking to quickly analyze the potential water quality benefits of implementing conservation easements in the Great Lakes region. A Google Sites-hosted version of this website can be accessed at the following link, a preview of which is shown in Figure 4.2. https://sites.google.com/umich.edu/epa-r5-model/home?authuser=0

EPA Region 5 Load Reduction Calculator

Input information regarding proposed land use change, acreage, and easement type below.

Proposed Land Use Change:

Residential

Acres of Sewered Land:

0

Acres of Unsewered Land:

100

SUBMIT

Results

Substance:	Load (lbs/yr):	Load Reduction with Agricultural Easement (lbs/yr):	Load Reduction with Open Space Easement (lbs/yr):
Biochemical Oxygen Demand (BOD)	1100	800	1060
Chemical Oxygen Demand (COD)	7100	4300	5600
Total Suspended Solids (TSS)	15400	100	13400
Total Dissolved Solids (TDS)	21800	12880	-2300
Total Nitrogen (TN)	310	70	290
Total Kjeldahl Nitrogen (TKN)	160	69	116
Dissolved Phosphorus (DP)	13	5	10
Total Phosphorus (TP)	40	22	27
Lead	11.7	11.5	11.16
Copper	2.4	1.96	2.2
Zinc	45	38.1	42
Cadmium	0.1	0.08	0.09

Figure 4.2. Web-based version EPA Region 5 Model Conservation Easement Load Reduction Calculator. All data sourced from the Illinois EPA.

To facilitate our second recommendation, we have worked with representatives of the Institute of Water Research to determine the best course of action to provide the City, as well as other local land conservancies, with an updated version of the Great Lakes Watershed Management System. This updated version would permit analysis within the Greenbelt District and be more finely tuned to the geography, geology, and hydrology of the area. More specifically, we recommend that the Greenbelt Program attempt to fund this project via the Technical Enhancement Funds available through the United States Department of Agriculture's Regional Conservation Partners Program (RCPP). These funds are designed to facilitate innovation that would otherwise not be available to a group of conservation practitioners, making it an ideal choice for the Greenbelt Program.

By utilizing the aforementioned tools and recommendations in this chapter, the Greenbelt Program can assess key ecosystem services related to water such as nonpoint source pollution mitigation. Further adaptation of these tools could facilitate reporting on other ecosystem services that were not included in this analysis but are largely impacted by changes in land use, including flooding, soil erosion, and climate regulation. Such information can be crucial to communicate to the public in order to garner further support for conservation efforts and raise awareness for the further protection of the ecosystem services provided by the parks and easements throughout the Greenbelt District.

Literature Cited

Arnold, J. G., Kiniry, J. R., Srinivasan, R., Williams, J.R., Haney, E. B., & Neitsch, S., L. (2012). Soil & Water Assessment Tool: Input/Output Documentation [PDF file]. Retrieved from https://swat.tamu.edu/docs

Bukhari, H., Elkin, J., Hemken, M., Lichten, N., Pettit, R., & Shattuck, S. (2015). Evaluation of different approaches for controlling phosphorus pollution in the Maumee River watershed [PDF file]. Retrieved from https://deepblue.lib.umich.edu/handle/2027.42/111006

Gathenya, M., Mwangi, H., Coe, R., & Sang, J. (2011). Climate-and land use-induced risks to watershed services in the Nyando River Basin, Kenya. *Experimental Agriculture, 47*(2), 339. https://doi.org/10.1017/S001447971100007X

Grizzetti, B., Lanzanova, D., Liquete, C., Reynaud, A., & Cardoso, A. C. (2016). Assessing water ecosystem services for water resource management. *Environmental Science & Policy, 61*, 194-203.

Immerzeel, W., Stoorvogel, J., & Antle, J. (2008). Can payments for ecosystem services secure the water tower of Tibet?. *Agricultural Systems, 96*(1-3), 52-63. https://doi.org/10.1016/j.agsy.2007.05.005

Jahre, J. (2020, October 5). *EnviroAtlas Benefit Category: Clean and Plentiful Water*. United States Environmental Protection Agency. https://www.epa.gov/enviroatlas/enviroatlas-benefit-category-clean-and-plentiful-water

Khan, F. A., & Ansari, A. A. (2005). Eutrophication: an ecological vision. *The Botanical Review, 71*(4), 449-482.

Leemans, R., & De Groot, R. S. (2003). Millennium Ecosystem Assessment: Ecosystems and human well-being: a framework for assessment.

Muleta, M. K., & Nicklow, J. W. (2005). Sensitivity and uncertainty analysis coupled with automatic calibration for a distributed watershed model. *Journal of Hydrology, 306*(1-4), 127-145. https://doi.org/10.1016/j.jhydrol.2004.09.005

Nejadhashemi, A. P., Woznicki, S. A., & Douglas-Mankin, K. R. (2011). Comparison of four models (STEPL, PLOAD, L-THIA, and SWAT) in simulating sediment, nitrogen, and phosphorus loads and pollutant source areas. *Transactions of the ASABE, 54*(3), 875-890.

Singare, P. U., Jagtap, A. G., & Lokhande, R. S. (2011). Water pollution by discharge effluents from Gove Industrial Area of Maharashtra, India: Dispersion of heavy metals and their Toxic effects. *International Journal of Global Environmental Issues, 11*(1), 28-36.

The Conservation Fund. (2019). City of Ann Arbor Greenbelt Program: Strategic Plan. Revised 2019. [PDF file]. Retrieved from https://www.a2gov.org/greenbelt/Pages/greenbelthome.aspx

United States Environmental Protection Agency (U.S. EPA). (2020, October 7). *Basic Information about Nonpoint Source (NPS) Pollution.* https://www.epa.gov/nps/basic-information-about-nonpoint-source-nps-pollution

Williams, D. C. (1993, March). *Why Are Our Regional Offices and Labs Located Where They Are? A Historical Perspective on Siting.* United States Environmental Protection Agency. https://www.epa.gov/history/why-are-our-regional-offices-and-labs-located-where-they-are-historical-perspective-siting

Appendix A: Maps of Field Sample Plot Locations

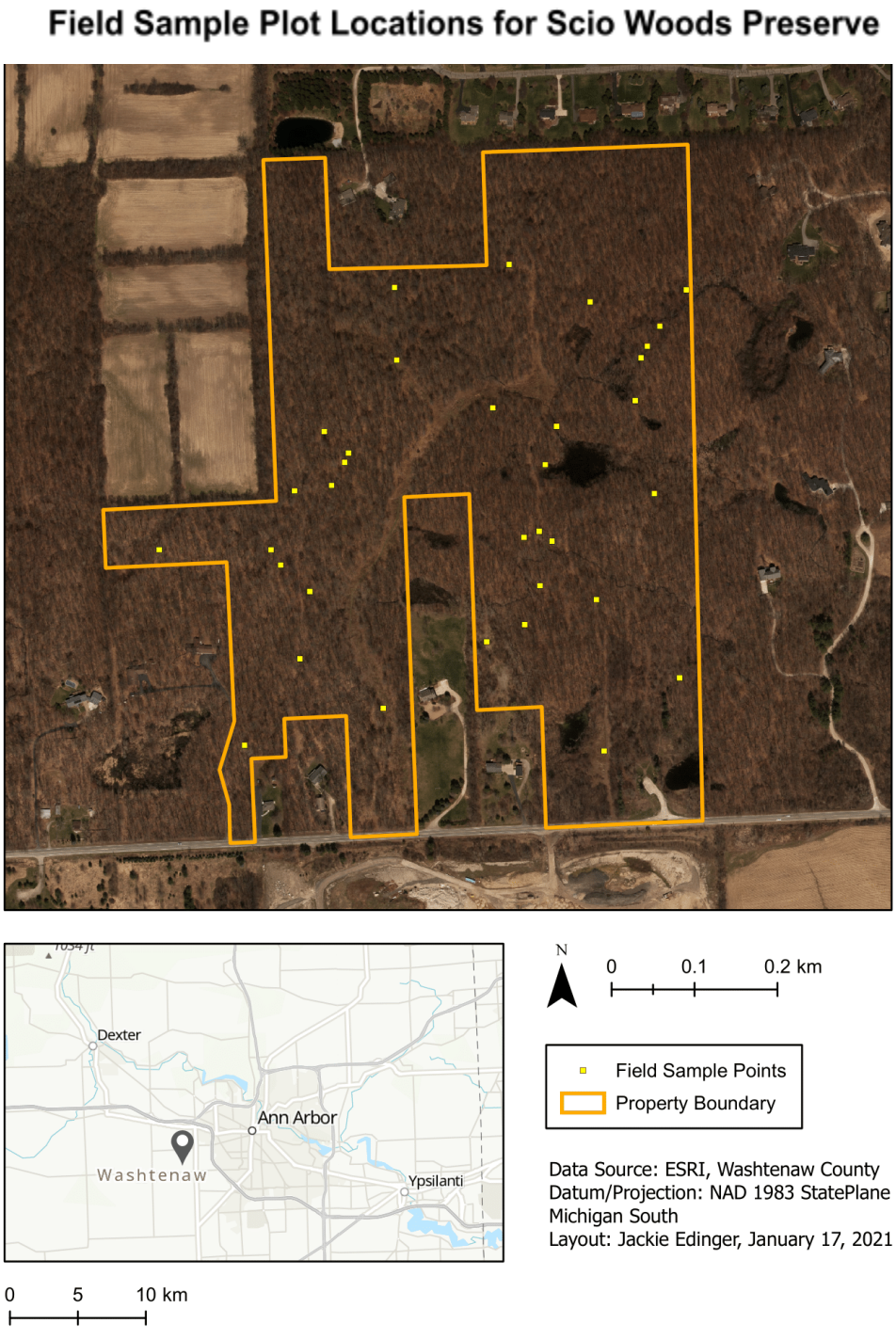

Field Sample Plot Locations for Brauer Preserve

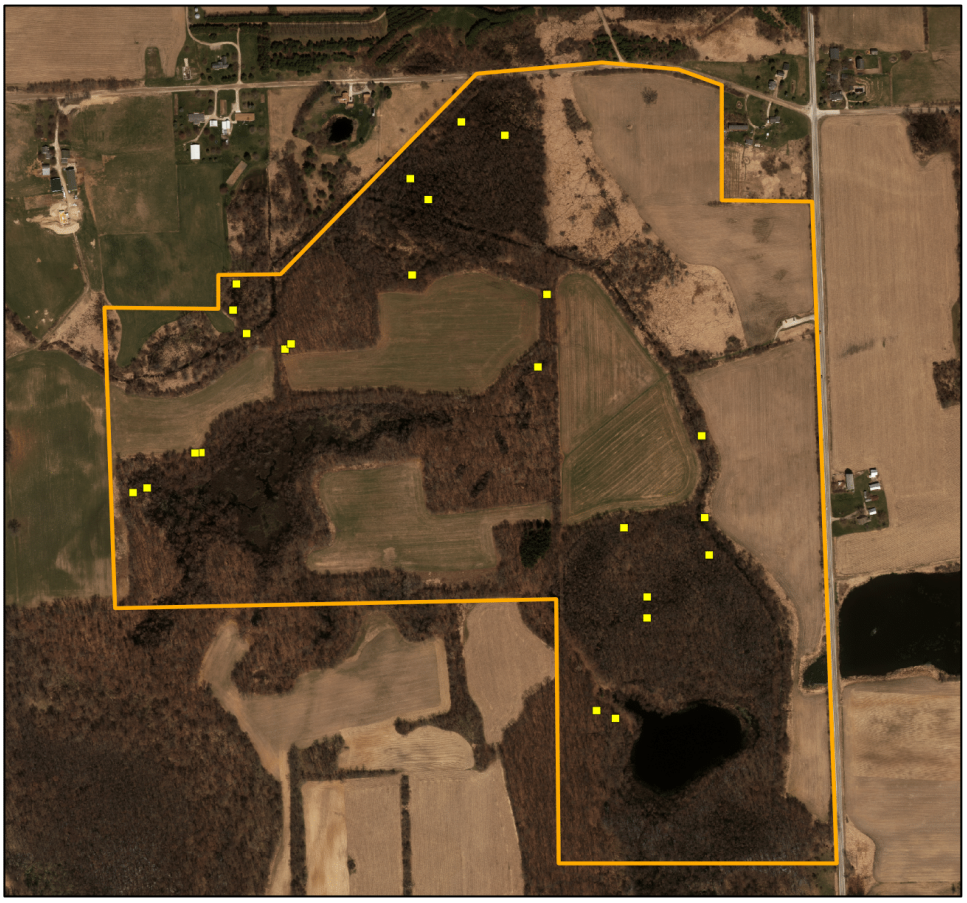

0 5 10 km

N

0 0.1 0.2 km

Field Sample Points
Property Boundary

Data Source: ESRI, Washtenaw County
Datum/Projection: NAD 1983 StatePlane Michigan South
Layout: Jackie Edinger, January 17, 2021

Field Sample Plot Locations for Creekshead Preserve

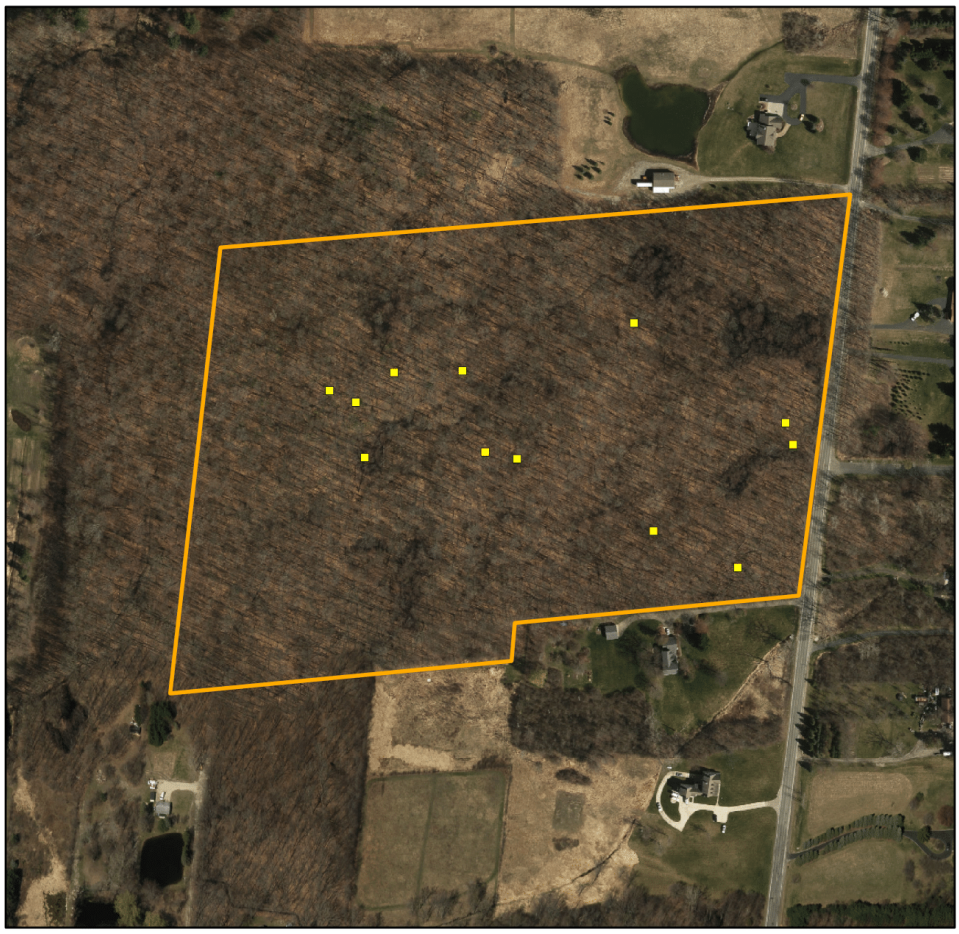

0 5 10 km

N

0 0.1 0.2 km

Field Sample Points
Property Boundary

Data Source: ESRI, Washtenaw County
Datum/Projection: NAD 1983 StatePlane Michigan South
Layout: Jackie Edinger, January 17, 2021

Appendix B: Field Data

Site 1: Scio Woods Preserve

Collection Date: 9/27/2020					
Plot #	**Tree #**	**Species Code**	**Species**	**DBH (cm)**	**Notes**
1	1	ACSA	*Acer saccharum*	14.0	
	2	ACSA	*Acer saccharum*	17.3	
	3	TIAM	*Tilia americana*	41.7	
	4	TIAM	*Tilia americana*	47.4	
	5	TIAM	*Tilia americana*	51.4	
	6	TIAM	*Tilia americana*	31.0	
2	1	CAOV	*Carya ovata*	36.9	
3	1	ACSA	*Acer saccharum*	21.7	
	2	ACSA	*Acer saccharum*	19.2	
	3	ACSA	*Acer saccharum*	15.6	
	4	QUAL	*Quercus alba*	46.5	
	5	QUAL	*Quercus alba*	26.2	
	6	QUAL	*Quercus alba*	51.2	
4	0	N/A	N/A	N/A	no trees in this plot
5	1	AIAL	*Ailanthus altissima*	16.9	
6	1	QURU	*Quercus rubra*	43.8	
	2	CACO	*Carya cordiformis*	36.7	
7	1	ACSA	*Acer saccharum*	12.4	
	2	ACSA	*Acer saccharum*	20.5	
	3	ACSA	*Acer saccharum*	15.1	
	4	ACSA	*Acer saccharum*	58.2	tag #1020
	5	OSVI	*Ostrya virginiana*	21.5	tag #1021
	6	FAGR	*Fagus grandifolia*	17.4	
	7	TIAM	*Tilia americana*	28.0	tag #1015
	8	PRSE	*Prunus serotina*	30.0	
	9	PRSE	*Prunus serotina*	29.9	
8	1	ACSA	*Acer saccharum*	16.2	
	2	CACO	*Carya cordiformis*	29.5	
	3	ACSA	*Acer saccharum*	12.3	
	4	TIAM	*Tilia americana*	44.3	
	5	ACSA	*Acer saccharum*	19.8	
9	1	ACSA	*Acer saccharum*	36.1	
	2	QUAL	*Quercus alba*	48.6	
	3	ACSA	*Acer saccharum*	16.1	
	4	ACSA	*Acer saccharum*	13.7	
10	1	CACO	*Carya cordiformis*	40.4	
	2	TIAM	*Tilia americana*	23.2	
	3	ACSA	*Acer saccharum*	20.7	
	4	ACSA	*Acer saccharum*	19.5	
	5	ACSA	*Acer saccharum*	13.3	
	6	CACO	*Carya cordiformis*	18.8	

Collection Date: 10/5/2020					
Plot #	**Tree #**	**Species Code**	**Species**	**DBH (cm)**	**Notes**
11	1	OSVI	*Ostrya virginiana*	15.9	
	2	OSVI	*Ostrya virginiana*	16.1	
	3	OSVI	*Ostrya virginiana*	13.3	
	4	ACSA	*Acer saccharum*	17.1	
	5	JUNI	*Juglans nigra*	37.4	

Site 1: Scio Woods Preserve (cont'd)

12	1	ACSA	*Acer saccharum*	14.7	
	2	QUAL	*Quercus alba*	28.4	
	3	QURU	*Quercus rubra*	13.4	
	4	ACSA	*Acer saccharum*	16.9	
	5	TIAM	*Tilia americana*	25.3	
	6	CAOV	*Carya ovata*	35.7	
	7	QUAL	*Quercus alba*	49.0	
	8	CAGL	*Carya glabra*	19.7	
13	0	N/A	*N/A*	N/A	no trees in this plot
14	1	QUAL	*Quercus alba*	47.5	
	2	CAOV	*Carya ovata*	36.5	
	3	QUAL	*Quercus alba*	32.8	
	4	ACSA	*Acer saccharum*	16.0	
	5	CAGL	*Carya glabra*	36.9	
15	0	N/A	*N/A*	N/A	no trees in this plot
16	1	FAGR	*Fagus grandifolia*	33.2	
	2	CAGL	*Carya glabra*	25.9	
	3	ACSA	*Acer saccharum*	19.2	
17	1	QUAL	*Quercus alba*	25.1	
	2	QUAL	*Quercus alba*	21.8	
	3	TIAM	*Tilia americana*	14.3	
	4	TIAM	*Tilia americana*	11.0	
	5	QURU	*Quercus rubra*	35.9	
	6	CAGL	*Carya glabra*	21.2	
	7	CAGL	*Carya glabra*	14.5	
	8	QUAL	*Quercus alba*	15.7	
	9	TIAM	*Tilia americana*	16.8	
	10	ACSA	*Acer saccharum*	11.9	
	11	OSVI	*Ostrya virginiana*	11.0	
18	1	TIAM	*Tilia americana*	26.4	*near big trees! 82cm dbh!!
	2	ACSA	*Acer saccharum*	49.9	
	3	ACSA	*Acer saccharum*	15.4	
19	1	QUAL	*Quercus alba*	58.5	
	2	ACSA	*Acer saccharum*	25.8	
	3	QUAL	*Quercus alba*	57.4	
	4	ACSA	*Acer saccharum*	30.6	
	5	ACSA	*Acer saccharum*	44.2	
20	1	ACSA	*Acer saccharum*	46.7	frog and pawpaw
	2	ACSA	*Acer saccharum*	42.2	
21	1	FAGR	*Fagus grandifolia*	11.2	

Collection Date: 10/6/2020					
Plot #	**Tree #**	**Species Code**	**Species**	**DBH (cm)**	**Notes**
22	1	JUNI	*Juglans nigra*	10.8	
	2	SAAL	*Salix alba*	15.1	
	3	SAAL	*Salix alba*	21.9	
	4	LITU	*Liriodendron tulipifera*	18.0	
	5	LITU	*Liriodendron tulipifera*	12.3	
	6	LITU	*Liriodendron tulipifera*	17.3	
23	1	PODE	*Populus deltoides*	52.0	plot from 9/27 points
	2	CAOV	*Carya ovata*	32.7	

Site 1: Scio Woods Preserve (cont'd)

24	1	TIAM	*Tilia americana*	58.3	
	2	CAGL	*Carya glabra*	38.0	
	3	ACSA	*Acer saccharum*	14.6	
	4	ACSA	*Acer saccharum*	16.6	
25	1	ACSA	*Acer saccharum*	12.3	plot from 9/27 points
	2	QUAL	*Quercus alba*	63.1	
26	1	ACSA	*Acer saccharum*	15.4	
	2	JUNI	*Juglans nigra*	31.4	
	3	PRSE	*Prunus serotina*	18.3	
	4	ACSA	*Acer saccharum*	22.8	
27	1	ACSA	*Acer saccharum*	10.9	
	2	CACO	*Carya cordiformis*	44.4	
	3	ACSA	*Acer saccharum*	14.2	
	4	ACSA	*Acer saccharum*	19.8	
	5	ACSA	*Acer saccharum*	23.4	
	6	ACSA	*Acer saccharum*	16.5	
	7	ACSA	*Acer saccharum*	13.5	
	8	ACSA	*Acer saccharum*	14.9	
	9	ACSA	*Acer saccharum*	21.4	
28	1	ACSA	*Acer saccharum*	63.2	
	2	PODE	*Populus deltoides*	39.0	
	3	ACSA	*Acer saccharum*	50.1	
29	1	ACSA	*Acer saccharum*	18.8	
	2	ACSA	*Acer saccharum*	18.7	
	3	ACSA	*Acer saccharum*	20.2	
	4	ACSA	*Acer saccharum*	17.5	
	5	ACSA	*Acer saccharum*	46.7	
	6	ACSA	*Acer saccharum*	19.4	
	7	ACSA	*Acer saccharum*	19.7	
30	1	TIAM	*Tilia americana*	50.3	
	2	ACSA	*Acer saccharum*	21.9	
	3	ACSA	*Acer saccharum*	52.1	
	4	ACSA	*Acer saccharum*	13.0	
	5	ACSA	*Acer saccharum*	13.1	
31	1	OSVI	*Ostrya virginiana*	11.0	plot from 9/27 points
	2	PRSE	*Prunus serotina*	27.0	
	3	ACSA	*Acer saccharum*	12.9	
	4	PRSE	*Prunus serotina*	19.3	
	5	OSVI	*Ostrya virginiana*	12.4	
32	1	ACSA	*Acer saccharum*	10.9	plot from 9/27 points
	2	ACSA	*Acer saccharum*	13.9	
	3	ACSA	*Acer saccharum*	18.3	
33	1	ACSA	*Acer saccharum*	33.1	plot from 9/27 points
	2	ACSA	*Acer saccharum*	16.6	
	3	CAGL	*Carya glabra*	20.6	
	4	TIAM	*Tilia americana*	17.7	
	5	TIAM	*Tilia americana*	28.6	

Site 2: Brauer Preserve

Collection Date: 10/10/2020					
Plot #	**Tree #**	**Species Code**	**Species**	**DBH (cm)**	**Notes**
1	1	ACRU	*Acer rubrum*	28.5	
	2	ACRU	*Acer rubrum*	43.1	
	3	ACRU	*Acer rubrum*	23.4	
	4	QUMA	*Quercus macrocarpa*	47.0	
	5	QUMA	*Quercus macrocarpa*	27.0	
	6	ACRU	*Acer rubrum*	37.1	
2	1	PRSE	*Prunus serotina*	30.2	plot is in poison ivy patch
	2	QURU	*Quercus rubra*	34.4	
	3	ACRU/ACSA	*Acer* ---	100.2	weird monster tree
3	1	ACRU	*Acer rubrum*	67.9	
	2	ACRU	*Acer rubrum*	36.5	
	3	ACRU	*Acer rubrum*	34.2	
	4	ACRU	*Acer rubrum*	29.9	
4	1	ACSA*	*Acer saccharinum*	19.9	
	2	ACSA*	*Acer saccharinum*	20.4	
5	1	ACSA*	*Acer saccharinum*	24.7	
	2	ACSA*	*Acer saccharinum*	34.9	
	3	ACSA*	*Acer saccharinum*	42.0	
6	1	ACSA*	*Acer saccharinum*	62.1	
	2	ACSA*	*Acer saccharinum*	51.6	
	3	ACSA*	*Acer saccharinum*	50.4	
	4	ULAM	*Ulmus americana*	14.8	
7	0	N/A	*N/A*	N/A	no trees in this plot
8	1	POGR	*Populus grandidentata*	26.6	
	2	ULAM	*Ulmus americana*	21.5	
9	1	ACSA	*Acer saccharum*	67.5	
10	1	ACSA	*Acer saccharum*	80.9	
	2	ULAM	*Ulmus americana*	22.8	
	3	ULAM	*Ulmus americana*	26.1	
	4	ULAM	*Ulmus americana*	22.0	
11	1	ACSA*	*Acer saccharinum*	52.7	
	2	ULAM	*Ulmus americana*	11.8	
	3	ACSA*	*Acer saccharinum*	28.6	
	4	ACSA*	*Acer saccharinum*	37.4	
12	1	ACRU	*Acer rubrum*	36.6	
	2	ACRU	*Acer rubrum*	44.4	
13	1	ACSA*	*Acer saccharinum*	20.5	
	2	ACSA*	*Acer saccharinum*	36.4	
	3	ACSA*	*Acer saccharinum*	41.3	
14	0	N/A	*N/A*	N/A	no trees in this plot
15	1	JUNI	*Juglans nigra*	26.5	
	2	ULAM	*Ulmus americana*	20.8	
	3	ULAM	*Ulmus americana*	14.5	

Site 2: Brauer Preserve (cont'd)

Collection Date: 10/24/2020					
Plot #	**Tree #**	**Species Code**	**Species**	**DBH (cm)**	**Notes**
16	1	ACSA*	*Acer saccharinum*	54.3	6 ft. buttonbush!
	2	ACSA*	*Acer saccharinum*	17.6	
	3	ACSA*	*Acer saccharinum*	17.4	
	4	ACSA*	*Acer saccharinum*	24.6	connected at base
	5	ACSA*	*Acer saccharinum*	18.7	
	6	ACSA*	*Acer saccharinum*	38.6	
17	1	ACSA*	*Acer saccharinum*	42.6	
	2	ACSA*	*Acer saccharinum*	18.2	
	3	ACSA*	*Acer saccharinum*	25.6	
	4	ACSA*	*Acer saccharinum*	34.4	connected at base
	5	ACSA*	*Acer saccharinum*	10.0	
	6	ACSA*	*Acer saccharinum*	23.6	
	7	ACSA*	*Acer saccharinum*	28.2	
	8	ACSA*	*Acer saccharinum*	65.7	
	9	ACSA*	*Acer saccharinum*	57.3	
18	1	PRSE	*Prunus serotina*	17.7	
	2	ACSA*	*Acer saccharinum*	12.5	
	3	ACSA*	*Acer saccharinum*	24.5	
	4	ACSA*	*Acer saccharinum*	15.4	
19	1	ACSA*	*Acer saccharinum*	23.4	
	2	ACSA*	*Acer saccharinum*	12.3	
	3	ULAM	*Ulmus americana*	22.0	
20	0	N/A	*N/A*	N/A	*Northern hackberry and common elder
21	1	ACSA*	*Acer saccharinum*	34.6	
	2	ACSA*	*Acer saccharinum*	27.8	
22	1	FRAM	*Fraxinus americana*	15.2	*bittersweet nightshade in plot
23	1	PRSE	*Prunus serotina*	12.7	
	2	QUVE	*Quercus velutina*	88.6	connected at base
	3	QUVE	*Quercus velutina*	43.6	measured above split at height of 1.5m
	4	QUVE	*Quercus velutina*	58.6	
24	1	PRSE	*Prunus serotina*	11.3	
	2	ULAM	*Ulmus americana*	24.9	
	3	PRSE	*Prunus serotina*	22.1	
	4	ACRU	*Acer rubrum*	17.1	
	5	ULAM	*Ulmus americana*	11.0	
	6	PRSE	*Prunus serotina*	18.6	
	7	QUVE	*Quercus velutina*	72.2	

*all ACSA in Brauer Preserve are silver maples, except in Plots 9 & 10 which are sugar maples

Site 3: Creekshead Preserve

Collection Date: 10/25/2020					
Plot #	**Tree #**	**Species Code**	***Species***	**DBH (cm)**	**Notes**
1	1	ACSA	*Acer saccharum*	21.9	
	2	CACO	*Carya cordiformis*	34.0	
	3	ACSA	*Acer saccharum*	12.0	
	4	TIAM	*Tilia americana*	44.8	
	5	ACSA	*Acer saccharum*	12.9	
	6	CACO	*Carya cordiformis*	30.6	
	7	ACSA	*Acer saccharum*	22.4	
2	1	QUMA	*Quercus macrocarpa*	19.3	
	2	QUMA	*Quercus macrocarpa*	13.7	
	3	QURU	*Quercus rubra*	34.1	
	4	QUMA	*Quercus macrocarpa*	17.1	
	5	QUMA	*Quercus macrocarpa*	32.1	
	6	QUMA	*Quercus macrocarpa*	19.5	
	7	QUMA	*Quercus macrocarpa*	19.2	
	8	QUMA	*Quercus macrocarpa*	13.5	
	9	ACSA	*Acer saccharum*	23.6	
	10	ACNI	*Acer nigrum*	15.0	
3	1	ACSA	*Acer saccharum*	11.7	
	2	TIAM	*Tilia americana*	18.2	
	3	TIAM	*Tilia americana*	48.9	
	4	ACSA	*Acer saccharum*	10.3	
	5	TIAM	*Tilia americana*	53.2	connected at base
	6	TIAM	*Tilia americana*	21.5	
	7	ACSA	*Acer saccharum*	30.6	
4	1	QURU	*Quercus rubra*	79.9	
	2	ACSA	*Acer saccharum*	41.6	connected at base
	3	ACSA	*Acer saccharum*	14.2	
5	1	TIAM	*Tilia americana*	22.9	
	2	FAGR	*Fagus grandifolia*	13.5	
	3	TIAM	*Tilia americana*	14.5	
	4	FAGR	*Fagus grandifolia*	27.6	
	5	TIAM	*Tilia americana*	45.9	
	6	FAGR	*Fagus grandifolia*	27.8	
6	1	FAGR	*Fagus grandifolia*	32.2	
	2	FAGR	*Fagus grandifolia*	36.0	
	3	ACSA	*Acer saccharum*	14.2	
	4	FAGR	*Fagus grandifolia*	14.0	
7	1	TIAM	*Tilia americana*	29.0	
	2	ACSA	*Acer saccharum*	10.2	
	3	ACSA	*Acer saccharum*	18.9	
	4	FAGR	*Fagus grandifolia*	11.2	

Site 3: Creekshead Preserve (cont'd)

8	1	ACSA	*Acer saccharum*	12.8	
	2	ACSA	*Acer saccharum*	48.7	
	3	FAGR	*Fagus grandifolia*	47.7	
9	1	QURU	*Quercus rubra*	26.0	
	2	ACSA	*Acer saccharum*	41.7	
	3	ACSA	*Acer saccharum*	16.0	
	4	FAGR	*Fagus grandifolia*	11.3	
	5	FAGR	*Fagus grandifolia*	12.5	
10	1	TIAM	*Tilia americana*	64.3	
	2	TIAM	*Tilia americana*	24.5	connected at base
	3	TIAM	*Tilia americana*	11.2	
	4	QURU	*Quercus rubra*	16.7	
11	1	ACRU	*Acer rubrum*	16.5	
	2	ACRU	*Acer rubrum*	41.3	
	3	ACRU	*Acer rubrum*	42.2	
	4	ACRU	*Acer rubrum*	15.5	
	5	ACRU	*Acer rubrum*	39.3	
	6	ACRU	*Acer rubrum*	27.0	connected at base
	7	ACRU	*Acer rubrum*	21.7	
	8	ACSA*	*Acer saccharinum*	32.0	
12	1	TIAM	*Tilia americana*	17.0	
	2	ACSA	*Acer saccharum*	14.2	
	3	ACSA	*Acer saccharum*	13.1	
	4	TIAM	*Tilia americana*	32.9	
	5	ACSA	*Acer saccharum*	18.0	

* all ACSA at Creekshead Preserve are sugar maples, except for Plot 8 which is a silver maple

Appendix C: Summary of Aboveground Carbon Storage by Property

Project Name	Biomass (kg)	Aboveground Carbon (kg)	Aboveground Carbon (Mg)	CO_2 Equivalent (metric tons CO_2)	EPA $ Conversion for Aboveground Carbon
Alexander, Robbin	732,829	366,414	366	1,344	$ 68,520.11
Bloomer, Tom & Rosanne	397,548	198,774	199	729	$ 37,171.03
Fishbeck, William & Betty (41 acres)	0	0	0	0	$ -
Fishbeck, William & Betty (116 acres)	598,717	299,358	299	1,098	$ 55,980.51
Kapp, Dale	1,425,764	712,882	713	2,614	$ 133,310.17
Cares, John & Jean	2,437,645	1,218,822	1,219	4,469	$ 227,921.86
Alexander, John and Beverly	238,957	119,478	119	438	$ 22,342.68
Honke (Cavanaugh)	744,698	372,349	372	1,365	$ 69,629.90
Maulbetsch	422,278	211,139	211	774	$ 39,483.32
Botero	749,387	374,693	375	1,374	$ 70,068.31
Fox	1,024,635	512,318	512	1,879	$ 95,804.28
Pellerito aka Lakeside Development LLC aka Mitigation Solutions aka Oakland	505,066	252,533	253	926	$ 47,224.10
Clark, Brad and Mary	1,123,255	561,628	562	2,059	$ 105,025.33
Landsberg, Carol P. Trust	1,172,774	586,387	586	2,150	$ 109,655.32
Merkel / Heller	856,602	428,301	428	1,570	$ 80,092.97
Smyth	1,124,307	562,154	562	2,061	$ 105,123.68
Whitney	1,743,716	871,858	872	3,197	$ 163,038.89
Webster Church	2,345,888	1,172,944	1,173	4,301	$ 219,342.49
Bloch (23 acres)	91,539	45,770	46	168	$ 8,558.98
Newton (Green Things)	688,270	344,135	344	1,262	$ 64,353.79
Gould	35,665	17,833	18	65	$ 3,334.73
Braun, Charles and Catherine	1,309,479	654,739	655	2,401	$ 122,437.39
Dudley, Open Roads Development	5,666,318	2,833,159	2,833	10,388	$ 529,805.59
Biltmore / Superior / Geddes aka DBN Investors LLC	789,742	394,871	395	1,448	$ 73,841.56
Pardon	133,329	66,665	67	244	$ 12,466.40
Nixon, William and Cherie	665,135	332,568	333	1,219	$ 62,190.71
Hilton, Walter Trust (Mason)	115,674	57,837	58	212	$ 10,815.63
Zeeb, Kenny	323,860	161,930	162	594	$ 30,281.18
Girbach (Vestergaard)	421,195	210,597	211	772	$ 39,382.06
Braun, Thomas & Theodore	889,909	444,955	445	1,632	$ 83,207.28
Ledwidge	574,748	287,374	287	1,054	$ 53,739.41
Geiger (213 acres)	67,556	33,778	34	124	$ 6,316.58
Geiger (116 acres)	943,418	471,709	472	1,730	$ 88,210.37
Lindemann and Weidmayer	534,028	267,014	267	979	$ 49,932.11

Thomas and Lobato	158,643	79,322	79	291	$ 14,833.28
VanNatter	52,430	26,215	26	96	$ 4,902.25
Bloch (33 acres)	778,365	389,183	389	1,427	$ 72,777.80
Ford-Goldsmith	308,685	154,342	154	566	$ 28,862.29
Boike (Maulbetsch)	23	12	0	0	$ 2.16
Drake - South	3,170,849	1,585,425	1,585	5,813	$ 296,477.08
Schultz, Robert	735,373	367,686	368	1,348	$ 68,757.99
Schumacher, Carol	504,207	252,103	252	924	$ 47,143.74
Hornback, Dan and Amy (Kadykowski)	2,076,656	1,038,328	1,038	3,807	$ 194,169.10
Wolf and Sheldon	5,512	2,756	3	10	$ 515.41
Novick, Jack and Kerry Kelly	453	226	0	1	$ 42.34
Drake - North	18,900	9,450	9	35	$ 1,767.17
Domino Farms aka DF Land Development (12 acres)	573,514	286,757	287	1,051	$ 53,624.03
Moore	106,534	53,267	53	195	$ 9,961.04
Polliey	49,196	24,598	25	90	$ 4,599.84
White aka McCleery	37,450	18,725	19	69	$ 3,501.60
VanCurler	5,372,843	2,686,421	2,686	9,850	$ 502,365.38
DF Land Development LLC (81 acres)	904,060	452,030	452	1,657	$ 84,530.34
Guenther - West	331,566	165,783	166	608	$ 31,001.74
Guenther - East	856,469	428,235	428	1,570	$ 80,080.59
Hall, James S. Revocable Trust	2,475,211	1,237,606	1,238	4,538	$ 231,434.34
Smith, Carol Trust	2,906,246	1,453,123	1,453	5,328	$ 271,736.45
Pringle, John and Beverly Mitchell (shared with LAC)	760,298	380,149	380	1,394	$ 71,088.53
Rogers	84,221	42,110	42	154	$ 7,874.72
Lada Rolling Acres, LLC	995,213	497,606	498	1,825	$ 93,053.25
DeVine-Koselka	3,359,476	1,679,738	1,680	6,159	$ 314,113.91
Seeley Farm	770,421	385,210	385	1,412	$ 72,034.98
Shatter Family Trust	688,310	344,155	344	1,262	$ 64,357.53
Stiles-Kaldjian	1,054,217	527,109	527	1,933	$ 98,570.20
Lepkowski	1,235,910	617,955	618	2,266	$ 115,558.65
Koch	50,631	25,315	25	93	$ 4,734.04
Stepien	546,459	273,229	273	1,002	$ 51,094.34
Haas	1,208,086	604,043	604	2,215	$ 112,957.10
Lambarth	1,497,117	748,558	749	2,745	$ 139,981.67
Boss & Bull Holdings, LLC	74,787	37,394	37	137	$ 6,992.67
Moehrle	549,374	274,687	275	1,007	$ 51,366.89

Totals	Biomass (kg)	Aboveground Carbon (kg)	Aboveground Carbon (Mg)	CO_2 Equivalent (metric tons CO_2)	EPA $ Conversion for Aboveground Carbon
	65,191,634	32,595,817	32,596	119,519	$ 6,095,473.15

To convert mass of aboveground carbon stored in kilograms to other metrics that communicate their value, we used a variety of available sources and conversion standards. The table below shows the social cost and carbon emission equivalents for all current Greenbelt properties. The social cost of carbon represents the societal costs, in terms of the long-term damage done to both the environment and human health, that are associated with the emission of one extra ton of CO_2 (U.S. EPA, 2016). Social cost and passenger vehicle mile emission estimates came from the EPA's Greenhouse Gases Equivalencies Calculator, airline mile emission estimates were sourced from BlueSkyModel, and yearly average household emission data was gathered using the CoolClimate Household Calculator (U.S. EPA, 2021; BlueSkyModel; CoolClimate Network). A different valuation model from Hungate et al. (2017) estimates the social cost of carbon at $42 to $400 per metric ton of C, with a median value of $137. The estimates from this model are lower than those calculated using the EPA social cost of carbon because the units of this model are metric tons of C while the units for the EPA model are metric tons of CO_2. Using the median value from the Hungate et al. (2017) model, we calculated the social cost of aboveground carbon storage for all Greenbelt properties to be $4,465,626.90.

Total Aboveground Carbon (kg)	Social Cost ($)*	Hungate et al. (2017)**	Passenger Vehicle Miles Equivalent (mi)	Airline Miles Equivalent (mi)	Avg. Annual Ann Arbor Household Emissions Equivalent (# of households)
32,595,817	$ 6,095,473.15	$4,465,626.90	80,682,715	1,348,245	2,716

* These calculations used the 2021 social cost of carbon value of $51/metric ton CO_2

** This is described by Hungate et al. (2017) as the median estimate of carbon reduction benefit with a value of $137/metric ton C

Literature Cited

BlueSkyModel. https://blueskymodel.org

CoolClimate Network. *Household calculator*. https://coolclimate.org/calculator

Hungate, B. A., Barbier, E. B., Ando, A. W., Marks, S. P., Reich, P. B., Van Gestel, N., ... & Cardinale, B. J. (2017). The economic value of grassland species for carbon storage. *Science Advances, 3*(4), e1601880.

United States Environmental Protection Agency (U.S. EPA). (2016, December). *Social Cost of Carbon* [PDF file]. https://www.epa.gov/sites/production/files/2016-12/documents/social_cost_of_carbon_fact_sheet.pdf

United States Environmental Protection Agency (U.S. EPA). (2021, March 11). *Greenhouse Gases Equivalencies Calculator - Calculations and References*. https://www.epa.gov/energy/greenhouse-gases-equivalencies-calculator-calculations-and-references

Appendix D: Map of Soil Types Found in the Greenbelt District

Soil Types of the Ann Arbor Greenbelt

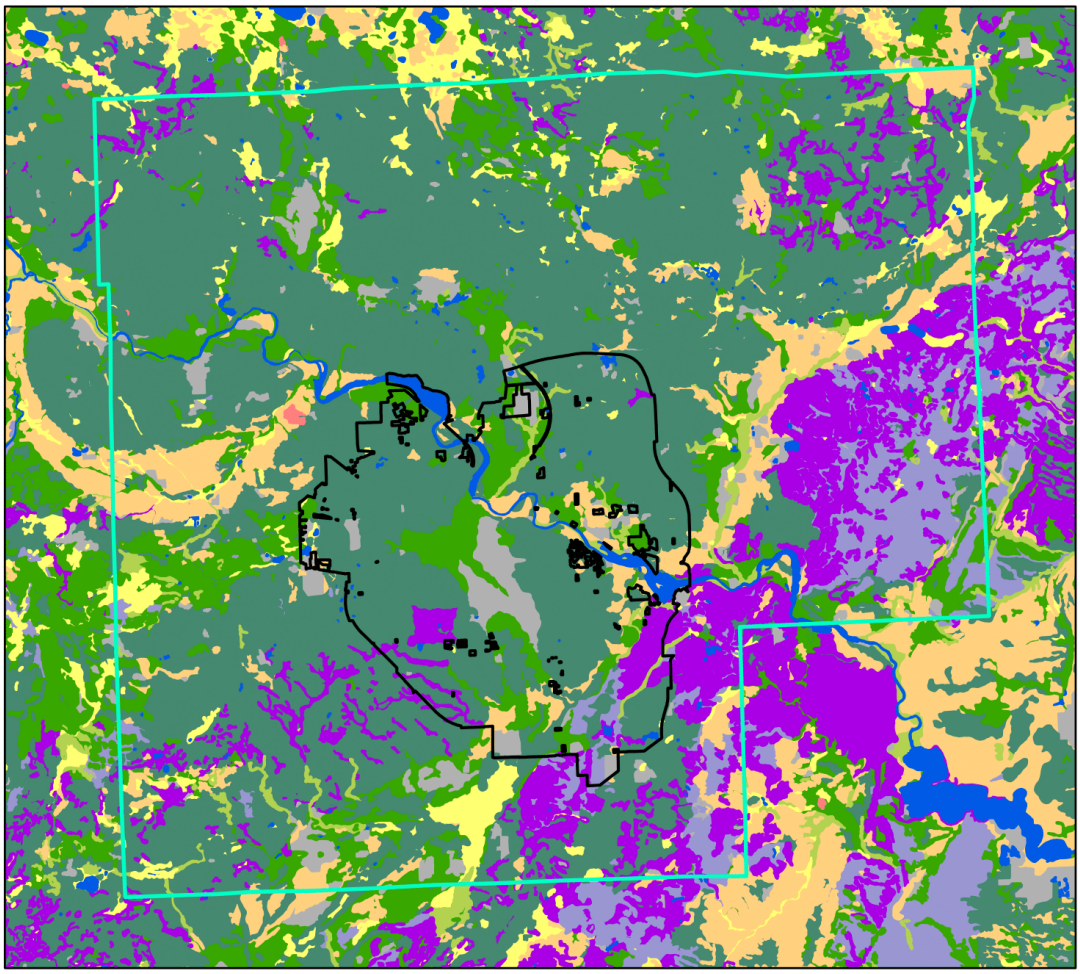

N

0 2 4 8 km

Data Source: NRCS Web Soil Survey
Datum/Projection: NAD 1983 StatePlane Michigan South
Map Layout: Jackie Edinger, 1/14/2021

Soil Type

- Clay Loams: Pewamo, St. Clair
- Silty Clay Loams: Hoytville, Nappanee
- Loams: Blount, Brookston, Conover, Kendallville, Macomb, Miami, Morley, Sebewa, Wawasee
- Sandy Loams: Cohoctah, Fox, Gilford, Kibbie, Kidder, Matherton, Metamora, Seward, Sisson, Wauseon, Ypsi
- Silt Loams: Pella, Sloan
- Mucks: Adrian, Edwards, Houghton, Palms
- Loamy Sands: Boyer, Oshtemo, Seward, Spinks, Thetford
- Sands: Oakville
- Other
- Water

- Ann Arbor City Boundary
- Greenbelt Boundary

Appendix E: Summary of Belowground Carbon Storage by Property

Project Name	Forest Soil Carbon (kg)	Wetland Soil Carbon (kg)	Total Belowground Carbon (kg)	Total Belowground Carbon (Mg)	CO_2 Equivalent (metric tons CO_2)	EPA $ Conversion for Soil Carbon
Alexander, Robbin	53,880	247,218	301,098	301	1,104	$ 56,305.79
Bloomer, Tom & Rosanne	166,044	1,569,516	1,735,559	1,736	6,364	$ 324,552.53
Fishbeck, William & Betty (41 acres)	0	0	0	0	0	$ -
Fishbeck, William & Betty (116 acres)	498,922	58,069	556,991	557	2,042	$ 104,158.19
Kapp, Dale	340,861	104,315	445,175	445	1,632	$ 83,248.56
Cares, John & Jean	719,254	241,116	960,370	960	3,521	$ 179,590.88
Alexander, John and Beverly	111,275	47,513	158,788	159	582	$ 29,693.68
Honke (Cavanaugh)	253,124	1,359,905	1,613,029	1,613	5,914	$ 301,639.19
Maulbetsch	172,213	1,601,561	1,773,774	1,774	6,504	$ 331,698.77
Botero	262,790	4,212,790	4,475,580	4,476	16,411	$ 836,941.06
Fox	734,321	80,059	814,380	814	2,986	$ 152,290.39
Pellerito aka Lakeside Development LLC aka Mitigation Solutions aka Oakland	197,595	369,054	566,648	567	2,078	$ 105,964.23
Clark, Brad and Mary	8,742	1,019,168	1,027,910	1,028	3,769	$ 192,220.91
Landsberg, Carol P. Trust	588,876	1,414,184	2,003,060	2,003	7,345	$ 374,575.72
Merkel / Heller	251,221	25,819	277,040	277	1,016	$ 51,807.01
Smyth	208,129	0	208,129	208	763	$ 38,920.40
Whitney	2,510,091	5,988,566	8,498,657	8,499	31,162	$ 1,589,263.37
Webster Church	44,484	1,298,287	1,342,772	1,343	4,924	$ 251,100.56
Bloch (23 acres)	4,980	86,829	91,808	92	337	$ 17,168.31
Newton (Green Things)	330,965	134,056	465,020	465	1,705	$ 86,959.62
Gould	0	0	0	0	0	$ -
Braun, Charles and Catherine	921,222	390,070	1,311,292	1,311	4,808	$ 245,213.77
Dudley, Open Roads Development	1,641,390	94,994	1,736,384	1,736	6,367	$ 324,706.75
Biltmore / Superior / Geddes aka DBN Investors LLC	349,643	74,128	423,772	424	1,554	$ 79,246.06
Pardon	89,513	47,621	137,134	137	503	$ 25,644.36
Nixon, William and Cherie	276,189	58,779	334,968	335	1,228	$ 62,639.54

Hilton, Walter Trust (Mason)	48,425	7,673	56,098	56	206	$ 10,490.46
Zeeb, Kenny	284,012	0	284,012	284	1,041	$ 53,110.78
Girbach (Vestergaard)	62,286	27,930	90,216	90	331	$ 16,870.53
Braun, Thomas & Theodore	690,653	4,264	694,917	695	2,548	$ 129,950.75
Ledwidge	85,991	0	85,991	86	315	$ 16,080.41
Geiger (213 acres)	277,975	24,109	302,084	302	1,108	$ 56,490.23
Geiger (116 acres)	77,575	300,547	378,122	378	1,386	$ 70,709.48
Lindemann and Weidmayer	255,741	80,366	336,107	336	1,232	$ 62,852.53
Thomas and Lobato	10,850	0	10,850	11	40	$ 2,029.02
VanNatter	23,918	0	23,918	24	88	$ 4,472.74
Bloch (33 acres)	171,888	28,773	200,661	201	736	$ 37,524.01
Ford-Goldsmith	36,197	0	36,197	36	133	$ 6,768.88
Boike (Maulbetsch)	2,151	0	2,151	2	8	$ 402.30
Drake - South	282,368	488,402	770,770	771	2,826	$ 144,135.36
Schultz, Robert	219,998	55,408	275,406	275	1,010	$ 51,501.33
Schumacher, Carol	591,787	215,209	806,995	807	2,959	$ 150,909.48
Hornback, Dan and Amy (Kadykowski)	1,514,977	280,553	1,795,530	1,796	6,584	$ 335,767.21
Wolf and Sheldon	0	0	0	0	0	$ -
Novick, Jack and Kerry Kelly	34,193	0	34,193	34	125	$ 6,394.24
Drake - North	0	0	0	0	0	$ -
Domino Farms aka DF Land Development (12 acres)	217,793	13,701	231,494	231	849	$ 43,289.75
Moore	47,108	0	47,108	47	173	$ 8,809.23
Polliey	0	16,645	16,645	17	61	$ 3,112.62
White aka McCleery	14,323	0	14,323	14	53	$ 2,678.48
VanCurler	784,057	257,796	1,041,853	1,042	3,820	$ 194,828.34
DF Land Development LLC (81 acres)	377,239	501,359	878,598	879	3,222	$ 164,299.29
Guenther - West	18,867	38,404	57,271	57	210	$ 10,709.78
Guenther - East	460,284	0	460,284	460	1,688	$ 86,073.98
Hall, James S. Revocable Trust	618,644	579,314	1,197,958	1,198	4,393	$ 224,020.26
Smith, Carol Trust	546,760	964,729	1,511,489	1,511	5,542	$ 282,651.09
Pringle, John and Beverly Mitchell (shared with LAC)	386,462	134,047	520,509	521	1,909	$ 97,336.15

Rogers	17,078	0	17,078	17	63	$ 3,193.59
Lada Rolling Acres, LLC	175,632	226,655	402,287	402	1,475	$ 75,228.28
DeVine-Koselka	1,399,421	187,782	1,587,203	1,587	5,820	$ 296,809.60
Seeley Farm	278,233	23,383	301,616	302	1,106	$ 56,402.70
Shatter Family Trust	203,291	111,562	314,852	315	1,154	$ 58,877.94
Stiles-Kaldjian	1,334,490	540,049	1,874,539	1,875	6,873	$ 350,541.93
Lepkowski	181,391	381,207	562,598	563	2,063	$ 105,206.78
Koch	8,438	0	8,438	8	31	$ 1,577.84
Stepien	82,812	40,364	123,177	123	452	$ 23,034.22
Haas	774,854	0	774,854	775	2,841	$ 144,899.08
Lambarth	147,046	180,256	327,302	327	1,200	$ 61,206.08
Boss & Bull Holdings, LLC	17,405	38,938	56,343	56	207	$ 10,536.20
Moehrle	107,501	126,852	234,353	234	859	$ 43,824.39

Totals	Forest Soil Carbon (kg)	Wetland Soil Carbon (kg)	Total Belowground Carbon (kg)	Total Belowground Carbon (Mg)	CO_2 Equivalent (metric tons CO_2)	EPA $ Conversion for Soil Carbon
	23,605,839	26,399,893	50,005,732	50,006	183,356	$ 9,351,156.96

Appendix F: Soil & Water Assessment Tool (SWAT) Input Files

Below is a table of all required and optional input files for the Soil & Water Assessment Tool (SWAT). Retrieved from SWAT 2012 Documentation (Arnold et al., 2012).

Input files for SWAT include:

file.cio (watershed level file)	Master watershed file. This required file contains the names of watershed level files and parameters related to printing.
.fig (watershed level file)	Watershed configuration file. This required file defines the routing network in the watershed and lists input file names for the different objects in the watershed.
.bsn (watershed level file)	Basin input file. This required file defines values or options used to model physical processes uniformly over the entire watershed.
.pcp (watershed level file)	Precipitation input file. This optional file contains daily measured precipitation for a measuring gage(s). Up to 18 precipitation files may be used in each simulation and each file can hold data for up to 300 stations. The data for a particular station is assigned to a subbasin in the subbasin input file (.sub).
.tmp (watershed level file)	Temperature input file. This optional file contains daily measured maximum and minimum temperatures for a measuring gage(s). Up to 18 temperature files may be used in each simulation and each file can hold data for up to 150 stations. The data for a particular station is assigned to a subbasin in the subbasin input file (.sub).
.slr (watershed level file)	Solar radiation input file. This optional file contains daily solar radiation for a measuring gage(s). The solar radiation file can hold data for up to 300 stations. The data for a particular station is assigned to a subbasin in the subbasin input file (.sub).
.wnd (watershed level file)	Wind speed input file. This optional file contains daily average wind speed for a measuring gage(s). The wind speed file can hold data for up to 300 stations. The data for a particular station is assigned to a subbasin in the subbasin input file (.sub).
.hmd (watershed level file)	Relative humidity input file. This optional file contains daily relative humidity values for a measuring gage(s). The relative humidity file can hold data for up to 300 stations. The data for a particular station is assigned to a subbasin in the subbasin input file (.sub).
.pet (watershed level file)	Potential evapotranspiration input file. This optional file contains daily PET values for the watershed.

.cst (watershed level file)	Weather forecast input file. This optional file contains the statistical data needed to generate representative daily climatic data for the subbasins during the forecast period.
.cal (watershed level file)	Auto-calibration input file. This optional file contains the data needed to operate the auto-calibration algorithms.
crop.dat (watershed level file)	Land cover/plant growth database file. This required file contains plant growth parameters for all land covers simulated in the watershed.
till.dat (watershed level file)	Tillage database file. This required file contains information on the amount and depth of mixing caused by tillage operations simulated in the watershed.
pest.dat (watershed level file)	Pesticide database file. This required file contains information on mobility and degradation for all pesticides simulated in the watershed.
fert.dat (watershed level file)	Fertilizer database file. This required file contains information on the nutrient content of all fertilizers and manures simulated in the watershed.
urban.dat (watershed level file)	Urban database file. This required file contains information on the build-up/wash-off of solids in urban areas simulated in the watershed.
septic.dat (watershed level file)	Septic database file. This file contains information on septic systems.
.sub (subbasin level file)	Subbasin input file. This required file for each subbasin defines climatic inputs, tributary channel attributes, and the number and types of HRUs in the subbasin.
.wgn (subbasin level file)	Weather generator input file. This required file contains the statistical data needed to generate representative daily climatic data for a subbasin.
.pnd (subbasin level file)	Pond/wetland input file. This optional file contains information for impoundments located within a subbasin.
.wus (subbasin level file)	Water use input file. This optional file contains information for consumptive water use in a subbasin.
.rte (subbasin level file)	Main channel input file. This required file contains parameters governing water and sediment movement in the main channel of a subbasin.
.sep (subbasin level file)	Septic input file. This optional file contains information for septic systems.

.wwq (watershed level file)	Watershed water quality input file. This optional file contains parameters used to model QUAL2E transformations in the main channels.
.swq (subbasin level file)	Stream water quality input file. This optional file contains parameters used to model pesticide and QUAL2E nutrient transformations in the main channel of the subbasin.
.hru (HRU level file)	HRU input file. Required file for HRU level parameters. Catch-all file.
.mgt (HRU level file)	Management input file. This required file contains management scenarios and specifies the land cover simulated in the HRU.
.sol (HRU level file)	Soil input file. This required file contains information about the physical characteristics of the soil in the HRU.
.chm (HRU level file)	Soil chemical input file. This optional file contains information about initial nutrient and pesticide levels of the soil in the HRU.
.gw (HRU level file)	Groundwater input file. This required file contains information about the shallow and deep aquifer in the subbasin. Because land covers differ in their interaction with the shallow aquifer, information in this input file is allowed to be varied at the HRU level.
.res (reservoir file)	Reservoir input file. This optional file contains parameters used to model the movement of water and sediment through a reservoir.
.lwq (reservoir file)	Lake water quality input file. This optional file contains parameters used to model the movement of nutrients and pesticides through a reservoir.
rechour.dat recday.dat recmon.dat recyear.dat reccnst.dat (point source file)	Point source input files. These optional files contain information about loadings to the channel network from a point source. The type of file used to store the data depends on how the data is summarized (hourly, daily, monthly, yearly, or average annual).

Literature Cited

Arnold, J. G., Kiniry, J. R., Srinivasan, R., Williams, J.R., Haney, E. B., & Neitsch, S., L. (2012). Soil & Water Assessment Tool: Input/Output Documentation [PDF file]. Retrieved from https://swat.tamu.edu/docs